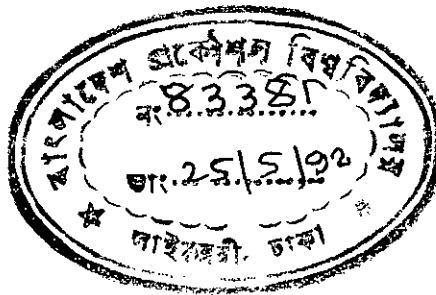


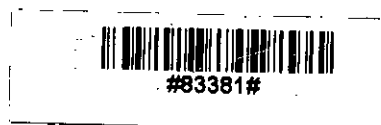
NATURAL CONVECTION FROM HOT CORRUGATED PLATES
TO A COLD FLAT PLATE

By
Chowdhury Md. Feroz

A Thesis
Submitted to the department of Mechanical Engineering
in partial fulfilment of the requirements for the degree
of
MASTER OF SCIENCE IN MECHANICAL ENGINEERING



BANGLADESH UNIVERSITY OF ENGINEERING AND TECHNOLOGY, DHAKA
April, 1992

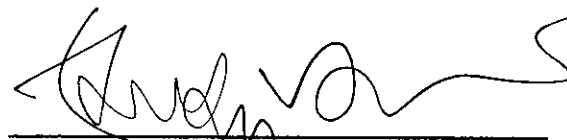


620.04
1992
Ch0

RECOMMENDATION OF THE BOARD OF EXAMINERS

The Board of Examiners hereby recommends to the Department of Mechanical Engineering, Bangladesh University of Engineering and Technology, Dhaka, the acceptance of the thesis, "NATURAL CONVECTION FROM HOT CORRUGATED PLATES TO A COLD FLAT PLATE", submitted by Chowdhury Md. Feroz, in partial fulfilment of the requirements for the degree of Master of Science in Mechanical Engineering.

Chairman :



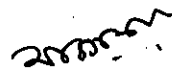
Dr. Md. Abdur Razzaq Akhanda
Professor
Dept. of Mechanical Engg.
BUET, Dhaka.

Member :



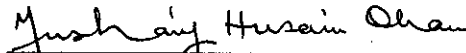
Dr. Md. Wahhaj Uddin
Professor & Head
Dept. of Mechanical Engg.
BUET, Dhaka.

Member :



Dr. Md. Abdur Rashid Sarker
Associate Professor
Dept. of Mechanical Engg.
BUET, Dhaka.

Member (External) :

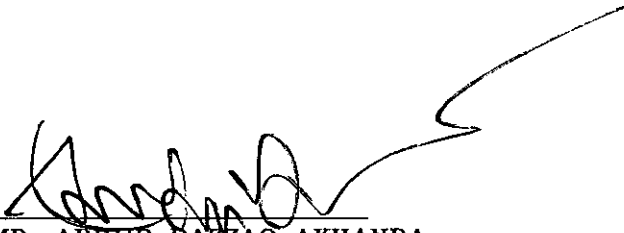


Prof. Musharrif Hussain Khan
Member
University Grants Commission
Dhaka, Bangladesh.

April, 1992.

CERTIFICATE OF RESEARCH

This is to certify that the work presented in this thesis is an outcome of the investigation carried out by the author under the supervision of Dr. Md. Abdur Razzaq Akhanda, Professor, Department of Mechanical Engineering, Bangladesh University of Engineering & Technology, Dhaka.



DR. MD. ABDUR RAZZAQ AKHANDA
Supervisor



CHOWDHURY MD. FERAZ
Author

ACKNOWLEDGEMENT

I wish to express my sincerest gratitude and indebtedness to Dr. Md. Abdur Razzaq Akhanda for his guidance and supervision throughout the entire period of the experimental investigation. His initiatives, encouragement, patience and invaluable suggestions are gratefully acknowledged without which this work would not have been possible.

I am truly grateful to Professor M. H. Khan for his constructive suggestions and advice during several phases of this investigation. Without his kind co-operation and guidance this work could not have been carried out properly.

The co-operation and inspiration extended by Associate Professors Dr. A.K.M. Sadrul Islam and Dr. Md. Abdur Rashid Sarker are acknowledged with gratitude.

Sincere thanks are offered to Mr. Rafiqul Islam, Foreman instructor, Carpentry shop, Md. Nazimuddin, Foreman instructor, Welding & Sheet Metal Shop, BUET, for their co-operation in fabricating and assembling different parts and components of the experimental set-up. Thanks are also due to Mr. Amir Hossain, Technician at the Heat Transfer Laboratory of Mechanical Engineering Department for his co-operation at different stages of the work. I would also like acknowledge the help of Mr. Md. Fakhrul Islam Hazra for Typing and Mr. Abdur Rahman for Drafting the figures.

Lastly, I would like to thank my wife who persistently kept me at my work and partly relieved me of family duties until this work was finished.

ABSTRACT

This experimental investigation deals with the steady state natural convection heat transfer from a hot corrugated plate to a cold flat plate through air placed above and parallel to it in an enclosed space. The surroundings of this space were adiabatic. Two types of corrugation, namely trapezoidal and rectangular, having same maximum width and height, were studied. The effects of the angle of inclination, the aspect ratio, the temperature potential and the Rayleigh number on average heat transfer coefficients were investigated.

The study covers the following ranges of parameter;

$9.84 \times 10^4 \leq Ra_L \leq 2.29 \times 10^6$, $0^\circ \leq \theta \leq 75^\circ$, $2.60 \leq A \leq 5.22$ and $10^\circ\text{C} \leq \Delta T \leq 35^\circ\text{C}$.

The results are compared with those available in the literature and found that, for the same aspect ratio but lower Rayleigh number, ($Ra_L = 0.40 \times 10^6$) the trapezoidal and rectangular corrugations are lower than Vee-corrugation by 34% and 38%, respectively, for all values of θ while the values are 15% and 18% when compared with sinusoidal corrugation. But the differences are lower at higher Rayleigh number. The following correlations were developed:

$$Nu_L = 0.0112 [Ra_L \cos\theta]^{0.521} [A]^{-0.4546}; \quad [\text{TRAPEZOIDAL CORRUGATION}]$$

$$Nu_L = 0.0102 [Ra_L \cos\theta]^{0.530} [A]^{-0.4923}; \quad [\text{RECTANGULAR CORRUGATION}]$$

Both of these correlations correlate data to $\pm 15\%$.

CONTENTS

	<u>Page</u>
RECOMMENDATION OF THE BOARD OF EXAMINERS	ii
CERTIFICATE OF RESEARCH	iii
ACKNOWLEDGEMENT	iv
ABSTRACT	v
CONTENTS	vi
NOMENCLATURE	viii
CHAPTER 1: INTRODUCTION	1
1.1 General	1
1.2 Natural Convection in an enclosure	2
1.2.1 Horizontal Fluid Layers	2
1.2.2 Inclined Fluid Layers	3
1.3 Motivation behind the Selection of the Problem	4
1.4 The Present Study	5
CHAPTER 2: LITERATURE REVIEW	8
2.1 General	8
2.2 Natural Convection Heat Transfer in Plane Horizontal Fluid Layers	9
2.3 Natural Convection Heat Transfer in Plane Inclined Fluid Layers	12
2.4 Natural Convection Heat Transfer in Vee-Corrugated Enclosure	14
2.5 Natural convection Heat Transfer in Sinusoidal-Corrugated Enclosure	16
CHAPTER 3: THEORY	17
3.1 Description of the Problem	17
3.2 Mathematical Equations	18

CHAPTER 4: EXPERIMENTAL SET-UP	19
4.1 General Description of the Set-up	19
4.2 The Test Section	20
4.2.1 The Hot Plate Assembly	20
4.2.2 The Outer Guard Heater Assembly	21
a. The Upper Outer Guard Heater Assembly	21
b. The Lower Outer Guard Heater Box	22
4.2.3 The Cold Plate Assembly	23
4.2.4 The Alingment Plate and Supporting Frame	24
4.3 The Reserve Water Tank	25
4.4 Instrumentation	26
CHAPTER 5: EXPERIMENTAL MEASUREMENTS AND TEST PROCEDURE	27
5.1 Temperature Measurement	27
5.2 Heat Flux Measurement	28
5.3 Test Procedure	28
5.4 Reduction of Data	31
CHAPTER 6: RESULTS AND DISCUSSION	32
CHAPTER 7: CONCLUSIONS AND RECOMMENDATIONS	38
7.1 Conclusions	38
7.2 Recommendations	40
REFERENCES	41
APPENDICES	
Appendix A: Design of the Test Rig	45
Appendix B: Conduction Correction	55
Appendix C: Determination of Emissivity of the Corrugated Surfaces	56
Appendix D: Correlations	57
FIGURES	61

NOMENCLATURE

<u>SYMBOL</u>	<u>MEANING</u>	<u>UNITS</u>
A	Aspect ratio, L/H [Mean plate spacing/amplitude of corrugation]	dimensionless
A_{COR}	Area of the test section of the experimental corrugated plate	m^2
A_{COLD}	Area of the cold plate	m^2
A_p	Area of any plane rectangular surface	m^2
A_i	Area of surface i	m^2
A_j	Area of surface j	m^2
A_s	Area of the wooden surface	m^2
C	Constant	dimensionless
C_p	Specific heat of air at constant pressure	kg/kJ °k
E_b	Emissive power for a black surface. σT^4	Watt/ m^2
E_c	Eckert number, $u^2/C_p \cdot \Delta T$	dimensionless
F	Shape factor [Fraction of black body radiation in a wave length band]	
Gr	Grashof number, $g \cdot \beta \cdot \Delta T d^3 / \nu^2$	dimensionless
g	Acceleration due to gravity	m/sec ²
h	Average natural convective heat transfer coefficient.	Watt/ m^2 °k
H	Amplitude of the corrugation	m
I_{safe}	Safe current capacity of the heater coil	ampere
J	Radiosity [Emissive power for a black surface, E_b]	Watt/ m^2
K	Thermal conductivity of air	Watt/m °k
L_c	Characteristics length ($= \sqrt{A_p}$)	m
L	Mean plate spacing	m

m	Exponent	dimensionless
n	Exponent	dimensionless
Nu_L	Average Nusselt number, hL/k	dimensionless
P	Pitch of corrugation	m
Pr	Prandtl Number, $\mu C_p/k$	dimensionless
q	Heat transfer rate	Watt/m ²
q"	Heat flux rate into the test hot plate	watt/m ²
r	Unit electrical resistance	ohms/m
R	Electrical resistance	ohms
Ra_L	Rayleigh Number based on mean plate spacings (L), g.B. $\Delta T.L^3/\nu\alpha$	dimensionless
s	Maximum width of corrugation	m
t	Time	Sec
T	Temperature	°k
T_a, T_∞	Ambient air temperature	°k
T_f	Fluid film temperature, $[T_{COR} + T_{COLD}]/2$	°k
T_{COR}	Temperature of the hot corrugated plate	°k
T_{COLD}	Temperature of the cold flat plate	°k
ΔT	Temperature difference between the hot corrugated plate & flat cold plate.	°k
ΔT_c	Conduction correction	°k
T_s	Temperature of the wooden surfaces	°k
u,v,w	Velocity components in the direction of x,y,z respectively	m/sec
V_{safe}	Safe voltage across the heater coil	volts
W	Width of the enclosure	m
x,y,z	Spatial coordinates	

X_{COR}	Longitudinal side of the test section of the corrugated plate	mm
X_{COLD}	Longitudinal side of the cold flat plate	mm
ΔX	Thickness along x direction.	m
Y_{COR}	Lateral side of the test section of the corrugated plate	mm
Y_{COLD}	Lateral side of the cold flat plate	mm

GREEK ALPHABET:

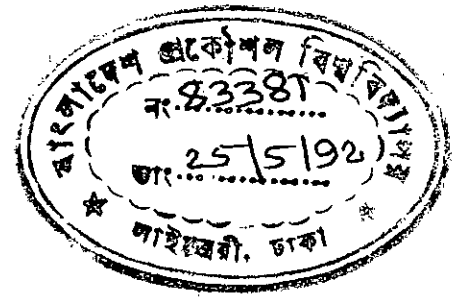
α	Thermal diffusivity, $k/\rho C_p$	m^2/sec
β	Volumetric thermal expansion coefficient, $1/T_f$	$1/^\circ k$
Δ	Difference	
ϵ	Long wave emissivities	dimensionless
ϵ_H	Hemispherical emittance	dimensionless
ϵ_s	Long wave emissivities of the wooden surfaces	dimensionless
θ	Tilt angle of inclination of the enclosed air layers with the horizontal.	degrees
ν	Kinematic viscosity of the convecting fluid (air)	m^2/sec
ρ	Density	kg/m^3
σ	Stefan Boltzman's constant [$=5.67 \times 10^{-8}$]	$Watt/m^2 \text{ } ^\circ k^4$
ϕ	Phase angle of the current	degree

SUBSCRIPTS:

r
t

DESIGNATION:

Rectangular corrugation
Trapezoidal corrugation



CHAPTER - 1

INTRODUCTION

1.1 General:

Motion in free convection fluid is due to buoyancy forces within the fluid, while in forced convection it is externally imposed. Buoyancy is due to the combined presence of a fluid density gradient and a body force. The body force is usually gravitational. There are several ways in which a mass density gradient may arise in a fluid but in the most common situation it is due to the presence of a temperature gradient. The density of gases and liquids depends on temperature, generally decreasing due to fluid expansion with increasing temperature.

Free convection currents transfer internal energy stored in fluid elements in the same manner as forced convection currents. However the intensity of mixing is generally less in free convection and consequently the heat transfer co-efficients in free convection are lower than those in forced convection.

The temperature distribution in natural convection depends on the intensity of the fluid currents which is really dependent on the temperature potential itself. So the qualitative and quantitative analyses of natural convection heat transfer are quite difficult. For this reason the theoretical analyses of natural convection heat transfer for most of the practical situations is absent in the literature. So, at this present stage the necessity of the experimental investigation is seriously felt.

1.2 Natural Convection in an Enclosure:

Engineering applications frequently involve heat transfer between surfaces that are at different temperatures and are separated by an enclosed fluid. The surfaces may be plane horizontal or vertical. Recently the heat transfer characteristics for non-plane [Vee corrugated and sinusoidal corrugated] horizontal as well as inclined fluid layers have been reported. The main feature of these types of natural convection heat transfer problems is that the boundary layer thickness, if there be any, is comparable with the dimensions of the enclosed fluid layers.

1.2.1 Horizontal Layers:

For fluids whose density decreases with the increase of temperature, no free convection currents occur in a fluid which is enclosed between two parallel horizontal plates as long as the temperature of the upper plate is higher than the temperature of the lower one. In that case heat will be transferred only by conduction. The situation is different when a fluid is enclosed between two horizontal surfaces of which the upper surface is at lower temperature than the lower one. For fluids whose density decreases with increasing temperature, this leads to an unstable situation. Benard [1900] mentioned this instability as a "top heavy" situation. In that case fluid is completely stationary and heat is transferred across the layer by the conduction mechanism only. Rayleigh [1916] recognized that this unstable situation must break down at a certain value of Rayleigh number

above which a convective motion must be generated. Jeffreys [1928] and Low [1929] calculated this limiting value of Ra_L to be 1708, when the air layer is bounded on both sides by solid walls. With the optical investigation in a trough filled with water carried out by Schmidt and Saunders [1938] this limiting value [$Ra_L = 1708$] also has been confirmed. Above this critical value of Ra_L a peculiar free convection flow pattern arises. The flow field becomes a cellular structure with more or less regular hexagonal cells. In the interior of these cells the flow moves in an upward direction and along the rim of the cells it returns down. According to Ostrach [1957] when the top and the bottom surfaces are rigid, the turbulence first appears at $Ra_L = 4380$ and the flow becomes fully turbulent at $Ra_L = 4500$ for plane horizontal air layers but at lower values of Ra_L for water with same boundaries.

1.2.2 Inclined Fluid Layers:

The problem associated with convective motion of an inclined fluid layer heated from below is more or less similar to horizontal fluid layer. Purely convective motion is gained after decaying of two distinct flow regimes - conductive regime and postconductive regime.

At very small Rayleigh number the motion is relatively simple. It consists of one large cell which fills the whole slot, the fluid rising on the hot wall, falling down the cold wall and turning at the opposite ends of the slot. This flow pattern is known as base flow according to Ayyaswamy [1973]. The heat transfer in this flow regime is purely conductive [i.e., $Nu = 1$]

except at the extreme ends where there is some convective heat transfer associated with the fluid turning. For air this conductive regime exists if the Rayleigh number is less than a critical value Ra_c . This limit has been defined by Buchberg et al. [1976] as follows:

$$Nu = 1 \quad \text{for} \quad Ra_L < 1708/\cos\theta$$

$$\text{i.e., } Ra_c = 1708/\cos\theta$$

At Ra_c , the base flow becomes marginally unstable and the resulting flow begins to take the form of steady longitudinal rolls i.e., rolls with their axis along the upslope.

At $Ra_L \gg Ra_c$, the flow becomes convective. The resulting flow begins to take the boundary layer structure with the resistance to heat transfer lying exclusively in two boundary layers, one on each of the boundary surfaces.

1.3 Motivation Behind the Selection of the Problem:

The free convective heat transfer across inclined fluid (air) layer heated from below is of importance in many engineering applications. It is of particular importance in flat-plate collectors where it can constitute the main mode of heat loss. Solar engineers are concerned about free convection heat loss from the absorber plate of the flat plate solar collector to the adjacent flat glass covers. The efficiency of the collector among other things increases with the decreasing of heat loss through the cover plates. Generally the absorber plate is made flat. Several studies have proved the advantageous effect of vee corrugated absorber plate

Close et al. [1968,1963]. Investigations carried out by Arnold et al. [1978], Buchberg et al. [1976], Graff et al. [1953], Difederico et al.[1966], Dropkin et al. [1966,1965,1959], Hart et al. [1971], Hollands et al. [1976, 1975, 1973, 1965], Koschmieder et al. [1974], O'Toole et al. [1961] and Schluter et al. [1965] have already discussed the natural convection heat transfer across air layer bounded by two parallel flat plates at different angles of inclination, including $\theta = 0^\circ$. Elsherbiny et al. [1977] studied the natural convection heat transfer from a vee corrugated plate to flat cold plate.

Kabir [1988] reported results on natural convection heat transfer from a hot sinusoidal corrugated plate to a cold flat plate for different aspect ratios and at different angles of inclination including horizontal.

Works were reported on natural convection heat transfer across air layer in an enclosure bounded by two flat plates, from a hot vee corrugated plate to a cold flat plate, and also heat transfer from a hot sinusoidal plate to a cold flat plate. But no work is reported on free convection heat transfer from a hot 'trapezoidal corrugated' plate to a cold flat plate and from a hot 'rectangular corrugated' plate to a cold flat plate. Hence through the present investigation an effort has been made to fill up the existing gap in the information on natural convection heat transfer.

1.4 The Present Study:

In the present study an experimental investigation on the natural convection heat transfer rate from a hot corrugated plate to a cold plate

with air as the working fluid was carried out. The geometry and dimensions of the corrugated plates tested are shown in figures 3.1a and 3.1b.

Main objectives of the present work were:

- a. To determine the average natural convective heat transfer co-efficients [h].
- b. To determine the dependence of average heat transfer co-efficient on aspect ratio [A].
- c. To study the variation of average heat transfer co-efficient with the angle of inclination [θ] of the corrugated plate with the horizontal.
- d. To observe the variation of average heat transfer co-efficient with different thermal potential [ΔT].
- e. To compare the results of this study with earlier relevant investigations.
- f. To develop possible correlations which will correlate all the experimental data within reasonable limit.

The experimental set-up of Kabir [1988] was redesigned and modified for the present investigation. Supply of power to the experimental rig by

electric heater was varied by using a Variac with the variation of aspect ratio to keep a particular constant thermal potential [ΔT]. The cold flat plate was cooled by continuous water circulation. In the fabrication of hot plate assembly, trapezoidal and rectangular corrugated G.I. Sheets of the same depth [amplitude] were used. The maximum width of the trapezoidal slot was equal to that of the rectangular slot. The amplitude and maximum width of the trapezoidal and rectangular corrugation were the same as that of Kabir [1988].

The aspect ratio was varied between 2.60 and 5.22 by changing the average plate spacing [L]. The angle of inclination covered was between 0° and 75° and the thermal potential range used in the experiment was from 10°C to 35°C . The Rayleigh number covered in this study was:

$$9.8 \times 10^4 \leq Ra_L \leq 2.29 \times 10^6$$

Correlations in the form of $Nu_L = C [Ra_L \cos\theta]^n [A]^m$ were developed. The results obtained in the present study are compared with other studies related to the problem under investigation.

CHAPTER - 2

LITERATURE REVIEW

2.1 General:

The free convection heat transfer through a layer of air bounded by two parallel plates heated from below is of importance in numerous engineering problems. Specially the free convection heat loss across an inclined air layer is of interest to the designers of solar collectors, because any reduction of heat loss from the absorber plate through the cover plates improves the efficiency of the collector.

Free convection currents occur in a fluid enclosed between two parallel horizontal plates if the temperature of the lower plate is higher than that of the upper one. For fluids whose density decreases with the increasing temperature, an unstable state, named as 'top heavy', is observed at a very small Rayleigh number. In this state, the fluid is completely stationary and heat is transferred across the fluid layer by a conduction mechanism. This unstable state breaks down at a certain critical value of Rayleigh number [The value depends on the boundary conditions].

At Ra_c , the unstable state becomes marginally unstable as any disturbance in the fluid will result in fluid motion with no dampening. This flow state is known as postconductive state. It is laminar and has nearly a hexagonal cell structure. The flow moves upward in the interior of these cells and returns downward along its rim.

At $Ra_L \gg Ra_c$, the flow becomes convective with the breaking down of laminar flow into turbulent flow. The resulting flow begins to take the boundary layer structure in which the resistance to heat transfer lie exclusively in two boundary layers on the boundary two surfaces.

2.2 Natural Convection Heat Transfer In Plane Horizontal Fluid Layers:

Most of the researches in heat transfer in confined spaces have been done with the parallel plates in a horizontal position. A considerable number of experiments have been conducted on air, on water and on oil and the results have been reported by investigators.

Thomson [1882] performed an experimental investigation on natural convection heat transfer through a layer of soapy water between horizontal plates heated from below. He noted the presence of cellular patterns in soapy water whose mean temperature was greater than the ambient. Benard [1900] also performed similar experimental investigation but his working fluid was paraffin oil and published photographs taken with a beam of parallel light which had passed through the layer of this paraffin oil. Those photographs clearly indicated the presence of a hexagonal cellular convection patterns. Sterling and Scriven [1964] concluded that the cellular convection patterns observed by Thomson & Benard were caused by surface tension rather than by thermal gradient.

Mull and Reiher [1930] performed most elaborated experiment on free convection heat transfer in horizontal air layer & presented their experimental results by plotting K_e/K_c versus Gr_L and obtained a smooth curve in the range of $2.1 \times 10^3 < Gr_L < 8.89 \times 10^8$. They assumed K_e as an equivalent thermal conductivity considering the effects of conduction, convection & radiation i.e., $K_e = K_c + K_r$, where K_c is an equivalent thermal conductivity taking into effects both conduction and convection, and K_r an equivalent thermal conductivity for radiation. Jakob [1946] plotted the data of Mull and Reiher in log-log coordinates and showed that there is at least one point of inflection in the curve and finally developed the following correlations:

$$\begin{aligned} Nu &= 0.195 [Gr_L]^{1/4}; & \text{for } 10^4 < Gr_L < 4 \times 10^5 \\ &= 0.068 [Gr_L]^{1/3}; & \text{for } Gr_L > 4 \times 10^5 \end{aligned}$$

Hollands, et al. [1974] carried out an experimental investigation on natural convection through an air-layer between two parallel copper plates, heated from below. They performed their experiment by varying pressure from 10 Pa to 700 kPa by inserting the plates in a pressure vessel. Actually the variation in of Ra over a wide range without altering the plate spacing or the temperature difference between the plates was attained through the variation pressure. Tests were carried out at mean plate spacings of 10mm, 25mm and 35mm covering the range of Ra from subcritical to 4×10^6 . They reported that when their data along with the data of Chu and Goldstein [1969] for air were analysed, the value of the index for Ra were the same

as one-third [1/3] while Chu and Goldstein for their data found that:

$$\text{Nu} \propto [\text{Ra}_L]^{0.294} \quad [\text{air}]$$

$$\text{Nu} \propto [\text{Ra}_L]^{0.278} \quad [\text{water}]$$

Rosby [1969] also reported different power law for different Prandtl number fluids as follows:

$$\text{Nu} \propto [\text{Ra}_L]^{0.281}; \quad \text{for silicon oil } [\text{Pr} = 11600]$$

$$\text{Nu} \propto [\text{Ra}_L]^{0.257}; \quad \text{for mercury } [\text{Pr} = 0.025]$$

Toole and Silveston [1961] developed the correlation equations for natural convection heat transfer across horizontal fluid layers by taking all the data available in the literature at that time. On the basis of Ra_L they differentiated the flow into the following three regions:

Initial region : $1700 < \text{Ra}_L < 3500$

Laminar region : $3500 < \text{Ra}_L < 10^5$

Turbulent region : $10^5 < \text{Ra}_L < 10^9$

They also developed the following correlations:-

$$\text{Nu} = 0.229 [\text{Ra}_L \cos\theta]^{0.22}; \quad 5900 \text{ Ra}_L \cos\theta < 10^5$$

$$\text{Nu} \propto [\text{Ra}_L]^{0.305}; \quad \text{for turbulent region.}$$

A number of investigators have also reported the 1/3 power law of dependency of Nusselt number on Rayleigh number. Mulkus [1963] and

Globe et al. [1959] also found the asymptotic behavior of Nusselt number and obtained $Nu \propto [Ra_L]^{1/3}$. Through numerical solution of the governing differential equations Herring [1965,1964] also predicted $Nu \propto [Ra_L]^{1/3}$ by neglecting the non-linear interaction terms.

2.3 Natural Convection Heat Transfer In Plane Inclined Fluid Layer:

Natural convection in inclined layers of fluid heated from below and cooled from above has received extensive attention owing to its importance in engineering applications, including solar heating.

Investigation was carried out by Graaf et al. [1953]. They performed measurements on heat transfer rate for the angles of inclination ranging from 0° to 90° in 10° steps and covered the range, $10^3 < Ra_L \cos\theta < 10^5$.

Dropkin et al. [1965] performed an experimental investigation of natural convection heat transfer in liquids [water, silicon oils and mercury] confined in two parallel plates, inclined at various angles with respect to the horizontal. They carried out their experiments in rectangular and circular containers having copper plates and insulated walls and covered the range, $5 \times 10^4 < Ra_L < 7.17 \times 10^8$ and $0.02 < Pr < 11560$. They got the following correlations:

$$Nu = C [Ra_L]^{1/3} [Pr]^{0.074}$$

where the constant C is a function of the angle of inclination. It varies from $C = 0.069$ for the horizontal plates to $C = 0.049$ for vertical plates.

Ayyaswamy et al. [1974] carried out a theoretical investigation on natural convection heat transfer in an inclined rectangular region and their results were limited to $0^\circ < \theta < 120^\circ$, $0.2 < A < 20$ and Ra up to 10^6 . But Ayyaswamy et al. [1973] investigated the boundary layer domain and observed that:

$$Nu_{(\theta)} = Nu_{(\theta = 90^\circ)} [\sin\theta]^{1/4}; \quad 0^\circ < \theta < 110^\circ.$$

Hollands et al. [1975] performed an experimental investigation on free convection heat transfer rates through inclined air layers of high aspect ratio (AR), heated from below. The covered range of Rayleigh number was from subcritical to 10^5 and angle of inclination was $0^\circ \leq \theta < 70^\circ$. They gave the following correlation:

$$\begin{aligned} Nu = 1 + 1.44 [1 - 1708/Ra_L \cos\theta]^* \\ [1 - (\sin 1.8\theta)^{1.6} \times 1708/Ra_L \cos\theta] + \\ [(Ra_L \cos\theta)^{1/3}/(5830^{1/3}) - 1]^* \end{aligned}$$

[* denotes that when the arguments inside the bracketed terms become negative, the value of bracketed terms must be taken as zero].

Computation of natural convection heat transfer characteristics of flat plate enclosures, using interferometric techniques, was carried out by Randall et al. [1977]. The effects of Grashof number, tilt angle and aspect ratio on both the local and average heat transfer co-efficient were determined. The Grashof number range tested was 4×10^3 to 3.1×10^5 and the aspect ratio,

defined as the ratio of enclosure length to plate spacing, varied between 9 and 36. The angles of inclination of the enclosure were 45°, 60°, 75° and 90°. They reported that the average heat transfer rate at an angle of inclination of 90° decreased by 18% from that at 45° and developed the following correlation:

$$Nu_L = 0.118 [Gr_L Pr \cos^2 (\theta-45)]^{0.29}$$

2.4 Natural Convection Heat Transfer In Vee Corrugated Enclosure:

The experimental investigations on natural convection heat transfer from a horizontal lower vee corrugated plate to an upper cold flat plate for Rayleigh number from 7×10^3 to 7×10^5 were first carried out by Chinnappa [1970]. The vee angle was 60° and aspect ratios were 0.64, 0.931, 0.968, 1.1875 and 1.218. Experimental fluid was air in all the test runs. The following correlations were obtained:

$$Nu = 0.54 [Gr_L]^{0.36} ; \quad 7 \times 10^3 < Ra_L < 5.6 \times 10^4$$

$$Nu = 0.139 [Gr_L]^{0.278} ; \quad 5.6 \times 10^4 < Ra_L < 7 \times 10^5$$

Elsherbiny et al. [1977] investigated free convection heat transfer in air layers bounded by lower hot V-corrugated plate and upper cold flat plate for Rayleigh number $10 < Ra_L < 4 \times 10^6$ and angle of inclination 0, 30, 45 and 60 degrees. The V-angle was 60 degree and aspect ratios were 1.0, 2.5 and 4.0. Experimental fluid was air in all test runs. He found that the convective heat transfer across air layers bounded by V-corrugated and

flat plates was greater than those for two flat parallel plates upto a maximum of 50%.

The correlation given by them was as follows:

$$\begin{aligned} \text{Nu} = \text{Nu}_c + K [1 - \text{Ra}_c / \text{Racos}\theta]^* [\text{Ra}_c (\text{Sin } 1.8\theta)^{1.6} / \text{Ra} \cos\theta] \\ + B [(\text{Ra} \cos \theta)^{1/3} / (3377)^{1/3} - F]^* \end{aligned}$$

Where,

$$\text{Ra}_c = 1708 + 945 / (A - 0.5)^{0.923}$$

$$K = 1.44 [1 - 1.15/A + 6.74/A^2 - 5.28/A^3]$$

$$B = 1.33 / \cos (\theta - 23.5)$$

$$F = 1.515 - 3.417 \times 10^{-2} \theta + 1.289 \times 10^{-3} \theta^2 - 1.158 \times 10^{-5} \theta^3$$

θ is in degrees and the asterisk brackets go to zero when the arguments inside them are negative.

Randall [1977] studied the average heat transfer co-efficients for natural convection between a V-corrugated plate and a parallel flat plate. He used interferometric techniques to find out the temperature distribution in the enclosed air space. From this temperature distribution he found the wall temperature gradient and hence estimated the local heat transfer co-efficient. The measurements were carried out for $10^3 < \text{Gr} < 3 \times 10^5$. The vee angle was 60° and aspect ratios were 0.75, 1 and 2, angle of inclination were 0° , 45° and 60° . Finally the following correlation was obtained:

$$\text{Nu} = C. \text{Gr}_L^n.$$

where,

0	A	C	n
0°	0.75	0.060	0.41
	1.0	0.060	0.41
	2.0	0.043	0.41
45°	0.75	0.75	0.36
	1.0	0.082	0.36
	2.0	0.037	0.41
60°	0.75	0.162	0.30
	1.0	0.141	0.30
	2.0	0.027	0.42

2.5 Natural Convection Heat Transfer In Sinusoidal Corrugated Enclosures:

The experimental investigation on the natural convection heat transfer from a lower horizontal sinusoidal corrugated plate to an upper cold flat plate for a range of Rayleigh number 5.50×10^3 to 2.34×10^6 and angle of inclination $[\theta]$ 0° to 75° was carried out by Kabir [1988]. The sinusoidal leading angle was 72° and aspect ratios covered were 2.0 to 5.75. Experimental fluid was air in all the test runs. Finally the following correlation was obtained:

$$Nu_L = 0.0132 [Ra_L \cos\theta]^{0.51} [A]^{-0.35}$$

The above equation correlates all the experimental data within $\pm 10\%$ and is valid for $5.56 \times 10^3 \leq Ra_L \leq 2.3 \times 10^6$, $1 \leq A \leq 5.75$ and $0^\circ \leq \theta \leq 75^\circ$.

CHAPTER - 3

THEORY

3.1 Description of the Problem:

The natural convection heat transfer in an inclined rectangular enclosure is a function of temperature difference between the hot and cold plates, boundary conditions, angle of inclination of the enclosure with the horizontal and the properties of confined convective fluid. The rectangular region of the present investigation were carried out for two sets of bottom and upper plates. In one set it had a lower hot trapezoidal corrugated plate and upper cold flat plate as shown in figure 4.2a and in the other set a bottom hot rectangular corrugated plate and an upper cold flat plate, as shown in figure 4.2b. The side walls of the enclosure were made plane and adiabatic. The convective fluid was air.

The spacing between the hot and cold plate was varied for varying aspect ratio 'A' defined as the ratio of mean plate spacing to amplitude of corrugation of the present experimental set-up. The vertical side walls of the enclosure and the bottom hot corrugated plates were maintained at the same temperature. At steady state the heat flux [q''] to the cold flat plate was by conduction, convection and radiation. But for Rayleigh numbers well above the critical value, conduction heat transfer was considered insignificant. So total heat flux, q'' had two components. Convection heat flux, q''_{conv} and radiation heat flux, q''_r [$q''_{conv} \gg q''_r$].

The radiative heat-flux, q_r'' was calculated by using the formula derived in appendix - A by considering hot corrugated plate & cold flat plate behaved as black bodies. The convective heat flux q_{conv}'' was calculated by subtracting the value of q_r'' from the total heat flux, q'' . Heat flux from the hot corrugated plate was calculated by measuring the current & the voltage supply of the main heater. The equations required for calculating q_r'' , q_{conv}'' & natural convective heat transfer co-efficient [h] are given in 3.2.

3.2 Mathematical Equations:

The mathematical equations that were used to calculate h, Nu_L and Ra_L are given below:

$$q_r'' = A_{COR} \cdot \sigma \cdot \epsilon_{COR} \cdot [(T_{COR})^4 - (T_{COLD})^4] \dots\dots\dots [3.1]$$

$$q'' = VI \cos \phi / A_{COR} \dots\dots\dots [3.2]$$

$$h = [q'' - q_r''] / [T_{COR} - T_{COLD}] \dots\dots\dots [3.3]$$

$$Nu_L = h \cdot L / K \dots\dots\dots [3.4]$$

$$Ra_L = \frac{g \cdot \beta \cdot [T_{COR} - T_{COLD}] \cdot L^3}{\nu \cdot \alpha} \dots\dots\dots [3.5]$$

All properties of air were evaluated at film temp.

$$T_f = [T_{COR} + T_{COLD}] / 2.$$

CHAPTER-4

EXPERIMENTAL SET-UP

4.1 General Description of the Set-up:

Figures 4.1[a & b] and 4.2[a & b] represent schematically the experimental setup and the test section respectively. The angle of inclination of the test section was varied by an alignment plate in the range, 0° to 90° at a step of 15° . The air gap depth was varied by changing the position of the cold plate in relation to the hot plate from 49.5mm to 99.5mm. Experimental hot plate assembly was heated by the main electric heater sandwiched in between the hot corrugated plates. The guard heater assemblies were also heated by the guard electric heaters sandwiched in between the inner and the outer wooden strips. The cold flat plate was placed above the hot corrugated assembly by four vertical clamps, fixed on the upper guard heater. This cold plate assembly was cooled by passing a steady flow of cooling water from the overhead tank. A digital milli-voltmeter was used to measure the temperature of the test section of the hot plate and cold plate through thermocouple no. 1 to 9 and 39 to 41 respectively. It was also used to monitor the surface temperatures of the guard heater assemblies through 27 Chromel-Alumel thermocouples. To obtain the total heat input to the experimental test section of the hot plate, the input current to the corresponding heater [main heater] was measured by a precision ammeter. The voltage across the main heater was measured by a precision digital voltmeter.

4.2 The Test Section:

The test section consisted of

- a. The hot plate assembly
- b. The outer guard heater assembly
- c. The cold plate assembly
- d. The alignment plate and supporting frame.

4.2.1 The Hot Plate Assembly:

The hot plate assembly was made of two sets of G.I. sheets, each 456mm X 534mm, one with rectangular and another with trapezoidal corrugation. An asbestos cloth of 12mm thick was placed on the upper side of the lower corrugated plate to insulate it electrically from the electrical heaters placed on the asbestos cloth. Another asbestos cloth was placed over the heaters to make the two corrugated plate well insulated from the sandwiched electrical heaters. There were three heaters on the hot plate assembly. One was used to heat the experimental hot plate section and the other two heaters were used as end and side guard heaters around the test section. These guard heaters were provided to reduce the end conduction losses from the experimental hot plate to a minimum level. For this purpose these guard heater sections were separated from the experimental hot plate section by cutting the top corrugated plate into five pieces forming separate guard heater sections and the central experimental hot plate section. The experimental hot plate section was 152mm x 230mm; 152mm across the corrugation and 230mm along the corrugation. There were two

troughs, one full crest and two half crests in the experimental hot plate section.

The end and side guard heater sections were 152mm wide on all the sides of the experimental hot plate section. Thus the over all dimension of the hot plate assembly was 456mm x 534mm. This hot plate assembly was placed inside a rectangular ring 483mm X 560mm. The rectangular ring was made of 76mm wide and 19.05mm thick wooden strip. Details of the hot plate assembly have been shown in figures 4.3a and 4.3b and details of design and fabrication process of the heaters are given in the Appendix-A.

4.2.2 The Outer Guard Heater Assembly:

The outer guard heater assembly was used to isolate the test hot plate section thermally from the surrounding surfaces except from the top. This assembly mainly consisted of upper guard heater ring and lower guard heater box. By varying the heat input to the outer guard heater assembly the temperature difference between the test hot plate and its surrounding surfaces could be made insignificant. Under this condition all the heat input to the experimental hot plate section would be transferred by conduction, convection and radiation to the cold flat plate only which was placed above the hot plate.

4.2.2a The Upper Outer Guard Heater Ring:

The upper outer guard heater ring was a rectangular shaped structure

which consisted of the following sections:

- a. Inner wooden rectangular ring
- b. Inner asbestos rectangular ring
- c. Outer asbestos rectangular ring
- d. Outer wooden rectangular ring

The test section was placed inside this guard heater. The outer wooden ring having outside dimensions of 579mm x 660mm was made of 12mm thick wooden strip. The inside dimension of the inner wooden ring was 483mm x 564mm. The inner and outer wooden rings were held together with a 579mm X 660mm outside dimension, 12mm thick and 48mm wide wooden annular ring at the top of the upper guard heater assembly. The height of the upper guard heater assembly was 139mm. The inner and outer asbestos rectangular rings were fitted inside the annular space between the outer and inner rectangular wooden rings. The outer asbestos ring 127mm wide was fitted inside the outer wooden ring and the inner asbestos ring of the same width was fitted outside the inner wooden ring. The heater made by warapping 29 SWG nichrome wire on the mica sheet was sandwiched in between the inner and the outer asbestos ring. The capacity of the heater was 105 Watt. A cross section of the upper outer guard heater assembly is shown in figure 4.4.

4.2.2b The Lower Outer Guard Heater Box:

The lower outer guard heater box was rectangular in shape and consisted of the following sections:

- a. Inner wooden rectangular box
- b. Inner asbestos rectangular box
- c. Outer asbestos rectangular box
- d. Outer wooden rectangular box.

The outer wooden box having outside dimension of 579mm X 660mm X 76mm was made of 12mm thick wooden strip. The outside dimension of the inner wooden box was 507mm X 588mm X 40mm. The outer asbestos box having dimension of 555mm X 636mm X 64mm was fitted cover the inner surface of the outer wooden rectangular box and the inner asbestos box having dimension of 531mm X 612mm X 52mm was fitted over the outer surface of the inner wooden box i.e. over the inner surface of the outer asbestos box. Two separate Nichrome heaters were sandwiched in between the inner and the outer asbestos rings, one was lower bottom guard heater and the other was lower side guard heater. A cross section of the lower outer guard heater assembly is shown in figure 4.5.

4.2.3 The Cold Plate Assembly:

The cold plate assembly was a sealed 550mm X 470mm X 19.05mm rectangular box made of 3.175mm thick mild steel plates painted with black plastic paint. Provision of water circulation was made from the reserve tank through inlet and outlet connections. The outlet and inlet connections were placed on the upper (outer) surface of this box. The flat bottom surface of this assembly, facing the corrugated plate was acting as a receiver of heat that was convected and radiated from the hot corrugated

plate. The whole cold plate assembly was placed above the hot corrugated plate and held by the vertical clamps, fixed on the upper outer guard heater assembly. These clamps had arrangements to change the spacing between the hot corrugated plate and the cold flat plate from 19.5mm to 109.5mm in steps of 10mm. The cold plate assembly is shown in figure 4.6.

4.2.4 The Alignment Plate and Supporting Frame:

The hot and the cold plate assembly with the guard heaters was placed inside of a rectangular frame made of 38.1mm X 38.1mm X 6.35mm mild steel angle on the two side supports of this frame, each of them is attached with the plate assembly by means of two bolts. Another two bolts were fixed at the centre of the two opposite longitudinal sides of the frame and passed through the holes of the side supports so that the frame and the plate assembly with the guard heaters could swivel about a horizontal axis i.e. the lateral axis of the hot plate through these bolts. The rectangular frame is shown in figure 4.7.

Two circular disc of mild steel having diameter of 102mm and thickness of 6.35mm namely as alignment plates were connected at the centre of the two opposite lateral sides of the rectangular frame by means of two screws passed through 6.5mm diameter holes located on each disc at 40mm apart and the holes of the two 57mm X 57mm hanging side supports made of 6.35mm thick mild steel sheet that were welded with the supporting frame at its centre. These discs had also several holes of diameter 6.5mm along a circle of radius 38mm. The angle of inclination of the test section was

varied by means of these holes by changing the inclination angle from 0° to 90° in steps of 15° . One of the alignment plate is shown in figure 4.8.

A supporting stand consisting of two pairs of legs 915mm apart connected by a flat mild steel bar. The height of this stand was 460mm. The rectangular frame along with the two alignment plates was connected with this stand at the top centre of its legs by means of two bolts passed through the 16mm diameter central holes of the alignment plates and the two holes located at the centre of the two lateral sides of the frame so that the frame and the plate assembly with the guard heaters could also swivel about a horizontal axis i.e. the longitudinal axis of the hot plate. The connection between the rectangular frame and the supporting stand is shown in figure 4.9.

The angle of inclination of the test section of the hot corrugated plate could set at a desire value by means of two screws passed through the corresponding peripheral holes of diameter 6.5mm of the alignment plates as mentioned above and the two holes 76mm apart located at the top of the two legs of the supporting stand. The supporting stand is shown in figure 4.10.

4.3 The Reserve Water Tank:

The reserve water tank was really an overhead tank - a simple cylindrical drum made of galvanized iron sheet. The water level in the tank was kept constant during experiments by controlling the water flow using the inlet

and outlet valves of this tank. The cold plate assembly was cooled by passing a steady flow of cooling water from this tank.

4.4 Instrumentation:

In the present investigation provisions were made for measuring angle of inclination, air gap between the hot and the cold plates and the temperature at different points of the experimental setup. The details of these instrumentation and measurements are presented in the next chapter.

CHAPTER - 5
EXPERIMENTAL MEASUREMENTS
AND
TEST PROCEDURE

5.1 Temperature Measurement:

Temperatures of the different sections of the experimental set-up were measured by forty-one 36 SWG Chromel-Alumel thermocouples connected to a calibrated millivoltmeter of DM-6018C having a range of -50°C to 750°C [for K type] to show the temperature directly through two selector switches [CROPIVCO] each having 24 points. Out of them nine thermocouples no. 1 to 9, were fixed on the bottom surface of the test section of the hot corrugated plate and five thermocouples no. 37 to 41, were fixed on the bottom surface of the cold plate facing the corrugated plate and the rest were fixed on the guard heating sections. The position of thermocouples are shown in figures 5.1 to 5.5. The thermocouples were calibrated in a constant temperature water bath for 31°C to 100°C . There was a maximum variation of 2.25% between the actual and the standard reading within the working range of the experiment. The calibration curve for thermocouple no. 5 is shown in fig.5.6 as an illustration.

The temperature of the exposed top surface of the experimental hot corrugated plate [T_{COR}] was determined after necessary conduction correction. Appendix B contains the outline of the procedure for calculating the conduction correction.

5.2 Heat Flux Measurement:

Heat flux from the hot corrugated plate was calculated by measuring the current and the voltage supply of the main heater since the heat flux is equal to the heat input [power] to the test section of the hot plate divided by the projected surface area of heat transfer of the same plate.

The voltmeter of model LEADER LDM-853A was employed to measure the voltage across the main heater which supplied the necessary heat to the test section of the hot plate. The voltmeter had the range of 0.2-1000V with an accuracy of + 0.3%.

The precision ammeter of model WESTING HOUSE 93623E was employed to measure the current supplied to the test section of the hot plate. This ammeter had the range of 0 to 2.5 amps. and the accuracy of $\pm 0.1\%$.

5.3 Test Procedure

Two specimens, one trapezoidal corrugated plate and the other rectangular corrugated plate were employed. For both the cases the variables measured were temperature difference [ΔT], angles of inclination of the air layer [θ] and the air gaps [L]. The experimental fluid was air at atmospheric pressure. Experiments were carried out under steady state, first on trapezoidal corrugated plate and then on

rectangular corrugated plate. The overall test procedure was as follows:

- a. Before starting the experiment the room temperature was recorded for selecting T_{COR} to maintain a steady ΔT [say, $\Delta T = T_{COR} - T_{COLD} = 10^{\circ}C$] since $T_{COLD} \approx T_{ROOM}$
- b. The spacing between the hot corrugated plate and the cold flat plate was measured as the distance between the bottom surface of the cold plate and the mid section of the troughs and crest of the corrugated plate [Fig. 4.2a & 4.2b]. The spacing L i.e. air gap of $L=99.5mm$ was kept by fixing the cold plate to the appropriate holes of the clamps fixed on the upper outer guard heater assembly.
- c. Then the rig was aligned to horizontal position for angle of inclination $\theta = 0^{\circ}$.
- d. Next all the heater circuits were switched on and at the same time, the water line of the cold plate was opened.
- e. By regulating the Variac of each heater, the temperatures, monitored by thermocouples no. 1 to 36, connected to the test section and the guard heater sections, were made equal. The cold plate was also maintained at the room temperature by controlling the water flow through it to maintain ΔT constant during a particular test run.

- f. From the readings of thermocouples no. 1 to 9 and 37 to 41 temperatures of the hot plate and the cold plate respectively were recorded. Readings of ammeter and voltmeter connected to the test section of the hot plate was also noted.
- g. All the operations so far performed in steps [e] and [f] were repeated for inclination angles $\theta = 30^\circ, 45^\circ$ and 75° keeping air gap, $L = 99.5\text{mm}$ constant throughout.
- h. By changing the air gap, [L] to the other values of 89.5mm, 79.5mm, 69.5mm, 59.5mm and 49.5mm operations from step [c] to step [g] were repeated.
- i. Next for other values of ΔT i.e. for 18°C , 26°C and 35°C all the operations described in steps [b] to [h] were repeated.

Thus ninety six [96] sets of data for each corrugation were recorded.

The ranges of different parameters in the investigations were as follows:

For Trapezoidal Corrugation:

Raleigh Number, $Ra_L = 9.8 \times 10^4$ to 2.29×10^6

Heat flux, $q'' = 12$ to 111 W/m^2

Temperature difference
 between hot plate and Cold plate,
 $\Delta T = 10^{\circ}\text{C}$ to 35°C

Temperature of the
 hot plate,
 $T_{\text{COR}} = 36^{\circ}\text{C}$ to 65°C

Inclination angle, $\theta = 0^{\circ}$ to 75°

Air gap,
 $L = 49.5\text{mm}$ to 99.5mm .

For Rectangular Corrugation:

Raleigh Number, $Ra_L = 9.8 \times 10^4$ to 2.29×10^6

Heat flux, $q'' = 10$ to 102 W/m^2

Temperature difference
 between hot plate and Cold
 plate,
 $\Delta T = 10^{\circ}\text{C}$ to 35°C

Temperature of the hot plate,
 $T_{\text{COR}} = 36^{\circ}\text{C}$ to 65°C

Inclination angle,
 $\theta = 0^{\circ}$ to 75°

Air gap,
 $L = 49.5\text{mm}$ to 99.5mm .

5.4 Reduction of Data:

For calculating convective heat transfer co-efficient, convective heat flux was required. But the heat flux, q'' obtained from the readings of voltmeter and ammeter was the combination of convective and radiative heat flux. So in calculating convective heat flux, the radiative heat flux was deducted from the measured heat flux. To find out the radiative heat Stefan-Boltzman equation for grey surface [equation 3.1] was used. In appendix-C, the outline for obtaining the emissivity of the test section of the hot corrugated plate has been given.

CHAPTER 6

RESULTS AND DISCUSSION

An experimental investigation of steady state natural convection heat transfer from a hot corrugated plate through air to a cold flat plate placed parallel to the hot plate and the assembly being inclined at various angles with respect to horizontal was carried out for finite rectangular enclosure having adiabatic surroundings. Two types of corrugation were employed - trapezoidal and rectangular having same height of corrugation. The experiments covered a range of Rayleigh number 9.84×10^4 to 2.29×10^6 and angle of inclination of 0° to 75° .

The temperature distribution over the experimental hot corrugated plate both for trapezoidal and rectangular corrugation and for cold plate for different aspect ratios [A] and different inclination angles [θ] was found to be such that an isothermal hot and cold surfaces was easily assumed. The temperature distribution for a typical illustration for the hot and the cold plate is shown in figures. 6.1 & 6.2 and figures 6.3 & 6.4 respectively.

To study the effect of aspect ratio on heat transfer rate across rectangular regions for various angles of inclination [θ] and ΔT for both types of corrugation, graphs 6.5 to 6.8 were plotted for h vs. A for a particular θ with different values of ΔT and graphs 6.9 to 6.12 for h vs. A for a particular ΔT with different values of θ . From graphs 6.5 to 6.8 it is observed that for both types of corrugation "h" increases with the increase of aspect ratio for every ΔT . But the limiting value of aspect ratio upto which, "h" increases are found to be different for different ΔT and for different corrugations. From graphs 6.9

to 6.12 it is observed that for both $0^\circ \leq \theta_t \leq 75^\circ$ and $0^\circ \leq \theta_r \leq 75^\circ$ heat transfer co-efficients increase with the increase of aspect ratio upto a certain value of "A". But this limiting value of aspect ratio is found to be different for different inclination angle $[\theta]$ for trapezoidal as well as rectangular corrugations for different temperature difference $[\Delta T]$. The values of h are found to be maximum for aspect ratios between 4 to 5.5 for both trapezoidal corrugation and for rectangular corrugation. The reason of such occurrence is that the increase of gap between the hot corrugated plate and the cold flat plate increases the aspect ratio and permits better mixing of the fluid leading to enhancement of heat transfer rate. But this enhancement of heat transfer rate has got a certain limit and beyond this limit heat transfer co-efficients are found to decrease with the increase of aspect ratio. Because beyond this limiting values of "A" the convective currents appear to be weak to reach the cold flat plate and transfer less heat after crossing a larger distance. From these figures it is also clear that at a particular temperature difference for both types of corrugation "h" decreases with the increase of angle of inclination $[\theta]$ for all aspect ratios. The physical reason as given above is also applicable here. This is also due to the fact that the Rayleigh number for breaking down of unstable situation in order to set convective motion within the fluid increases with the increase of angle of inclination i.e., critical Rayleigh number for horizontal fluid layer is equal to $\cos\theta$ times of critical Rayleigh number for inclined fluid layer.

The effect of temperature potential i.e. the temperature difference between the hot corrugated plate and cold flat plate on heat transfer rate for various angles of inclination $[\theta]$ and aspect ratios $[A]$ for both types of corrugation, graphs 6.13 to 6.18 were plotted for h vs. ΔT for a particular "A" with different values of

θ. From these graphs it is clear that average heat transfer coefficient increases more or less linearly with the increasing of temperature potential. Because for higher value of ΔT heat fluxes are also higher which enhance heat transfer i.e. increase convective heat transfer coefficient for both types of corrugation.

Results are presented in terms of Nusselt number and angle of inclination for a particular aspect ratio [A] and Rayleigh numbers [Ra_L] in figures 6.19 to 6.24 for trapezoidal corrugation and figures. 6.25 to 6.30 for rectangular corrugation. From these figures it is clear that at a constant aspect ratio and Rayleigh number, Nusselt number decreases with the increase of angle of inclination for both types of corrugation. Nusselt number is also found to be maximum at $\theta = 0^\circ$ [horizontal] for all Rayleigh numbers. This is due to the fact that as angle of inclination [θ] increases from 0° the hydrodynamic instabilities begin to interfere with the motion induced by thermal instabilities. But thermal instabilities are dominant at lower angles of inclination.

Figures 6.31 to 6.36 show the relationship between the Nusselt number and $Ra_L \cos\theta$ for different values of aspect ratios and angles of inclination [θ]. From these figures it is observed that for both types of corrugation Nusselt number increases with the increasing of Rayleigh number at a particular aspect ratio and angle of inclination. The reason for such behaviour is due to the fact that at a constant aspect ratio and angle of inclination, Rayleigh number increases with the increasing of temperature potential [ΔT]. Again increase in ΔT increases the heat flux which inturns increases convective heat transfer co-efficient leading to the increase of Nu_L .

Comparison:

Figures 6.5 to 6.12 show the effect of aspect ratio on average heat transfer coefficient for different ΔT and angles of inclination for both trapezoidal and rectangular corrugation. The nature of variation of the convective heat transfer coefficient with different aspect ratios and angle of inclinations for both type configurations is more or less same. The convective heat transfer coefficients for trapezoidal corrugation are higher than that for rectangular corrugation for different values of ΔT and angles of inclination for every aspect ratio that was covered in this experimental investigation by a maximum of 6%. The enhanced values of convective heat transfer coefficients for trapezoidal corrugation than rectangular corrugation for different values of ΔT and θ are to the geometry of corrugation. As for example, at $\theta = 0^\circ$ the rectangular corrugated surface becomes partly horizontal and partly vertical while the trapezoidal corrugated surface becomes partly horizontal and partly inclined. The trapezoidal corrugated surface having the same amplitude gave better heat transfer performance than rectangular corrugated surface because better clearance between the adjacent ribs of trapezoidal corrugation may permit better clearance for inflow and outflow of convecting fluid.

Figures 6.37 and 6.38 give the comparison of Nusselt number of the present study with the Nusselt number of the works of Elsherbiny [1977] and Kabir [1988]. For the same aspect ratio and for lower Rayleigh number $Ra_L = 0.40 \times 10^6$, the Nusselt numbers of the trapezoidal and rectangular corrugations [present study] are lower than Elsherbiny's values by an average of 34% and 38% respectively for all values of θ . For the same Rayleigh number, the Nusselt

numbers of the trapezoidal and rectangular corrugations [present study] are also found lower than Kabir's values by an average of 15% and 18% respectively for all angles of inclination. But the differences are lower at higher Rayleigh number as for example at $Ra_L = 1.0 \times 10^6$, the present investigations with trapezoidal and rectangular corrugations show average decrease of 29% and 32% in the values of Nusselt number respectively from those found by Elsherbiny while the values are 12% and 16% when compared with Kabir's works.

The experimental data of Elsherbiny and Kabir have been plotted along with the present work in figure 6.39 for $A = 2.6$ and figure 6.40 for $A = 4.17$. The values of Nusselt number for aspect ratio of 4.17 are greater than those for $A = 2.6$ for the present study as well for the works of Kabir and Elsherbiny. The dependency of Nu_L on $Ra_L \cos\theta$ for different works as shown in these figures is given below:

For lower aspect ratio, $A = 2.60$

References:

$$Nu_L \propto [Ra_L \cos\theta]^{0.3249}; \quad \text{ELSHERBINY [VEE-CORRUGATION]}$$

$$Nu_L \propto [Ra_L \cos\theta]^{0.4807}; \quad \text{KABIR [SINUSOIDAL CORRUGATION]}$$

Present Study:

$$Nu_L \propto [Ra_L \cos\theta]^{0.4878}; \quad \text{TRAPEZOIDAL CORRUGATION}$$

$$Nu_L \propto [Ra_L \cos\theta]^{0.5169}; \quad \text{RECTANGULAR CORRUGATION}$$

For higher aspect ratio, $A = 4.17$

References:

$$Nu_L \propto [Ra_L \cos\theta]^{0.3773}; \quad \text{ELSHERBINY [VEE-CORRUGATION]}$$

$$Nu_L \propto [Ra_L \cos\theta]^{0.5168}; \quad \text{KABIR [SINUSOIDAL CORRUGATION]}$$

Present Study:

$$Nu_L \propto [Ra_L \cos\theta]^{0.5283}; \text{ TRAPEZOIDAL CORRUGATION}$$

$$Nu_L \propto [Ra_L \cos\theta]^{0.5467}; \text{ RECTANGULAR CORRUGATION}$$

The correlations for both types of corrugation arrived from the present experimental data as shown in appendix-D are given by the following equations:

$$Nu_L = 0.0112 [Ra_L \cos\theta]^{0.521} [A]^{-0.4546}, \quad \text{[TRAPEZOIDAL CORRUGATION]}$$

$$Nu_L = 0.0102 [Ra_L \cos\theta]^{0.530} [A]^{-0.4923}, \quad \text{[RECTANGULAR CORRUGATION]}$$

Where, $9.80 \times 10^4 \leq Ra_L \leq 2.29 \times 10^6$

$$2.60 \leq A \leq 5.22$$

$$0^\circ \leq \theta \leq 75^\circ$$

The above correlating equations for trapezoidal and rectangular corrugations correlate all most all the data to within $\pm 15\%$.

CHAPTER - 7

CONCLUSIONS AND RECOMMENDATIONS

This chapter presents the conclusions drawn from the experimental investigation of natural convection from two types of hot corrugated namely trapezoidal and rectangular plate to a cold flat plate. The recommendations for the extension of the present study are also included in this chapter.

7.1 Conclusions:

- [1] For both trapezoidal and rectangular corrugation the natural convective heat transfer co-efficient [h] is found to be dependent on temperature potential [ΔT], angle of inclination [θ] and aspect ratio [A].
- [2] The average natural convective heat transfer co-efficient for trapezoidal and rectangular corrugations is found increase with the increase of aspect ratio upto a certain limit and then has a tendency to decrease with further increase of aspect ratio. The maximum value of "h" occurs for both types of corrugation for aspect ratio between 4.0 to 5.5.
- [3] The dependency of average natural convective heat transfer coefficient [h] on temperature potential [ΔT] is found more or less linear for both types of corrugation.
- [4] For both types of corrugation the convective heat transfer co-efficient decreases with the increase of angle of inclination [θ].

- [5] The maximum values of average natural convective heat transfer coefficient are experimentally found to be $3.051 \text{ w/m}^2 \text{ }^\circ\text{C}$ and $2.9 \text{ w/m}^2 \text{ }^\circ\text{C}$ for trapezoidal and rectangular corrugations respectively.
- [6] The average Nusselt number $[\text{Nu}_L]$ decreases with the increase of angle of inclination. The maximum values of average Nusselt number are experimentally found to be 10.41 and 9.66 for trapezoidal and rectangular corrugations respectively.
- [7] The linear relationship between the Nusselt number and $\text{Ra}_L \cos\theta$ for all aspect ratios and for both types of corrugation is found in the logarithmic plot of Nu_L Vs. $\text{Ra}_L \cos\theta$.
- [8] The average natural convective heat transfer co-efficient can be calculated by using the following correlating equations:

$$\text{Nu}_L = 0.0112 [\text{Ra}_L \cos\theta]^{0.521} [\text{A}]^{-0.4546}; \quad [\text{TRAPEZOIDAL CORRUGATION}]$$

$$\text{Nu}_L = 0.0102 [\text{Ra}_L \cos\theta]^{0.530} [\text{A}]^{-0.4963}; \quad [\text{RECTANGULAR CORRUGATION}]$$

Where,

$$9.80 \times 10^4 \leq \text{Ra}_L \leq 2.29 \times 10^6$$

$$2.60 \leq \text{A} \leq 5.22$$

$$0^\circ \leq \theta \leq 75^\circ$$

7.2 Recommendations:

- [1] An experiment can be carried out with higher aspect ratio [$A > 5.22$] to get the effect of it on heat transfer rate & for conforming the dependency of natural convective heat transfer coefficient on aspect ratio.
- [2] An experiment can also be done with trapezoidal and rectangular corrugated plates of different pitches and amplitudes to get the effect of geometry on heat transfer rate.
- [3] Further investigation can be carried out with hot plate of square corrugation.
- [4] The effect of Prandtl number on the natural convection heat transfer can be investigated by performing the similar experiment with different convective fluid e.g., water, silicon oil, etc.
- [5] A comprehensive investigation of natural convection heat transfer of the similar type may be carried out over a wider range of Rayleigh number.
- [6] The entire investigation can be carried out by interferometric techniques for conforming the flow pattern of the convective fluid within the region.

REFERENCES

- Arnold, J.N., Catton, I., and Edwards, D.K., 1976, "Experimental Investigation of Natural Convection in Inclined Rectangular Regions of differing Aspect Ratios", *J. Heat Transfer*, Vol. 98, pp. 67-71.
- Ayyaswamy, P.S., and Catton, I., 1974, "Natural Convection Flow in a Finite Rectangular Slot Arbitrarily Oriented with Respect to the Gravity Vector," *International Journal of Heat and Mass Transfer*, Vol. 17, pp. 173-184.
- Ayyaswamy, P.S., and Catton, I., 1973, "The Boundary Layer regime for Natural Convection in a differentially Heated, Tilted Rectangular Cavity", *J. Heat Transfer*, *Trans. ASME Series C*, Vol. 95, pp. 543 - 545.
- Benard, H., 1900, *Rev. Gen. Sci. Pures Appl.* vol. 11, pp.1261-1271.
- Buchberg, H., Catton, I., and Edwards, D.K., 1976, "Natural Convection in Enclosed Spaces; A Review of Application to Solar Energy Collection", *J. Heat Transfer*, Vol. 98, No. 2, pp. 182-188.
- Burmeister, L.C., 1983, "Convective Heat Transfer", John Wiley and Sons, Inc.
- Channrasekhar, S., 1961, "Hydrodynamic and Hydromagnetic stability", Clarendon Press, Oxford.
- Chinnappa, J.C.V., 1970, " Free convection in Air Between a 60° Vee-Corrugated Plate and Flat Plate", *International Journal of Heat and Mass Transfer*, Vol. 13, pp. 117-123.
- Chu, T.Y., and Goldstein, R.J., 1973, "Turbulent Convection in a Horizontal Layer of Water", *Journal of Fluid Mechanics*, Vol. 60, pp. 141-159.
- Chu, T.Y., and Goldstein, R.J., 1969, "Thermal Convection in a Horizontal Layer of Air", *Prog. Heat and Mass Transfer*, Vol. 2, pp. 55-75.
- Close, D.J., Dunkle, R.V., and Robeson, K.A., 1968, "Design and Performance of a Thermal Storage Air-Conditioning Systems", *Mech. Chem. Eng. Trans. Inst. Engrs. Aust.*, Vol. 4, pp. 45.
- Close, D.J., 1963, "Solar Air Heaters for Low and Moderate Temperature Applications", *Solar Energy*, Vol. 7, No. 3, pp.117-124.
- David P. Dewitt, and Frank P. Incropera, 1985 " Introduction to Heat Transfer".
- De Graff, J.G.A., and Van der Held, F.E.M., 1953, "The Relation Between the Heat Transfer and the Convection Phenomena in Enclosed Plane Air layers", *Appl. Sci. Res. A*, Vol. 3, pp. 393-409.

- Difederico, I., and Foraboschi, F.P., 1966, " A Contribution to the Study of Free Convection in a Fluid Layer Heated from Below", International Journal of Heat and Mass Transfer, Vol. 9, pp. 1351-1360.
- Dropkin, D., and Somerscales, E., 1966, "Experimental Investigation of the Temperature Distribution in a Horizontal Layer of Fluid heated from Below", International Journal of Heat & Mass Transfer, Vol.9, pp. 1189-1204.
- Dropkin, D., and Somerscales, E., 1965, " Heat Transfer by Natural Convection in Liquids Confined by Two Parallel Plates which are Inclined at Various Angles with respect to the Horizontal", Journal of Heat Transfer, Series C, vol. 87, pp. 77-84.
- Dropkin, D., and Globe, S., E., 1959, "Natural convection Heat Transfer in Liquids Confined by Two Horizontal Plates and Heated from Below", Journal of Heat Transfer, Vol. 81, Series C, pp. 24-28.
- Eckert, E.R.G., and Carlson, W.O., 1969, " Natural Convection in an air Layer Enclosed Between Two Vertical Plates with Different Temperatures", International Journal of Heat and Mass Transfer, Vol. 2, pp. 102-120.
- Elsherbiny, S.M., Hollands, K.G.T., and Raithby, G.D., 1967, "Free Convection Across Inclined Air Layers with one Surface Vee-Corrugated", in Heat Transfer Solar Energy Systems, Howell, J.R., and Min, T., (eds.), American Society of Mechanical Engineerings, New York.
- Emery, A., Chu, N.C., 1969, " Heat Transfer Across Vertical Layers", ASME Journal of Heat Transfer, Vol. 91, pp. 391.
- Gryzagoridis, J., 1971, "Natural Convection from a Vertical Plate in Low Grashof Number Range", International Journal of Heat & Mass Transfer, Vol. 14, pp. 162-164.
- Hart, J., 1971, "Stability of the Flow in a Differentially Heated Inclined Box", Journal of Fluid Mechanics, Vol. 47, pp. 547-576.
- Herring, J.R., 1965, "Investigation of Problems in Thermal Convection", Journal Atmos. Sci. Vol. 20, pp. 325.
- Herring, J.R., 1964, "Investigation of Problems in Thermal Convection: Rigid Boundaries", Journal Atmos. Sci. Vol. 21, pp. 227.
- Hollands, K.G.T., Unny, T.E., Raithby, G.D. and Konicek, L., 1976, "Free Convective Heat Transfer Across Inclined Air Layers", Journal of Heat Transfer, Vol. 98, No. 2, pp. 189-193.
- Hollands, K.G.T., Raithby G.D. and Konicek, L., 1975, "Correlation Equations for Free Convection Heat Transfer in Horizontal Layers of Air and Water", International Journal of Heat and Mass Transfer, Vol. 18, P. 879-884.

- Hollands, K.G.T., and Konicek, L., 1973, "Experimental Study of the Stability of Differentially Heated Inclined Air Layers", *International Journal of Heat and Mass Transfer*, Vol. 16, pp. 1467-1476.
- Hollands, K.G.T., 1965, "Convective Heat Transport Between Rigid Horizontal Boundaries after Instability", *Physics Fluids*, Vol. 8, pp. 389-390.
- Hollands, K.G.T., 1963, "Directional Selectivity, Emittance and Absorptance Properties of Vee-Corrugated Surfaces", *Solar Energy*, vol. 7, pp. 108-116.
- Holman, J.P., 1981, "Heat Transfer", Fifth Edition, MacGraw-Hill Book Company.
- Jakob, M., 1949, "Heat Transfer", Vol.1, John Wiley and Sons, Inc. N.Y.
- Jakob, M., 1946, *Trans. ASME*, Vol. 68, pp. 189.
- Jeffreys, H., 1928, "Some Cases of Instability in Fluid Motion", *Proc. Roy. Soc. (London)*, (A), Vol. 118, pp. 195.
- Kabir Humayun, 1988, "An Experimental Investigation of Natural Convection Heat Transfer from a Hot Corrugated Plate to a Flat Plate", M.Sc. Engg. (Mechanical) Thesis, BUET.
- Koschmieder, E.L., and Pallas, S.G., 1974, "Heat Transfer Through a Shallow Horizontal Convecting Fluid Layer", *International Journal of Heat and Mass Transfer*, Vol.7, .991-1002.
- Low, A.R., 1929, "On the Criterion for Stability of a Layer of Viscous Fluid Heated from Below", *Proc. Roy. Soc. (London)*, (A), Vol. 125, pp. 180.
- Malkus, W.V.R., 1963, "Outline of a Theory of Turbulent Convection", *Theory and Fundamental Research in Heat Transfer*, edited by J.A. Clark, Pergamon Press, New York, pp. 203-212.
- Mull W., and Reiher H., 1930, "Experimental Investigation on Free Convection Heat Transfer in Horizontal Air Layers", *Gesundh-Ing.* 28(1), pp. 1-28.
- McAdams, W.H., 1949, "Heat Transmission", Third edition, MacGraw-Hill Book Company, Inc.
- Ostrach, S., 1957, "Convective Phenomena in Fluids Heated from Below", *Trans. ASME*, Vol. 79, pp. 299-305.
- O'Toole, J.L., and Siveston, P.L., 1961, "Correlations of Convective Heat Transfer in Confined Horizontal Layers", *A.I.Ch.E. Chem. Engrg. Progr. Symp. Ser.* Vol. 57(32), pp. 81-86.

- Ozoe, H., Sayma, H., and Churchill, S.W., 1975, "Natural Convection in an Inclined Rectangular Channel at Various Aspect Ratios and Angles: Experimental Measurements", International Journal of Heat and Mass Transfer, Vol. 18, pp.1425-1431.
- Randall, K.R. et al. "Interferometric Investigation of Convection in Slat-Flat Plate and Vee-Corrugated Solar Collectors," Solar Energy International Progress, pp.447-460.
- Rayleigh, L., 1916, "On Convection Currents in a Horizontal Layer of Fluid when the Higher Temperature is on the Underside", Phil. Mag. Vol. 32, pp.529.
- Rossby, H.T., 1969, " A Study of Benard Convection with and without Rotation", Journal of Fluid Mechanics, Vol. 36(2), pp.309-335.
- Schluter, A., Lortz, D., Busse, F., 1965, "On the Stability of Steady Finite Amplitude Convection", Journal of Fluid Mechanics, Vol. 23, pp.129-144.
- Schmidt, R.J., and Silveston, P.L., O.A., 1959, "Natural Convection in Horizontal Liquid Layers", Chem. Engrg. Progr. symp. Ser. 29, Vol. 55, pp.163-169.
- Schmidt, R.J., and Saunders, O.A., 1938, "On the Motion of Fluid Heated from Below", Proc. Roy. Soc. (London)(A), Vol. 165, pp. 216-218.
- Sterling, C.V., and Scriven, L.E., 1964, Journal of Fluid Mechanics, Vol. 19, pp.321.
- Thomson, J.J., 1882, Proc. Glasgow Phil. Soc., Vol. 13, pp.464.

APPENDIX - A
DESIGN OF THE TEST RIG

Design of the test rig had the following two aspects:

- [1] Heat Transfer Calculation
- [2] Electrical Heater Design

A1 Heat Transfer Calculations:

Heat transfer calculations included estimation of the steady state heat transfer rates from different exposed heated surfaces of the experimental rig under different design operating conditions as given below:

- [1] Calculation of rate of heat transfer from the hot corrugated plate to the cold flat plate by convection and radiation.
- [2] Calculation of rate of heat transfer from the exposed surfaces of the upper guard heater assembly to the ambient air by convection and radiation.
- [3] Calculation of rate of heat transfer from the exposed surfaces of the lower guards heater assembly to the ambient air by convection and radiation.

The above three items were estimated for two extreme design temperatures namely the maximum and minimum design temperatures. From the previous available experimental data it was observed that maximum heat transfer will occur when the rig is horizontal, and mean plate spacing is minimum while the test runs under maximum design temperature. Similarly minimum heat transfer will occur when the rig is vertical, mean plate spacing is maximum while the test runs under minimum design temperature.

A1.1 Calculation of Rate of Heat Transfer from the Hot Corrugated Plate to the Cold Flat Plate:

Heat transfer from the hot corrugated plate to the cold flat plate takes place by two different modes; natural convection and radiation. For design purpose it was assumed that the corrugated plate was a flat one. For computing heat transfer co-efficient approximately the following correlating equations by Jakob [1949] for horizontal [fig.A.1] and vertical [fig.A.2] positions of the test rig heated from below were used .

For horizontal position:

$$Nu_L = 0.195 [Gr_L]^{1/4}, \quad 10^4 < Gr_L < 4 \times 10^5 \dots\dots\dots [1]$$

$$Nu_L = 0.068 [Gr_L]^{1/3}, \quad Gr_L > 4 \times 10^5 \dots\dots\dots [2]$$

For vertical position:

$$Nu_L = 1, \quad Gr_L < 2000 \dots\dots\dots [3]$$

$$Nu_L = 0.18 [Gr_L]^{1/4} [H/L]^{-1/9}, \quad 2 \times 10^3 < Gr_L < 2 \times 10^5 \dots [4]$$

$$Nu_L = 0.065 [Gr_L]^{1/3} [H/L]^{-1/9}, \quad 2 \times 10^5 < Gr_L < 11 \times 10^6 \dots [5]$$

After knowing Nu_L , convective heat transfer co-efficient was found by using the following equation:

$$h = Nu_L \cdot K / L \dots\dots\dots [6]$$

And finally convective heat transfer rate was calculated by using the following equation:

$$q_{conv} = A_{COR} \cdot h \cdot [T_{COR} - T_{COLD}] \dots\dots\dots [7]$$

For estimating the radiation heat transfer rate following assumptions were made:

- Interior surfaces i.e., the hot corrugated plate & cold flat plate behaved as black bodies.
- Heat Transfer by convection was not taken into account.
- Side walls of the test rig were adiabatic.

In general radiation from a surface may be due to both reflection and emission. Since the interior surfaces as mentioned above were assumed to be black surfaces the radiation which emitted was absorbed without any reflection. Defining q_{i-j} as the rate at which radiation was emitted by a black surface i and was intercepted by black surface j , [Figure A.3] i.e.,

$$q_{i-j} = [A_i J_i] F_{ij} \dots\dots\dots [8]$$

Since radiosity equals emissive power for a black surface [$J_i = E_{bi}$],

hence

$$q_{i-j} = A_i F_{ij} E_{bi} \dots\dots\dots [9]$$

similarity

$$q_{j-i} = A_j F_{ji} E_{bi} \dots\dots\dots [10]$$

The net radiative exchanged between two surfaces:

$$q_{ij} = q_{i-j} - q_{j-i}$$

or $q_{ij} = A_i F_{ij} E_{bi} - A_j F_{ji} E_{bi} \dots\dots\dots [11]$

By reciprocity, $A_j F_{ji} = A_i F_{ij} \dots\dots\dots [12]$

According to Stefan - Boltzman law:

$$E_{bi} = \sigma T_i^4 \dots\dots\dots [13]$$

$$E_{bj} = \sigma T_j^4 \dots\dots\dots [14]$$

Now from equations [11], [12], [13] and [14]:

$$q_{ij} = A_i F_{ij} \sigma [T_i^4 - T_j^4] \dots\dots\dots [15]$$

Considering surfaces i and j as corrugated and flat plate respectively and assuming that the radiation emitted by the corrugated surface was intercepted by the cold flat plate [$F_{ij}=1$], the equation [15] took the following form:

$$q_{rad} = A_{COR} \sigma [T_{COR}^4 - T_{COLD}^4] \dots\dots\dots [16]$$

From equation [16] the radiation heat transfer was estimated.

A1.2 Calculation of Rate of Heat Transfer from the Exposed surfaces of the Upper Guard Heater Assembly to the Ambient Air by Convection and Radiation:

For horizontal position of the experimental rig, the exposed surfaces of the upper guard heater assembly consisted of two pairs of parallel vertical plane surfaces facing outward having dimensions of 660mm X 127mm & 579mm X 127mm.

For vertical position of the rig, one of the pairs of dimension 660mm X 127mm of the exposed surfaces of the upper guard heater assembly became horizontal; one facing upward and another facing downward. But the other pair of the exposed heated surfaces of dimension 579mm X 127mm remained vertical facing outward.

In the design the following correlations were used for estimating the rate of heat transfer from the exposed surfaces of the upper guard heater assembly:

- [i] For computing convective heat transfer co-efficient approximately the following correlating equation recommended by Gryzagoridis [1971] for vertical heated surfaces of height H [figure A.4] was used.

$$Nu_H = 0.555 [Gr_H Pr]^{1/4}, 10 < Gr_H < 10^9 \dots\dots\dots [17]$$

where,

Nu_H and Gr_H are based on length of the vertical surface.

[ii] For computing convective heat transfer co-efficient approximately for heated horizontal surfaces [figure A.5 and A.6] of characteristic length $L_c = \sqrt{\text{Area of the plate}} = A_p$ the following correlating equations recommended by McAdams [1949] were used.

$$Nu_{Lc} = 0.54 [Gr_{Lc} \cdot Pr]^{1/4}, 10^5 < Gr_{Lc} < 2 \times 10^7, [\text{For upward facing}].. [18]$$

$$= 0.14 [Gr_{Lc} \cdot Pr]^{1/3}, 2 \times 10^7 < Gr_{Lc} < 3 \times 10^{10}$$

$$Nu_{Lc} = 0.27 [Gr_{Lc} \cdot Pr]^{1/4}, 3 \times 10^5 < Gr_{Lc} < 3 \times 10^{10},$$

[For downward facing] [19]

Where, Nu_{Lc} and Gr_{Lc} are based on the characteristic length L_c of the plane as mentioned above.

The radiation heat transfer from these exposed heated surfaces were estimated by the following equation:

$$q_{rad} = A_s \cdot \epsilon_s \cdot \sigma \cdot [T_s^4 - T_o^4]..... [20]$$

A1.3 Calculation of Rate of Heat Transfer from the Exposed Surfaces of the Lower Guard Heaters Assembly to the Ambient Air by Convection and Radiation:

For horizontal position of the experimental rig, the exposed surfaces of the lower gaurd heater assembly consisted of two pairs of parallel vertical plane surfaces facing outward having dimension of 660mm X 64mm & 579mm X 64mm and the bottom surface 660mm X 579mm facing downward.

For vertical position of the rig, one of the pairs of surface having the dimension 660mm X 64mm of the lower gaurd heaters assembly became horizontal; one facing upward and another facing downward. But the other

pair of the exposed heated surfaces of dimension 579mm X 64mm remained vertical facing outward. The bottom face became vertical.

The required correlating equations for estimating both convective and radiative heat transfer rate from the exposed surfaces of the lower gaurd heater assembly were the same as described in the preceding section [A.1.2].

For both the lower and the upper gaurd heater assembly the sum of the heat convected and radiated from the exposed surfaces must be equal to the amount of heat conducted from gaurd heaters through asbestos & wooden strip layers. But during the design the exposed surface temperature [T_s] of the gaurd heaters assembly was not known. So T_s was assumed and estimation of conduction heat transfer was made. Then by using this surface temperature the amount of convective and radiative heat transfer wer calculated. The iterative solution was continued until the conduction heat transfer rate became equal to the sum of convective & radiative heat transfer. The equation used for estimating conduction heat transfer rate is given below:

$$q_{\text{cond}} = A_s \cdot \sum_{i=1}^2 K_i / L_i [T_g - T_s] \dots\dots\dots [21]$$

K_1 = The thermal conductivity of asbestos cloth = 0.192 W/m^ok

K_2 = The thermal conductivity of wooden strip = 0.130 W/m^ok

L_1 = The thickness of the asbestos cloth = 12mm

L_2 = The thickness of the wooden strip = 12mm

T_g = Temperature of the gaurd heating element $\approx T_{\text{COR}}$

Now by substituting the above values into eqn. [21] the conduction heat transfer rate was found to be:

$$q_{\text{cond}} = 26.833 A_s [T_g - T_s] \dots\dots\dots [22]$$

The present experimental investigation was carried out with a rectangular rig that was used by Kabir [1988]. So the results of the heat transfer calculations for rig design were taken from Kabir's work.

A2 Heater Design:

Six heaters were used in the experimental sections. Actually only one heater was used in the experimental test section and the other five heaters acted as guard heaters. Each of these heaters had separate controlling variac through which power input to the heaters were controlled during experiment. Power required for each heater was estimated from heat transfer calculations shown in A1.

The details of the heater design are given below:

Power [P] taken by the electric heater of resistance R can be determined by the following equation:

$$P = I_{\text{safe}}^2 \times R \dots\dots\dots [23]$$

If r be the resistance of the heating wire per meter of length then for a heater of power P the length of the heating wire will be:

$$L = R/r \dots\dots\dots [24]$$

By knowing I_{safe} and power [P] taken by each electric heater the required resistance [R] was calculated from eqn. [23]. For a particular heating wire, internal resistance "r" is fixed. So, by putting the values of R and r into eqn. [24] required length for each heater was determined.

The ratings of the heating wires were as follows:

Type 1: Resistance, $r = 39.37$ ohms/m
 Current carrying capacity = 0.75 amps.

Type 2: Resistance, $r = 26.25$ ohms/m
 current carrying capacity = 1.5 amps.

The particulars of the heating arrangement that were used are given in following tabular form:

Heater No. and Name	Maximum Power Requirement (Watt)	Type	Length (cm)	Location	Variatc Connected with Heater	
					Safe Installed Capacity (Watt)	Safe Voltage (Volt)
1. Experimental hot corrugated plate heater	15.74	1-Nicrome Wire	72.0	Experimental test section Figs.4.3[a & b]	22.5	30
2. Outer side gaurd heater	83.40	1-Nicrome Wire	376.60	Longitudinal sides of the test section Figs.4.3[a & b]	22.5	30
3. Outer end gaurd heater	20.79	1-Nicrome Wire	93.87	Lateral sides of the test section Figs.4.3[a & b]	90	120
4.Upper outer gaurd heater	97.60	2-Nicrome wire	165.24	Upper gaurd heater ring Figs.4.4[a & b]	180	120
5.Bottom guard heater	113.02	1-Nicrome Wire	510.34	Lower gaurd heater box Figs. 4.5[a & b]	90	120
6.Lower outer gaurd heater	43.17	1-Nicrome wire	194.93	Lower gaurd heater box Figs.4.5 [a & b]	45	60

APPENDIX - B
CONDUCTION CORRECTION

The one dimensional fourier conduction equation is;

$$q'' = K_c \cdot \Delta T_c / \Delta x \quad [\text{For one layer of conductive zone}] \dots\dots\dots [1]$$

$$= T_c / \Sigma(\Delta x_i / k_i) \quad [\text{For two or more layers of conductive zone}] \dots\dots\dots [2]$$

As shown in figure B.1 it is observed that under steady state heat conduction the resistance to the heat conduction will consist of the resistances offered by the upper asbestos cloth layer and upper corrugated plate [G.I. Sheet].

The thermal conductivity of asbestos cloth, $K_1 = 0.157 \text{ W/m}^\circ\text{k}$.

The thermal conductivity of G.I. Sheet, $K_2 = 70 \text{ W/m}^\circ\text{k}$.

The thickness of asbestos cloth, $X_1 = 2.15052 \times 10^{-3} \text{ m}$.

The thickness of G.I. Sheet, $X_2 = 7.9375 \times 10^{-4} \text{ m}$

Assuming that there is no temperature difference at the interface of the lower corrugated plate and the interface of the lower guard heater box. So that the heat goes up towards the cold plate. It is also assumed that the temperature at the bottom surface of the lower corrugated plate is equal to the temperature at the interface of the two asbestos cloth.

Now by substituting the above values into equation [2] the conduction correction in temperature measurements was found to be:-

$$\Delta T_c = 0.0137089 q'' \dots\dots\dots [3]$$

Where, q'' will be taken as electrical heat input [W/m^2] per unit projected surface area of the experimental section of the hot corrugated plate.

APPENDIX - C

DETERMINATION OF EMISSIVITY OF THE CORRUGATED SURFACE

The accuracy in predicting the radiation heat transfer from the experimental hot corrugated plate to the cold flat plate largely depends on the precise determination of the long wave emissivity and hemispherical emissivity of the corrugated surface.

Both the trapezoidal and rectangular corrugated plates were painted dull black by plastic paint. Hollands [1963] developed the method of determination of the hemispherical emissivities of the Vee-corrugated surfaces using the emissivity of the plane surface. When a plane G.I. sheet is uniformly painted to dull black with black paint, its emissivity can be taken as the emissivity of the black paint. From table 3.6 of "Journal of Solar Energy", H.P. Gary; Vol. 1, John Wiley and Sons, Ltd. [1982] the emissivity of the black paint was found to be 0.94. The emissivity of the G.I. corrugated [painted black] plate was assumed to be the same as that of plane G.I. sheet [painted black]. Considering this value of the emissivity, the hemispherical emissivity of the trapezoidal corrugated plate having opening angle of 72° was found to be 0.97 [using figure C.2]. Similarly the hemispherical emissivity of the rectangular corrugated plate having opening angle of 90° was found to be 0.95 [using figure C.2].

APPENDIX-D

CORRELATIONS

D.1 Correlations of Natural Convection Heat Transfer in an Inclined Rectangular Region:

Difedeviso and Foraboschi [1966] carried out experimental investigations on natural convection heat transfer in an inclined rectangular region with different convecting fluids and developed correlation in the following form:

$$Nu = C [Ra_a]^n [Pr]^m \dots\dots\dots [1]$$

Kabir [1988] carried out an experimental investigation of natural convection heat transfer across air layer from a hot sinusoidal corrugated plate to a flat cold plate enclosed in a rectangular region inclined at various angle with respect to horizontal for various aspect ratios [A] and developed the following correlation:

$$Nu_L = 0.0132 [Ra_L \cos\theta]^{0.51} [A]^{-0.35}, \dots\dots\dots [2]$$

Where,

$$5.56 \times 10^3 \leq Ra_L \leq 2.34 \times 10^6$$

D.2 Correlation of Natural Convection Heat Transfer from a Hot Corrugated Plate to a Cold Flat Plate:

The present study was the experimental investigation of steady state natural convection from a hot corrugated plate to a cold flat plate. Two types of corrugation namely trapezoidal and rectangular having same amplitude and pitch were used. The required correlation was arrived at by considering the effect of the followings factors:

D.2a. Effect of Fluid Properties:

The most commonly used dimensionless parameters which include the effect of fluid properties in natural convection are as follows:

$$Pr = \mu C_p / k \quad \text{and}$$

$$Ra_L = g.\beta.\Delta T.L^3/\nu.\alpha$$

The present experimental investigations were carried out with only one convecting fluid [air], so Pr can be omitted in correlating equation. Therefore Nusselt number $[Nu_L]$, which measures the thermal convective property of the fluid mainly depends on Rayleigh number $[Ra_L]$. It was experimentally found that Nusselt number increases with the increasing Rayleigh number. For analysis of natural convection from inclined surface because of bouyance force, Ra_L is generally substituted by its vertical component i.e. $Ra_L \cos\theta$. So $Ra_L \cos\theta$ should include the contribution of the fluid property in natural convection. Let correlation of the following form be assume:

$$Nu_L \propto [Ra_L \cos\theta]^{n_t} \dots\dots\dots [3]$$

$$Nu_L \propto [Ra_L \cos\theta]^{n_r} \dots\dots\dots [4]$$

In this case using conventional techniques, the exponent n_t and n_r of $Ra_L \cos\theta$ were determined by plotting Nu_L vs. $Ra_L \cos\theta$ from the present experiment data as shown in figures 6.31 to 6.36 and the average of the

exponents were found to be, $n_t = 0.521$ and $n_r = 0.530$. So the correlations became:

$$Nu_L \propto [Ra_L \cos\theta]^{0.521} ; \quad [\text{TRAPEZOIDAL CORRUGATION}] \dots [5]$$

$$Nu_L \propto [Ra_L \cos\theta]^{0.530} ; \quad [\text{RECTANGULAR CORRUGATION}] \dots [6]$$

D.2b. Effect of Spacing between Hot and Cold Plates:

Elsherbiny [1977] and Kabir [1988] suggested the following dimensionless group to describe the contribution of plate spacing between hot corrugated plate and cold flat plate in natural convection in a rectangular enclosure heated from below:

$$A = L/H \dots \dots \dots [7]$$

In equation [7] "L" is mean plate spacing and "H" is amplitude of corrugation [fixed]. It was experimentally observed that average convective heat transfer coefficient for both types of corrugation increases with the increase of aspect ratio [A]. So, this dimensionless number also should include the contribution of spacing between hot and cold plates in free convection.

By including this dimensionless group the correlating equation became,

$$Nu_L \propto [Ra_L \cos\theta]^{0.525} [A]^{m_t} \dots \dots \dots [8]$$

$$Nu_L \propto [Ra_L \cos\theta]^{0.530} [A]^{m_r} \dots \dots \dots [9]$$

In this case also using conventional techniques, the exponent m_t of the group "A" was determined by plotting $Nu_L/[Ra_L \cos\theta]^{0.521}$ vs. A of the present experimental data for trapezoidal corrugation as shown in figures 7.1 to 7.4. Similarly the exponent m_r of the group "A" was determined by plotting $Nu_L/[Ra_L \cos\theta]^{0.530}$ vs. A of the present experimental data for rectangular corrugation as shown in figure 7.5 to 7.8. The average value of the exponents were found to be, $m_t = -0.4546$ and $m_r = -0.4923$.

So that,

$$Nu_L \propto [Ra_L \cos\theta]^{0.521} \cdot [A]^{-0.4546}; \quad [\text{TRAPEZOIDAL CORRUGATION}] \dots [10]$$

$$Nu_L \propto [Ra_L \cos\theta]^{0.530} \cdot [A]^{-0.4923}; \quad [\text{RECTANGULAR CORRUGATION}] \dots [11]$$

The graphical representation of the correlations for trapezoidal and rectangular corrugations are shown in figure D.1 and figure D.2 respectively. Both of these correlations correlate all most all the data to within $\pm 15\%$. The complete correlations for trapezoidal and rectangular corrugation are given by the following equations:

$$Nu_L = 0.0112 [Ra_L \cos\theta]^{0.521} \cdot [A]^{-0.4546}; \quad [\text{TRAPEZOIDAL CORRUGATION}] \dots [12]$$

$$Nu_L = 0.0102 [Ra_L \cos\theta]^{0.530} \cdot [A]^{-0.4923}; \quad [\text{RECTANGULAR CORRUGATION}] \dots [13]$$

Where,

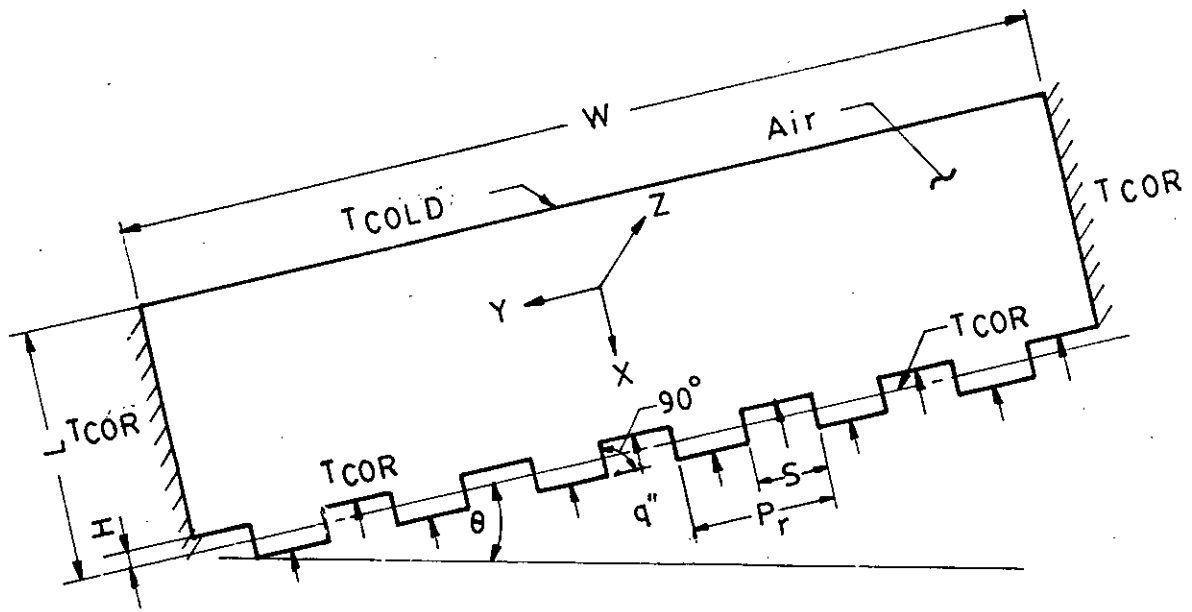
$$9.80 \times 10^4 \leq Ra_L \leq 2.29 \times 10^6$$

$$2.60 \leq A \leq 5.22$$

$$0^\circ \leq \theta \leq 75^\circ$$

FIGURES

All measurements are in millimeter unless otherwise mentioned.



$\theta = 0^\circ - 75^\circ$
 $L = 4.95 \text{ cm} - 9.95 \text{ cm}$
 $H = 1.905 \text{ cm}$
 $S = 8.0 \text{ cm}$
 $P_r = 16.0 \text{ cm}$
 $P_t = 13.52 \text{ cm}$
 $W = 63.5 \text{ cm}$

FIG. 3.1a SKETCH OF THE INCLINED AIR LAYERS BOUNDED BY RECTANGULAR CORRUGATED PLATE AND FLAT PLATE

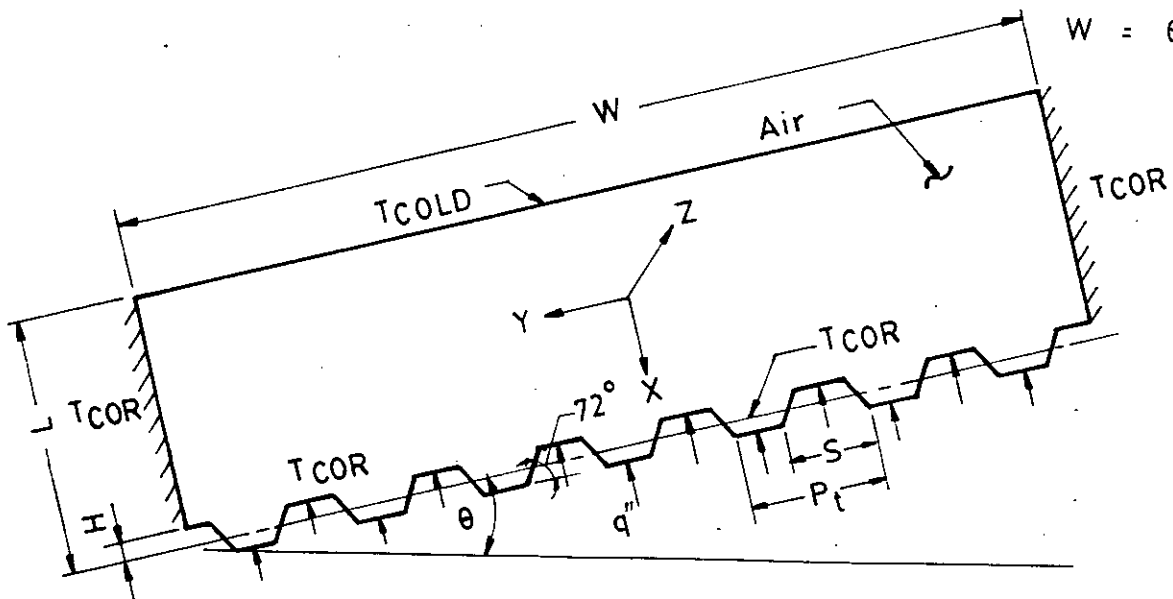


FIG. 3.1b SKETCH OF THE INCLINED AIR LAYERS BOUNDED BY TRAPEZOIDAL CORRUGATED PLATE AND FLAT PLATE

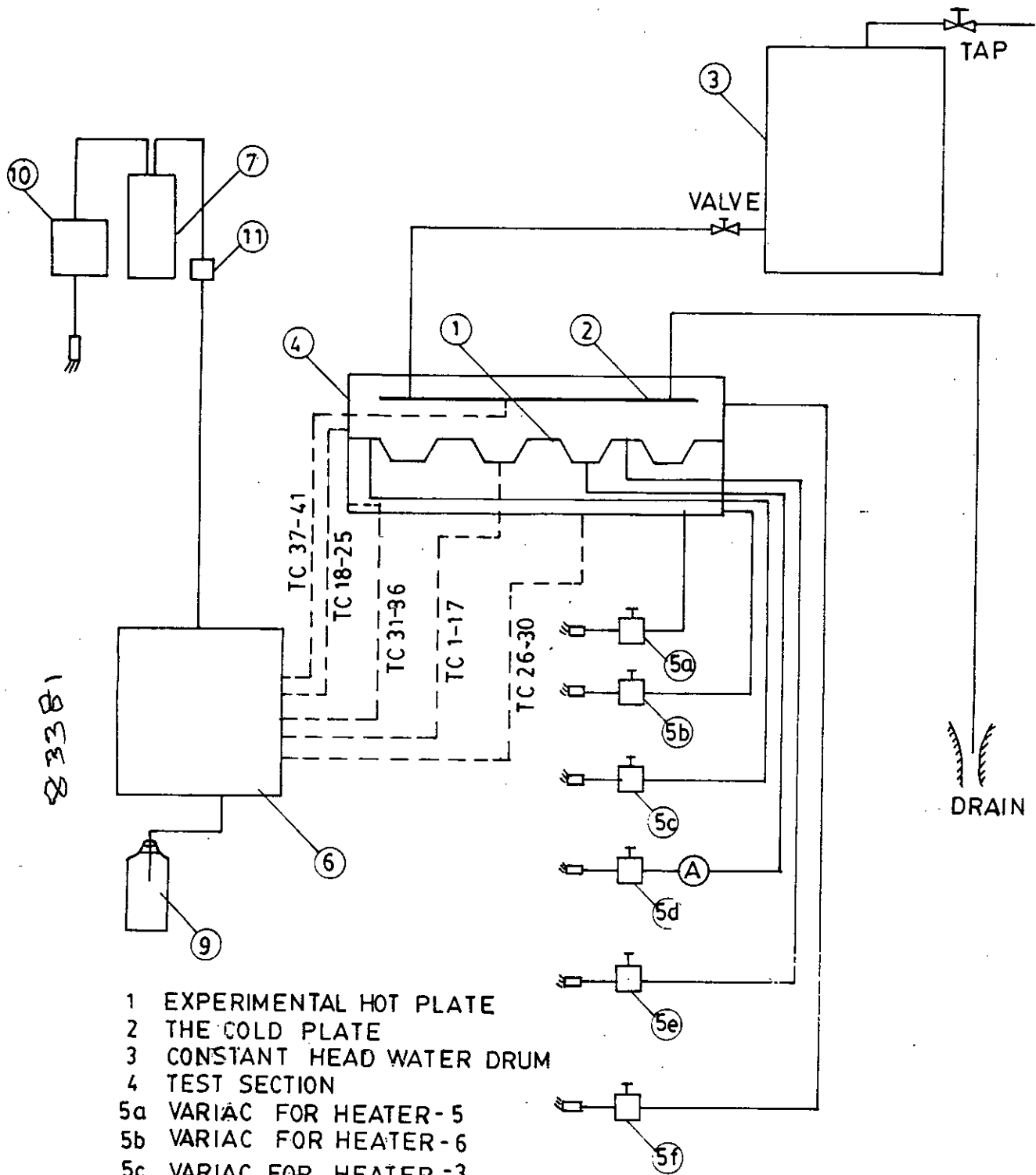
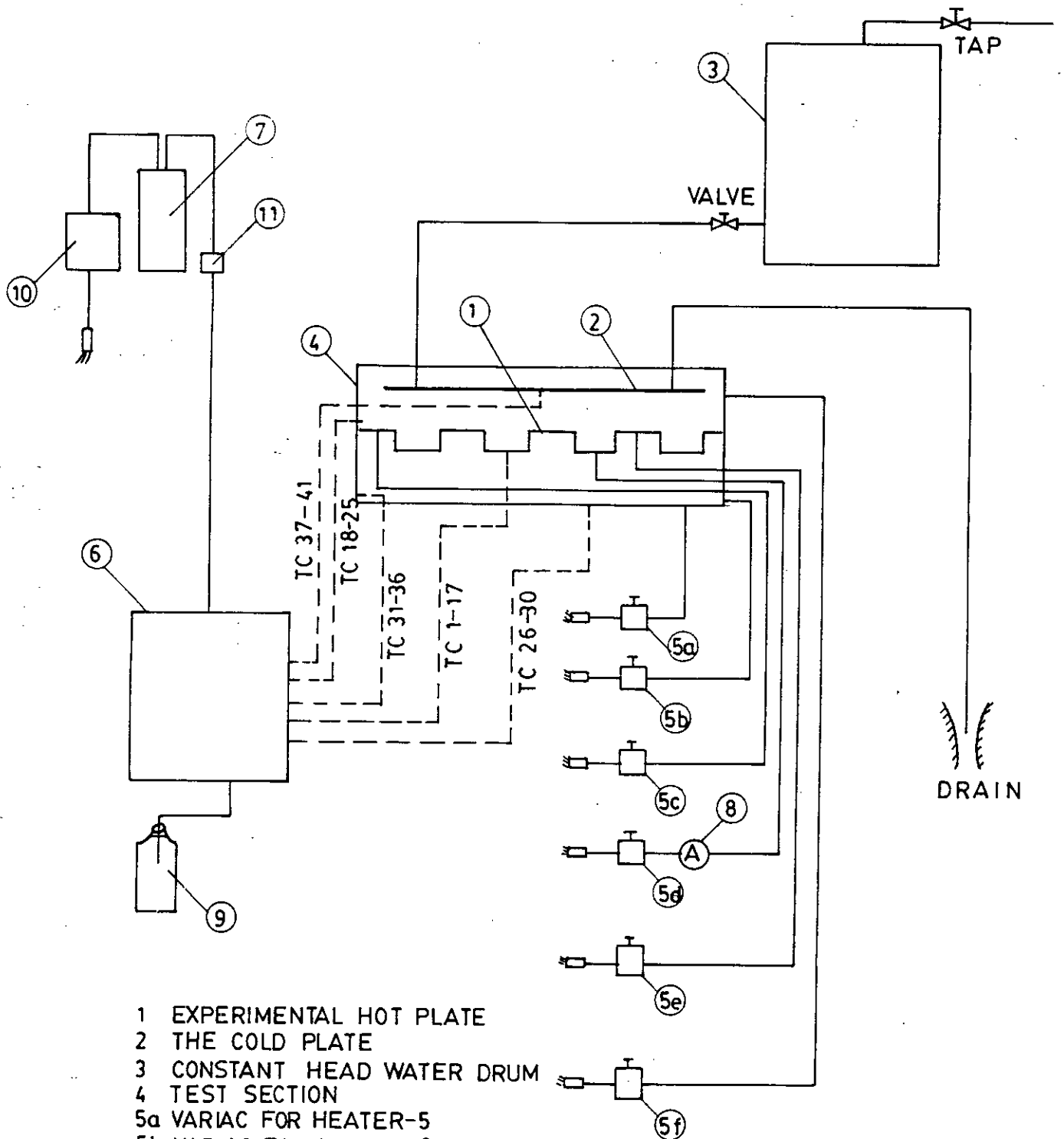
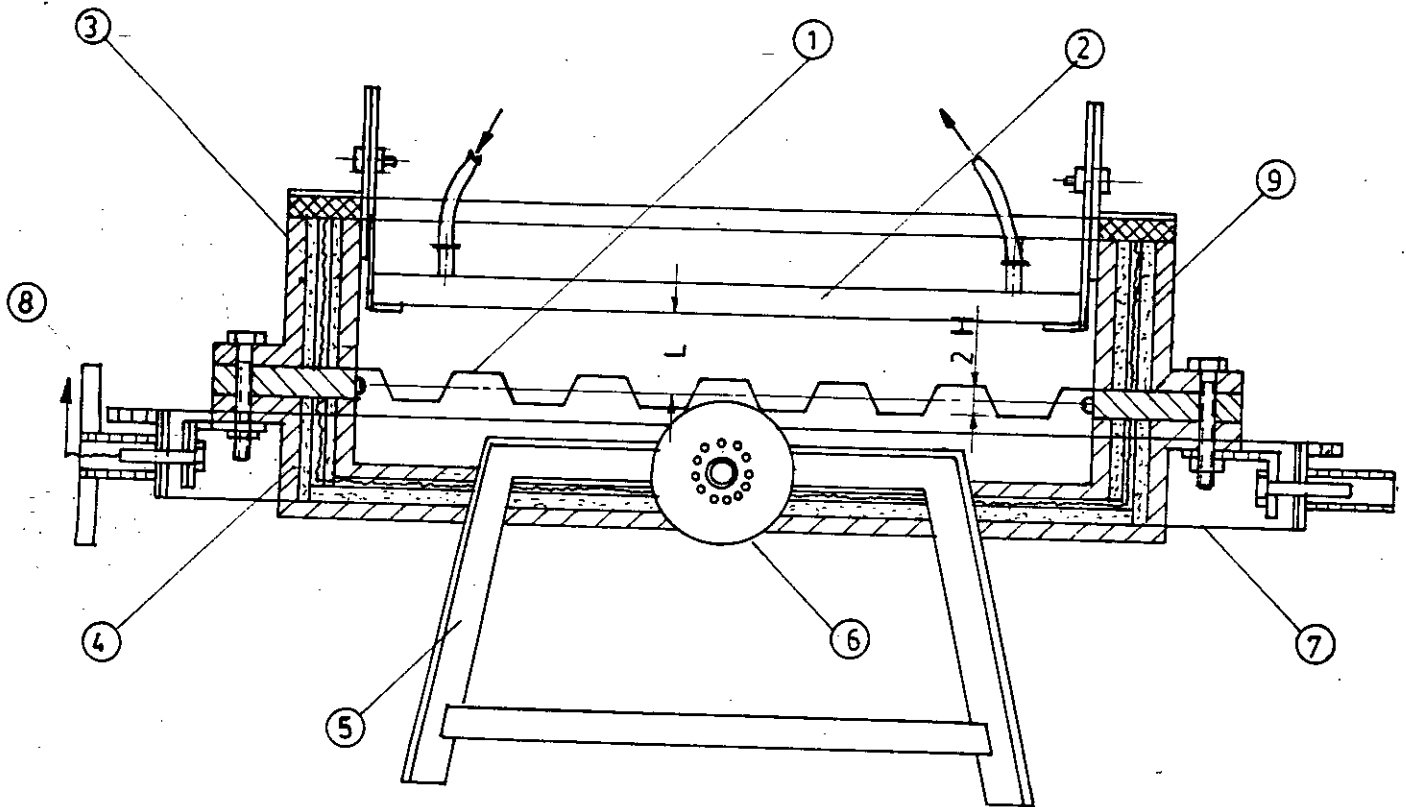


FIG. 4.1a SCHEMATIC DIAGRAM OF THE EXPERIMENTAL SETUP FOR TRAPEZOIDAL CORRUGATION



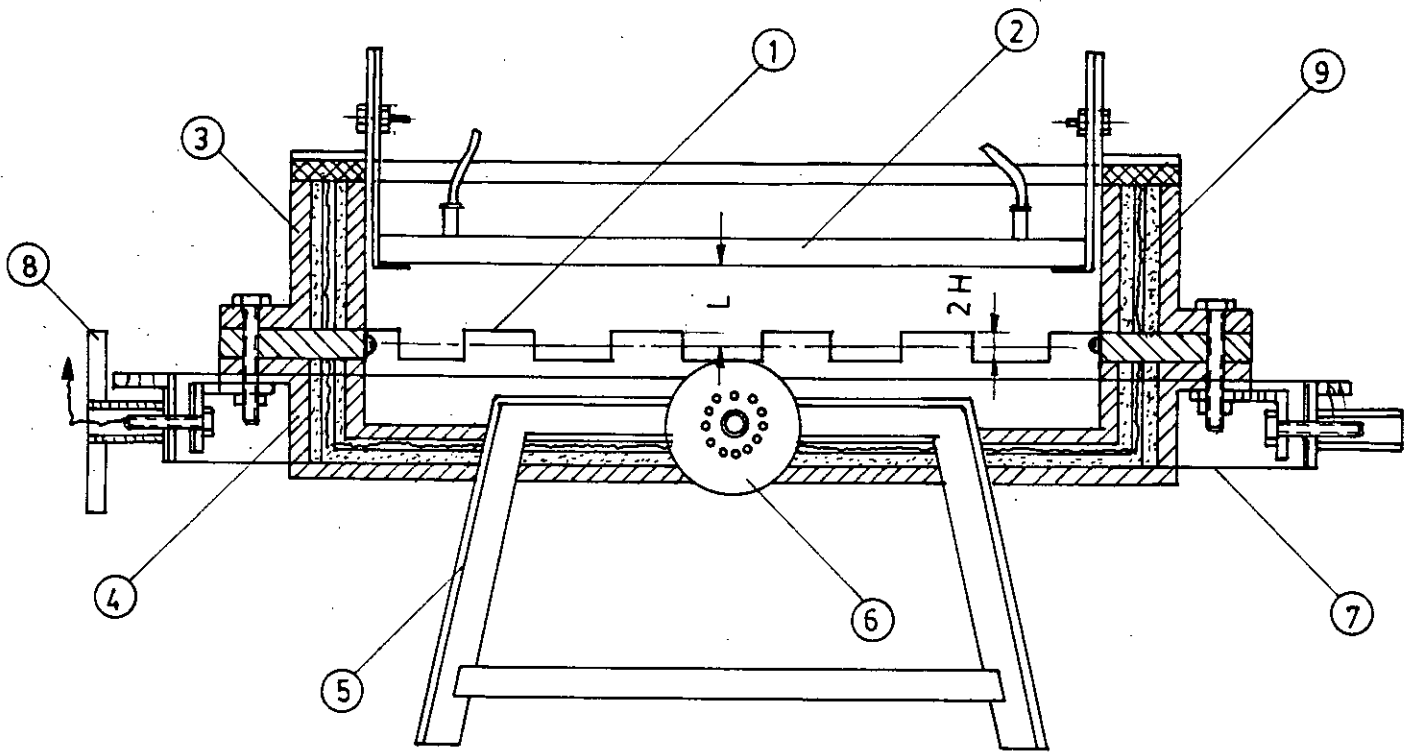
- 1 EXPERIMENTAL HOT PLATE
- 2 THE COLD PLATE
- 3 CONSTANT HEAD WATER DRUM
- 4 TEST SECTION
- 5a VARIAC FOR HEATER-5
- 5b VARIAC FOR HEATER-6
- 5c VARIAC FOR HEATER-3
- 5d VARIAC FOR HEATER-1
- 5e VARIAC FOR HEATER-2
- 5f VARIAC FOR HEATER-4
- 6 THERMOCOUPLE SELECTOR SWITCH
- 7 DIGITAL MICRO VOLT METER (DMM)
- 8 PRECISION AMMETER
- 9 COLD JUNCTION
- 10 VOLTAGE STABILISER
- 11 CONNECTOR TO DMM

FIG.4.1b SCHEMATIC DIAGRAM OF THE EXPERIMENTAL SETUP FOR RECTANGULAR CORRUGATION



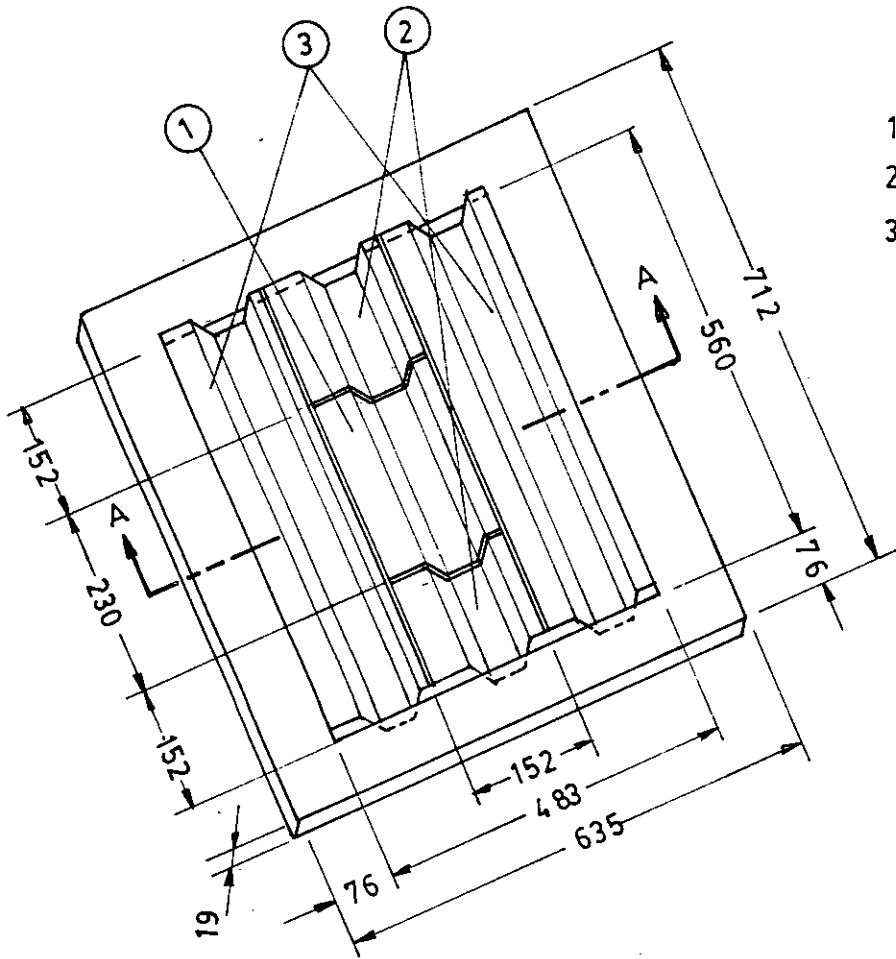
- 1. THE HOT PLATE ASSEMBLY
- 2. THE COLD PLATE
- 3. THE UPPER GUARD HEATER
- 4. THE LOWER GUARD HEATER
- 5. THE END RIG HOLDER
- 6. THE ALIGNMENT PLATE
- 7. THE SIDE RIG HOLDER
- 8. THE ALIGNMENT INDICATOR
- 9. NICHROME HEATER

FIG. 4.2a DETAILS OF THE TEST SECTION
FOR TRAPEZOIDAL CORRUGATION



- 1- THE HOT PLATE ASSEMBLY
- 2. THE COLD PLATE
- 3. THE UPPER GUARD HEATER
- 4. THE LOWER GUARD HEATER
- 5. THE END RIG HOLDER
- 6. THE ALIGNMENT PLATE
- 7. THE SIDE RIG HOLDER
- 8. THE ALIGNMENT INDICATOR
- 9. NICHROME HEATERS

FIG.4-2b DETAILS OF THE TEST SECTION
FOR RECTANGULAR CORRUGATION



- 1. EXPERIMENTAL HOT PLATE
- 2. OUTER END GUARD HEATER
- 3. OUTER SIDE GUARD HEATER

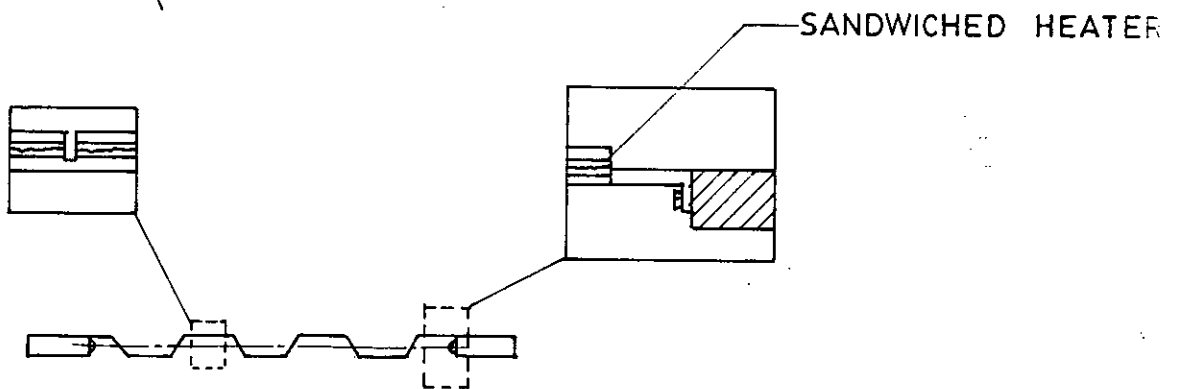
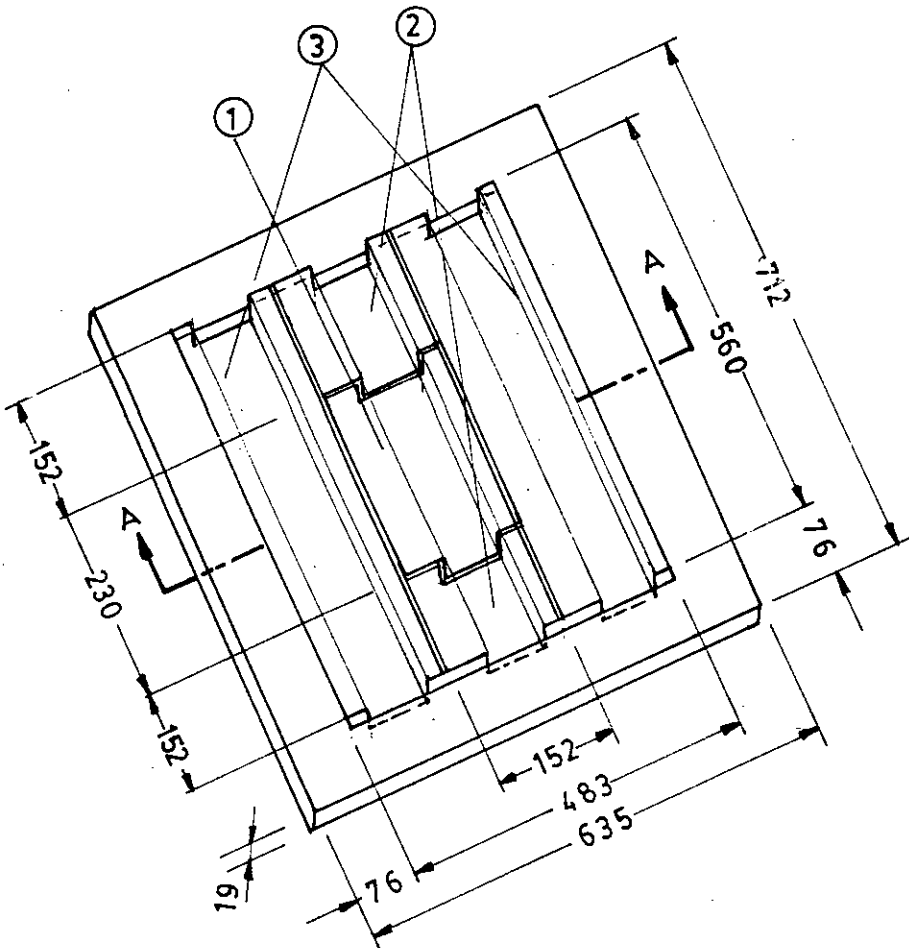


FIG. 4.3a DETAILS OF HOT PLATE ASSEMBLY FOR TRAPEZOIDAL CORRUGATION



1. EXPERIMENTAL HOT PLATE
2. OUTER END GUARD HEATER
3. OUTER SIDE GUARD HEATER

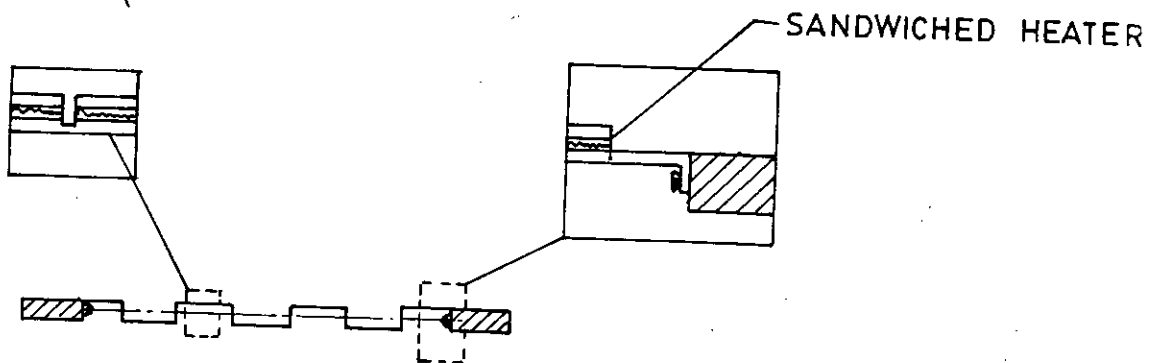
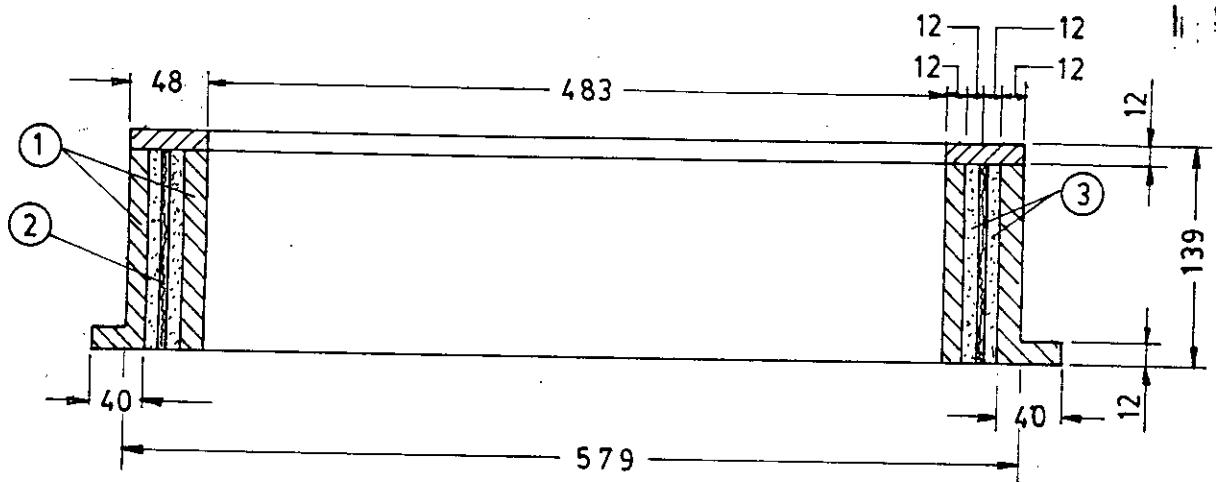
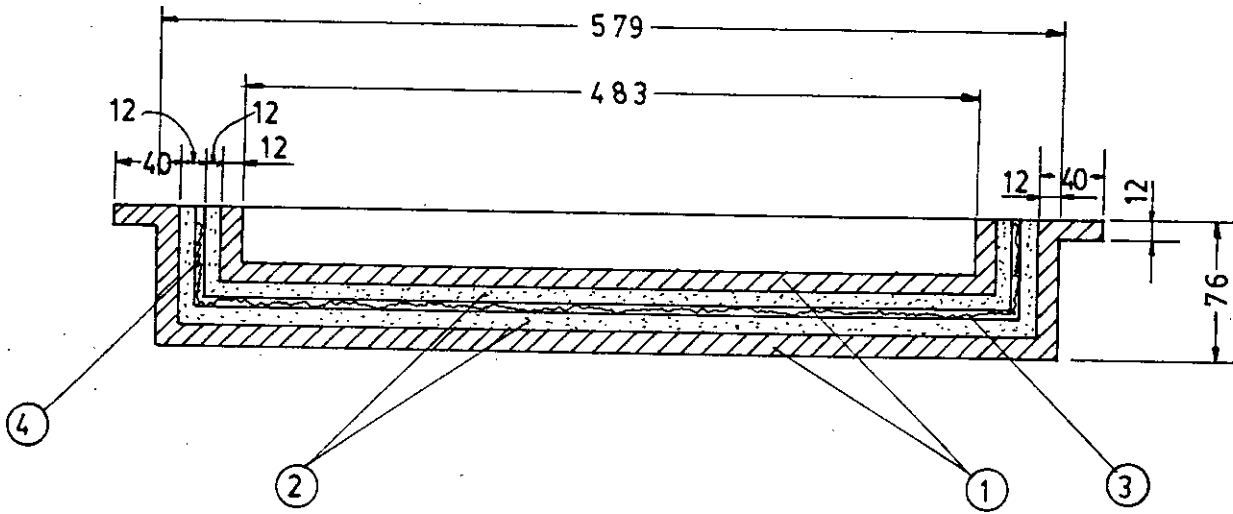


FIG.4.3b DETAILS OF HOT PLATE ASSEMBLY FOR RECTANGULAR CORRUGATION



- 1. INNER AND OUTER WOODEN RING
- 2. UPPER OUTER GUARD HEATER
- 3. INNER AND OUTER ASBESTOS RING

FIG. 4.4 DETAILS OF UPPER GUARD HEATER RING



- 1. INNER AND OUTER WOODEN BOX
- 2. ASBESTOS INSULATION
- 3. BOTTOM GUARD HEATER
- 4. LOWER OUTER GUARD HEATER

FIG. 4.5 DETAILS OF LOWER OUTER GUARD HEATER BOX

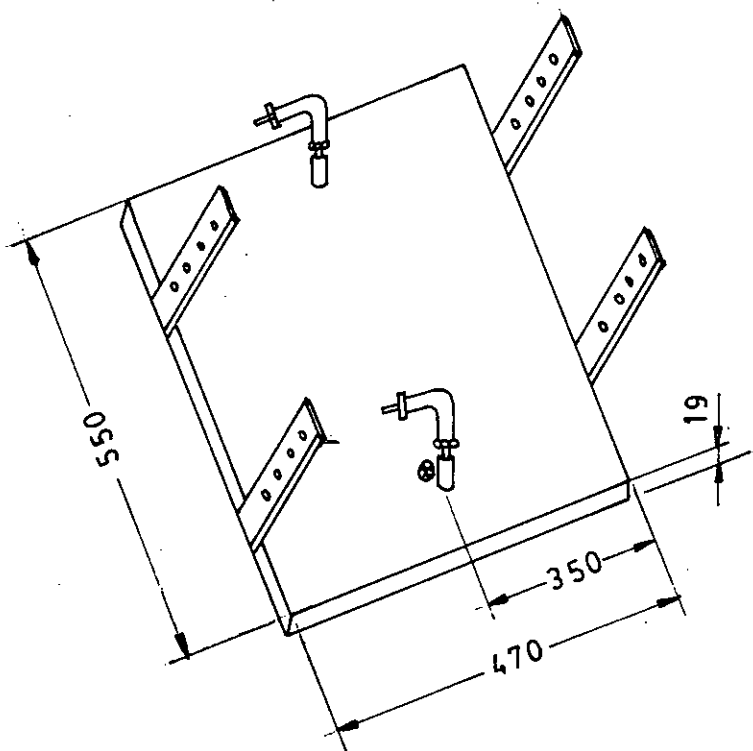


FIG. 4.6. DETAILS OF THE COLD PLATE ASSEMBLY

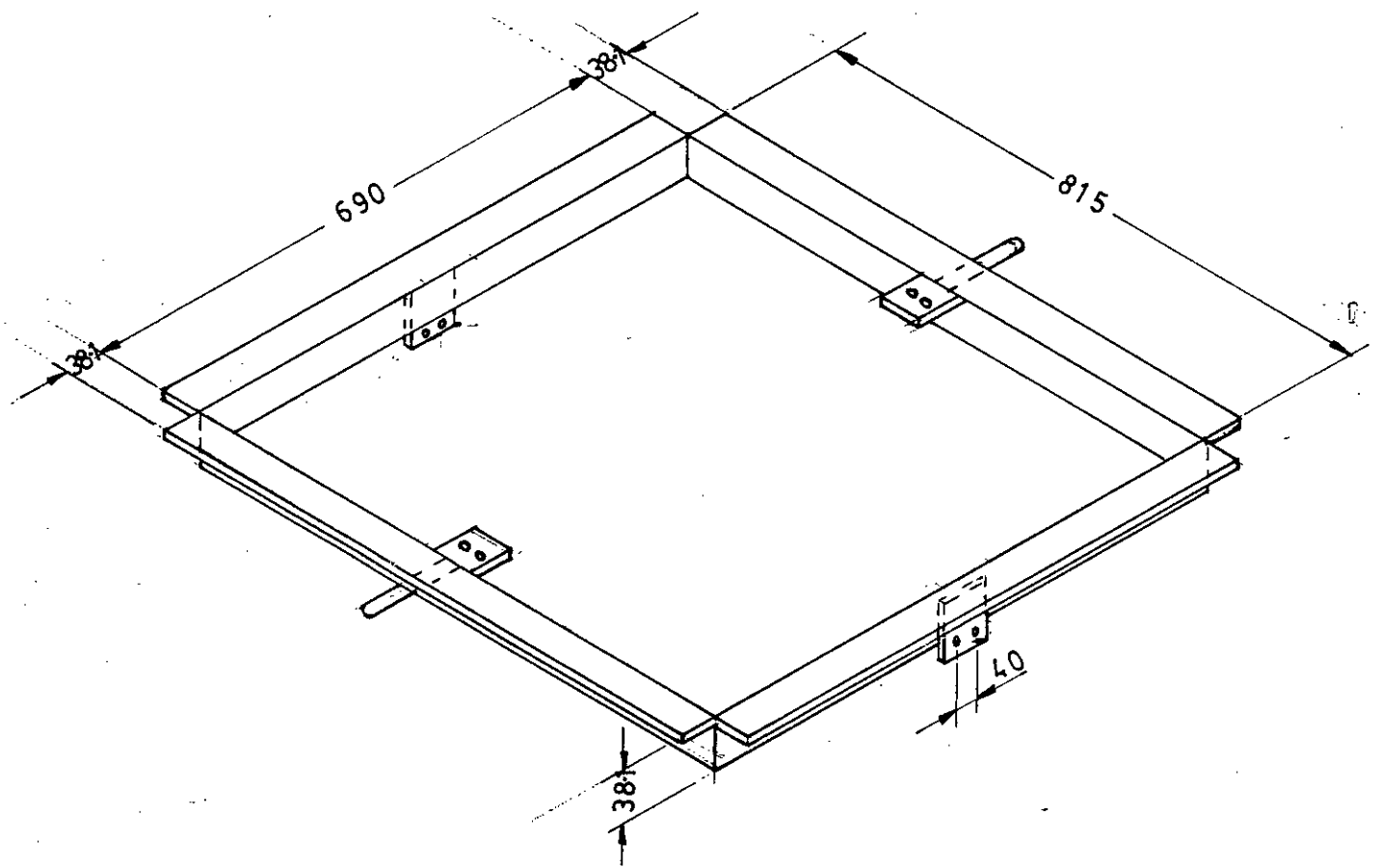


FIG. 4.7 THE RECTANGULAR SUPPORTING FRAME

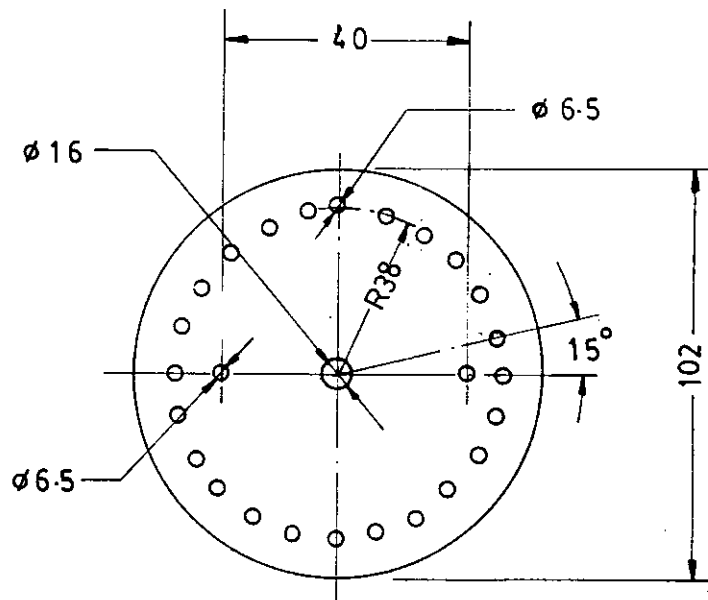
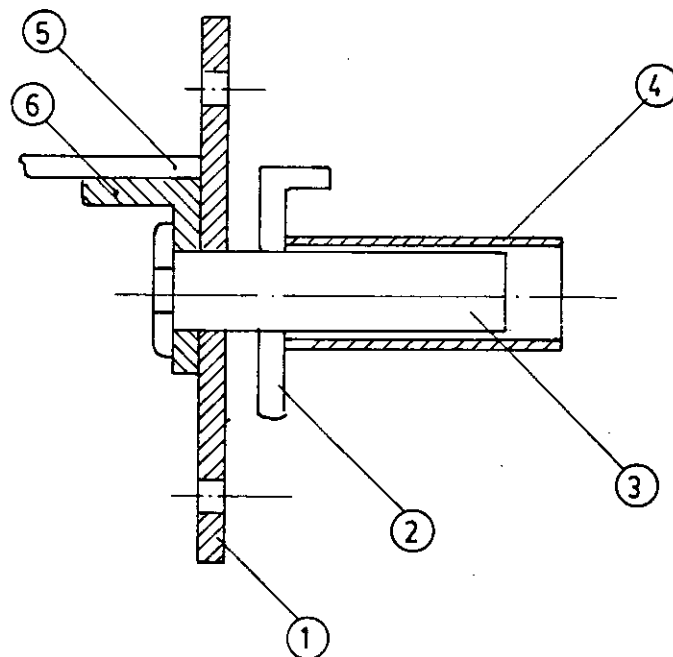


FIG. 4.8 THE ALIGNMENT PLATE



- 1. ALIGNMENT PLATE
- 2. SUPPORTING STAND
- 3. SUPPORTING BOLT
- 4. SUPPORTING BOLT HOLDER
- 5. SUPPORTING FRAME
- 6. OVER HANGING SIDE SUPPORT

FIG. 4.9 CONNECTION OF THE RECTANGULAR SUPPORTING FRAME WITH THE SUPPORTING STAND.

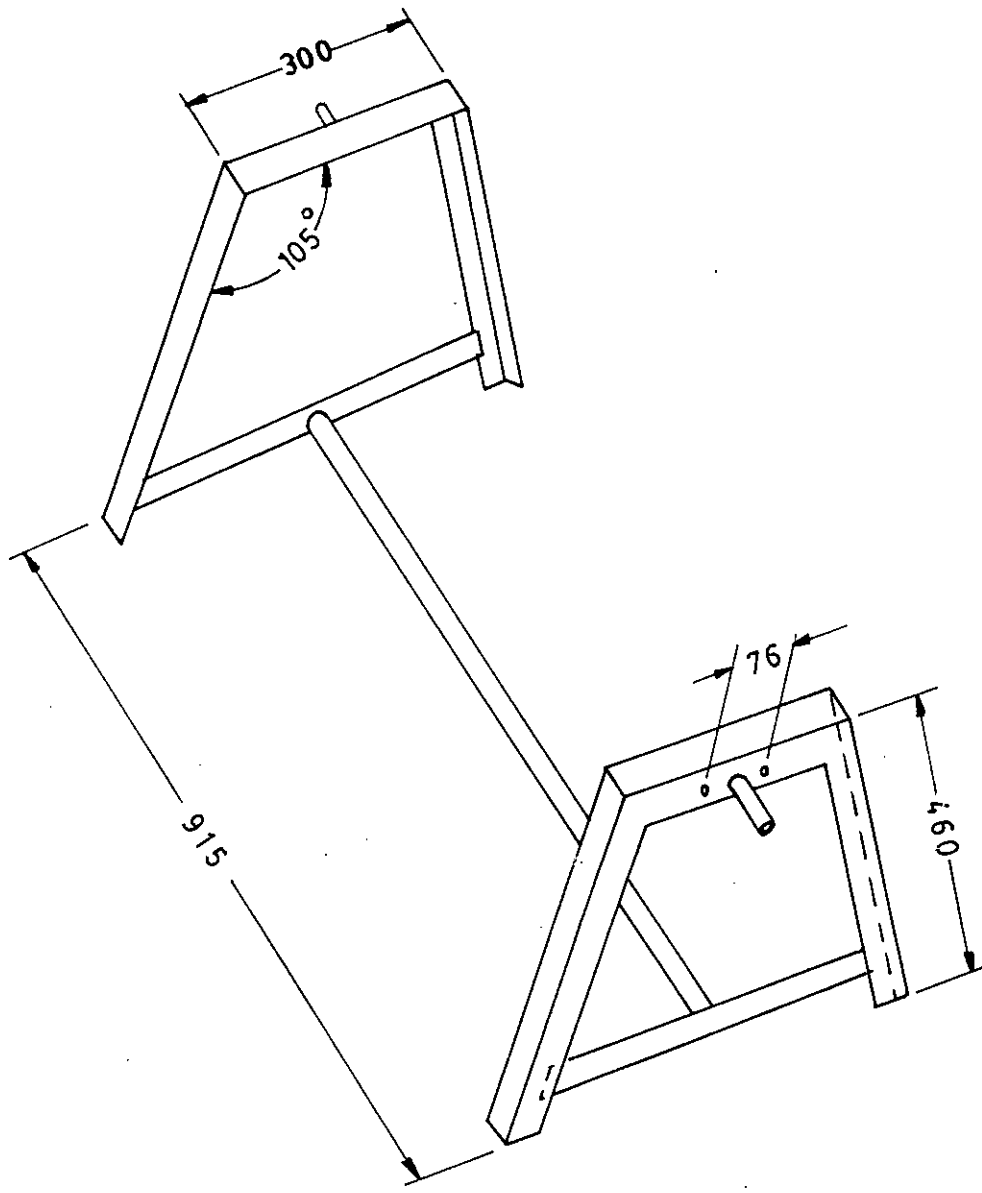


FIG. 4.10 THE SUPPORTING STAND

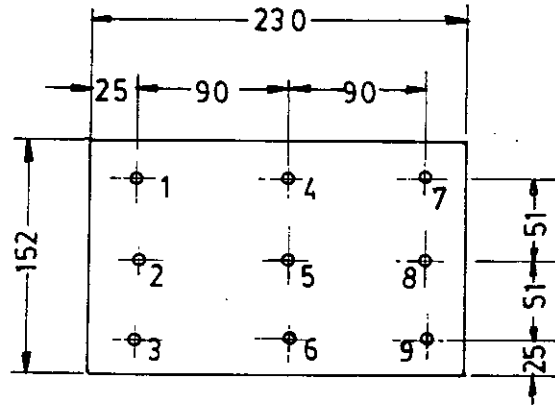


FIG. 5.1 POSITION OF THE THERMOCOUPLES IN THE TEST SECTION OF THE HOT PLATE

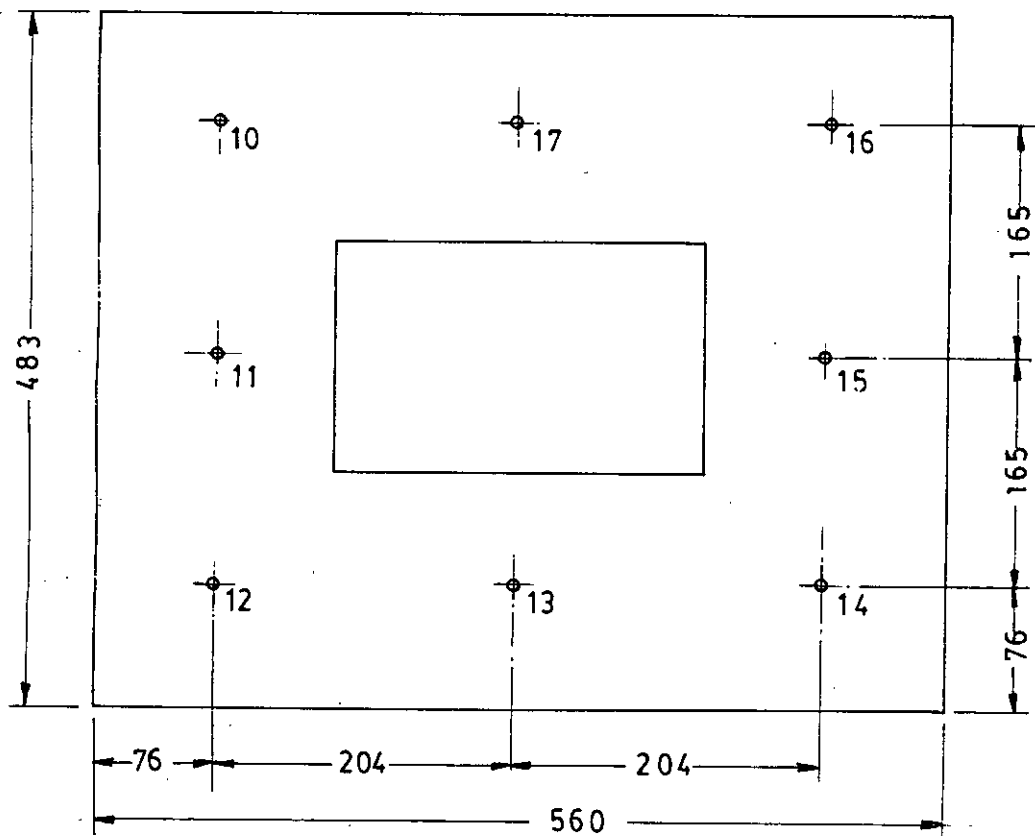


FIG. 5.2 POSITION OF THE THERMOCOUPLES IN OUTER END AND SIDE GUARD HEATERS SECTIONS.

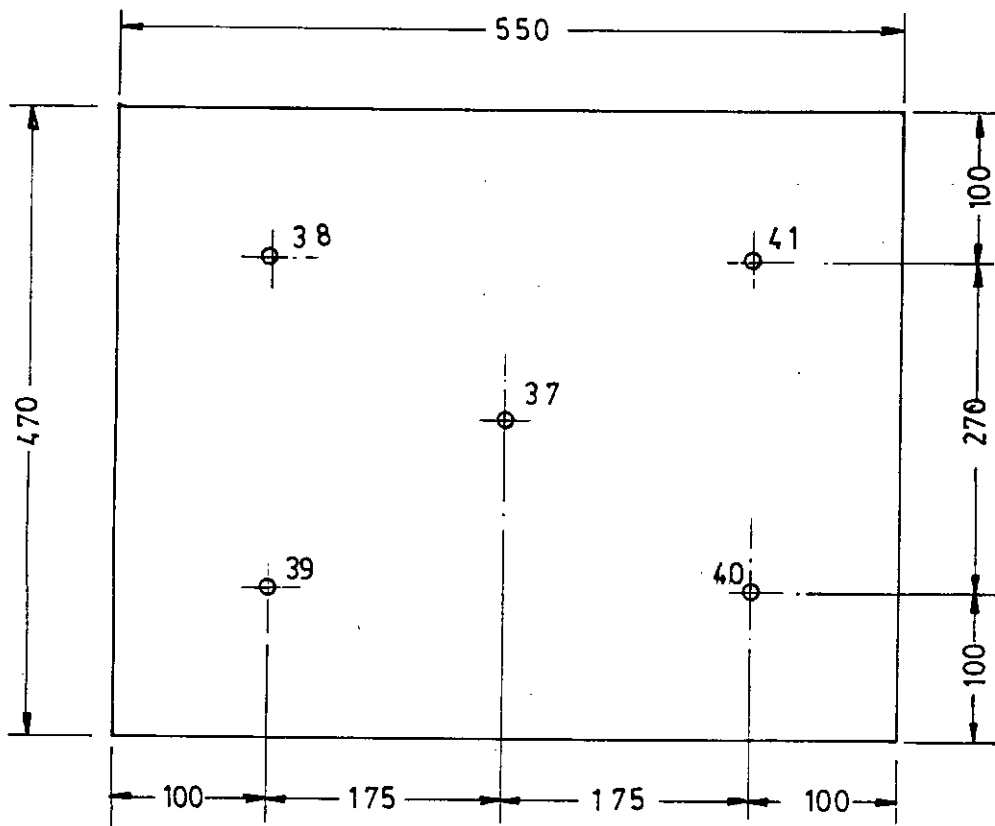


FIG. 5.3 POSITION OF THERMOCOUPLES IN COLD PLATE

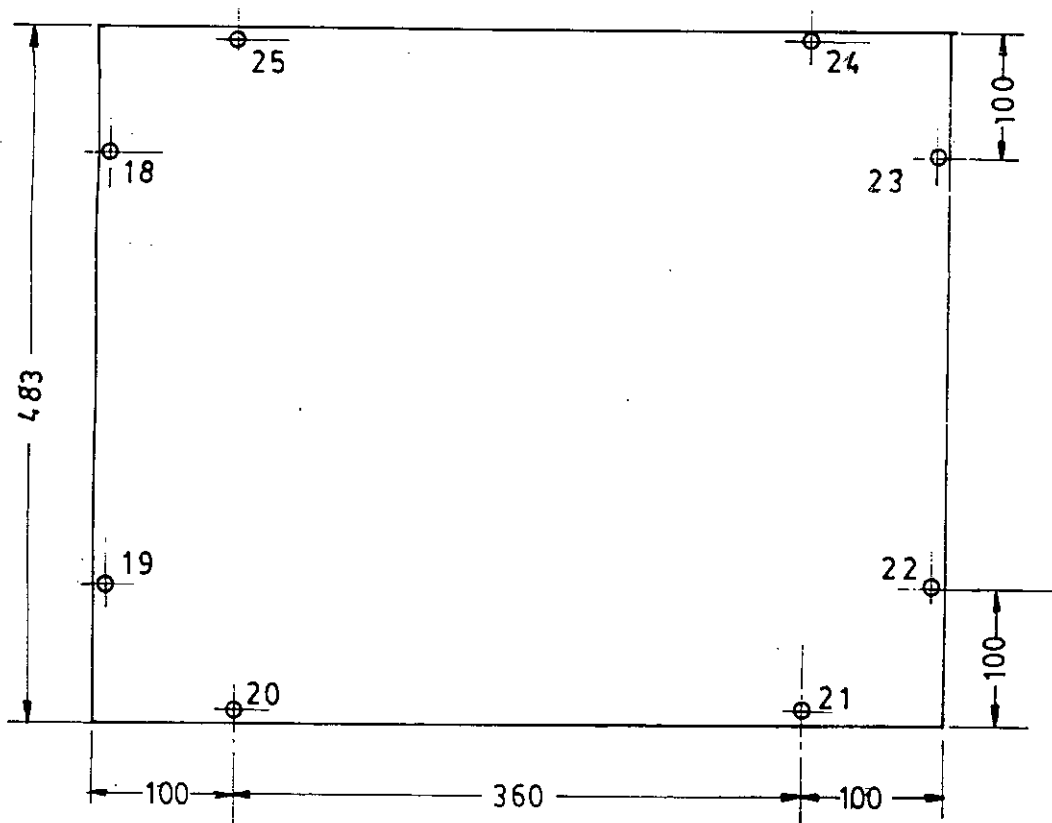


FIG. 5.4 POSITION OF THERMOCOUPLES IN UPPER OUTER GUARD HEATE RING

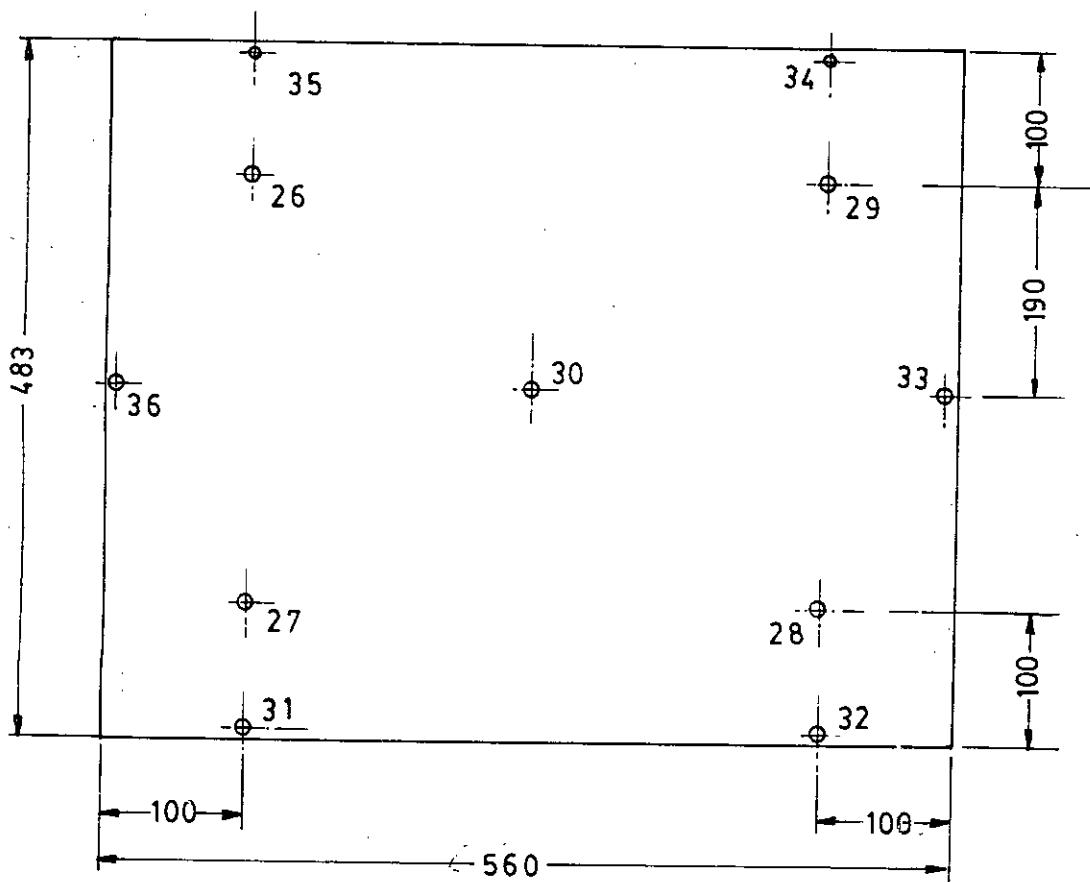


FIG. 5.5: POSITION OF THERMOCOUPLES IN LOWER OUTER GUARD HEATER BOX.

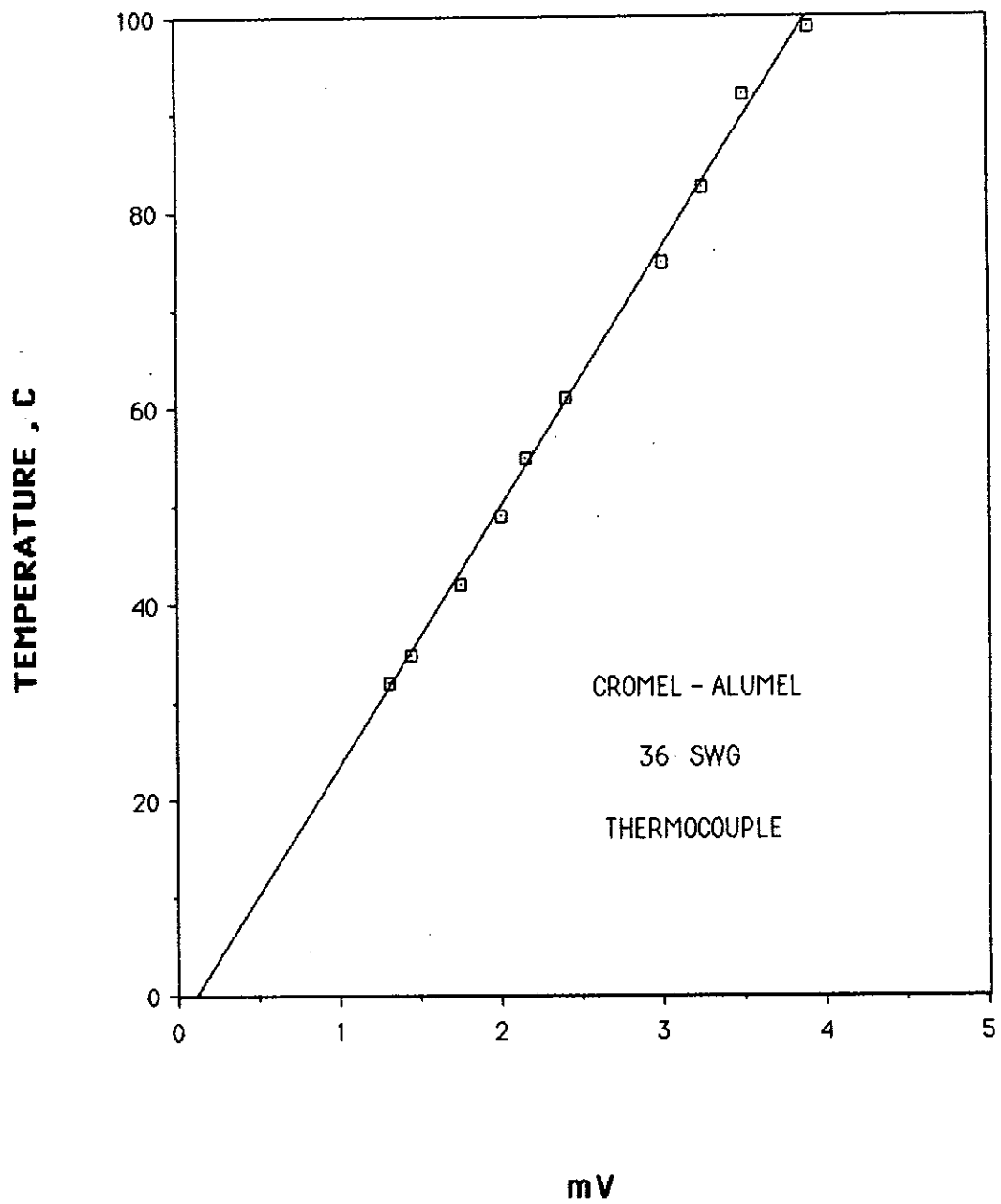
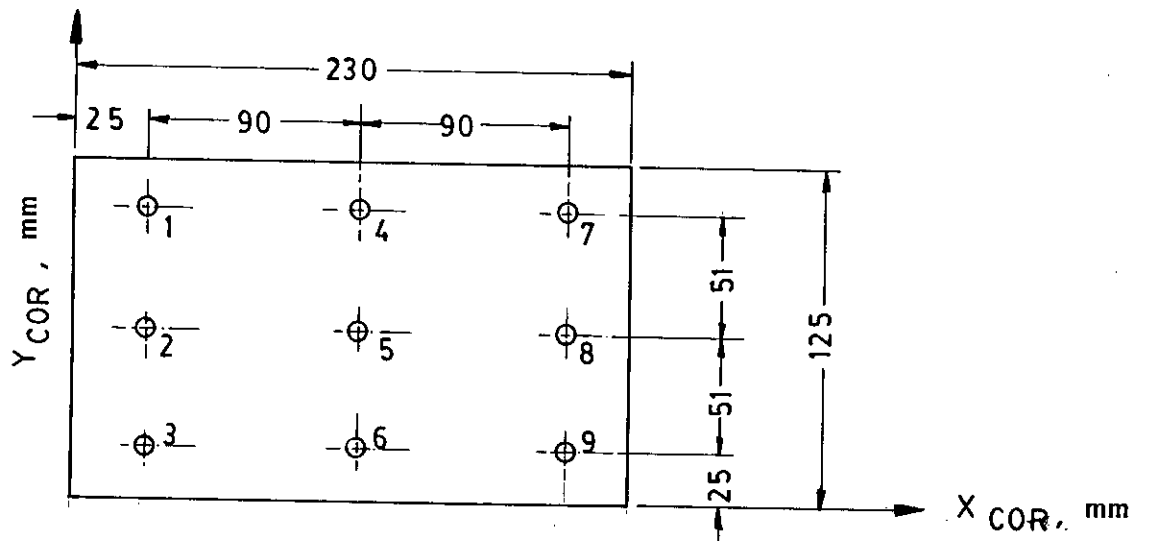


FIG. 5.6: THERMOCOUPLE CALIBRATION CURVE FOR THERMOCOUPLE NO.5



POSITION OF THE THERMOCOUPLES IN THE TEST SECTION OF THE HOT TRAPEZOIDAL CORRUGATED PLATE

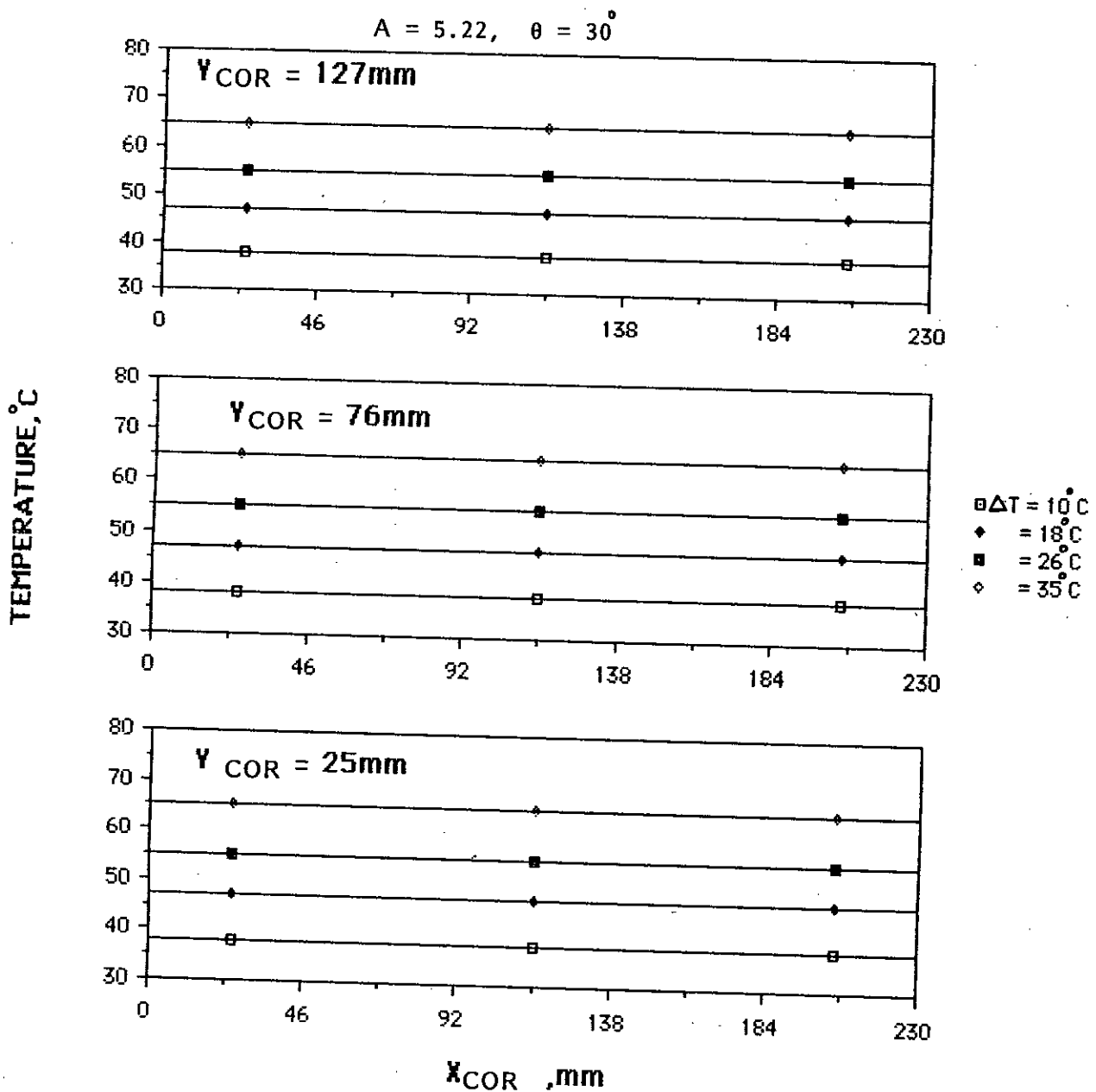
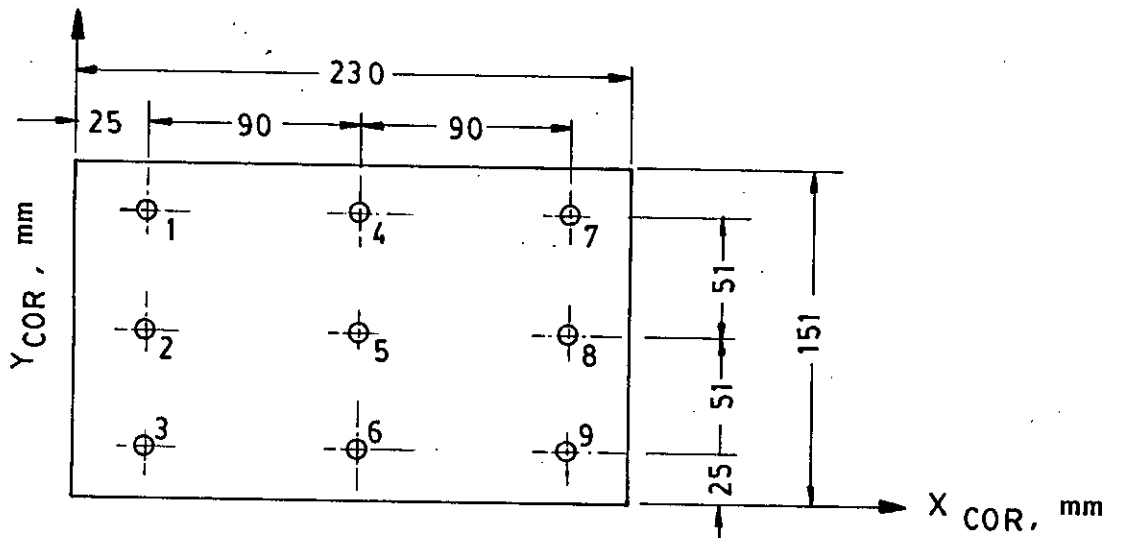


FIG. 6.1 TEMPERATURE DISTRIBUTION OVER THE TEST SECTION OF THE HOT TRAPEZOIDAL CORRUGATED PLATE



POSITION OF THE THERMOCOUPLES IN THE TEST SECTION OF THE HOT RECTANGULAR CORRUGATED PLATE

$$A = 4.70, \theta = 30^\circ$$

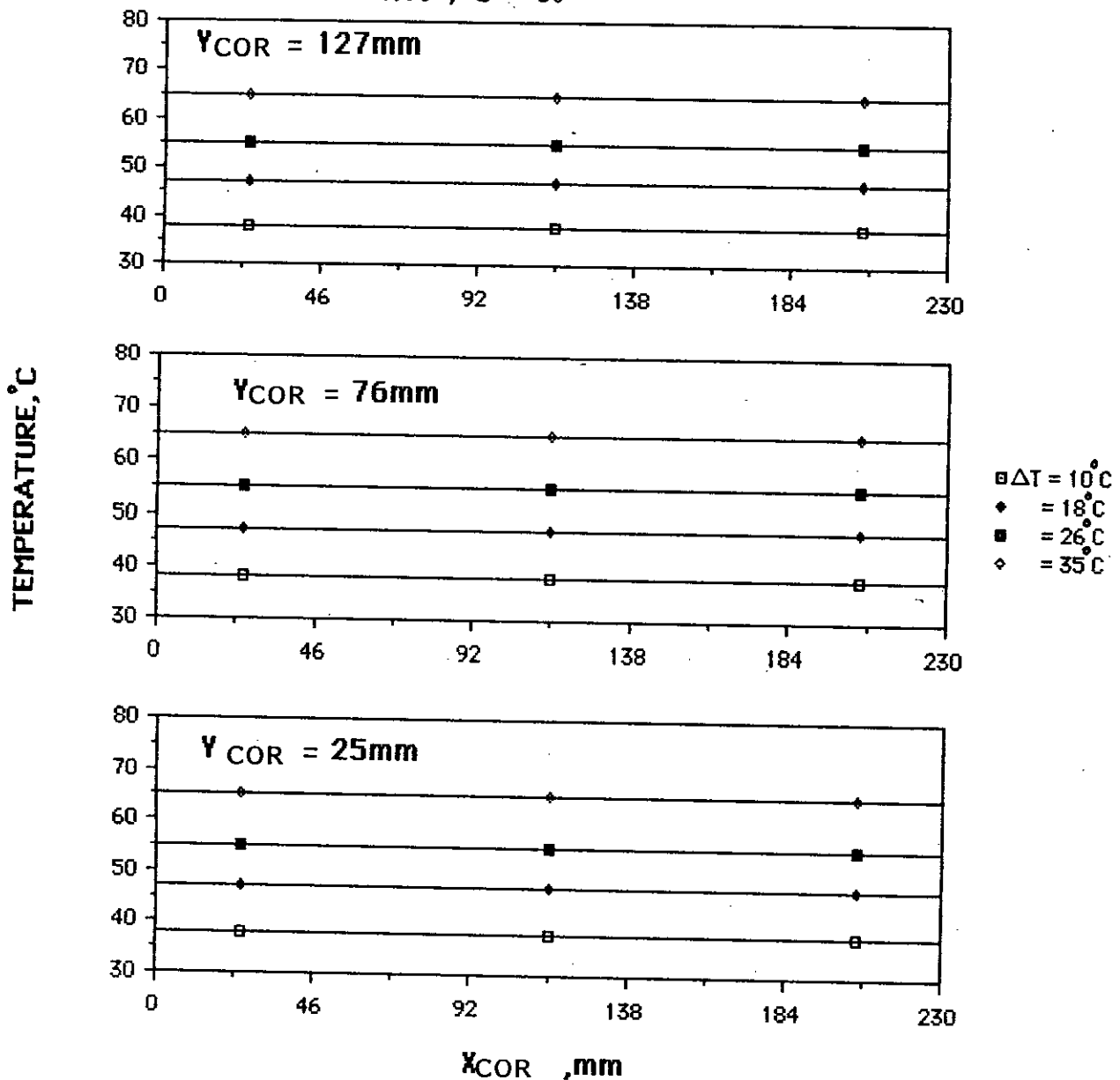
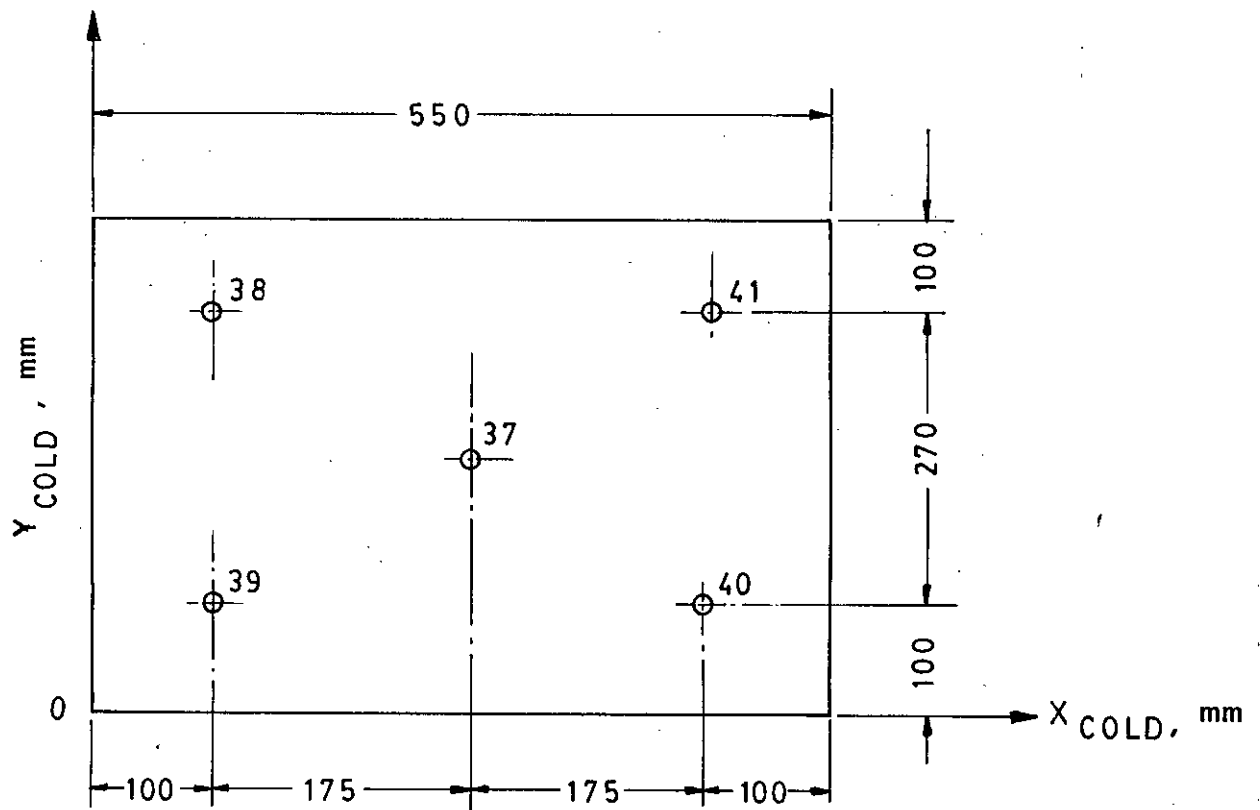


FIG. 6.2 TEMPERATURE DISTRIBUTION OVER THE TEST SECTION OF THE HOT RECTANGULAR CORRUGATED PLATE



POSITION OF THE THERMOCOUPLES IN THE COLD FLAT PLATE

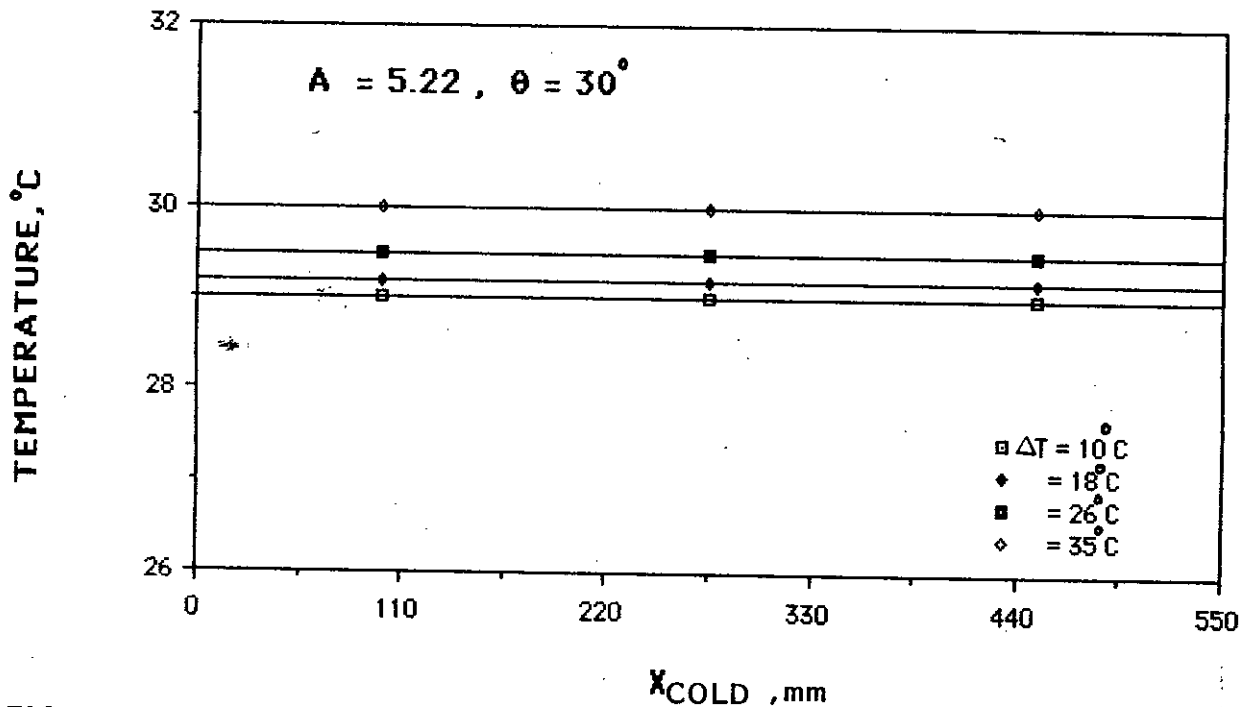
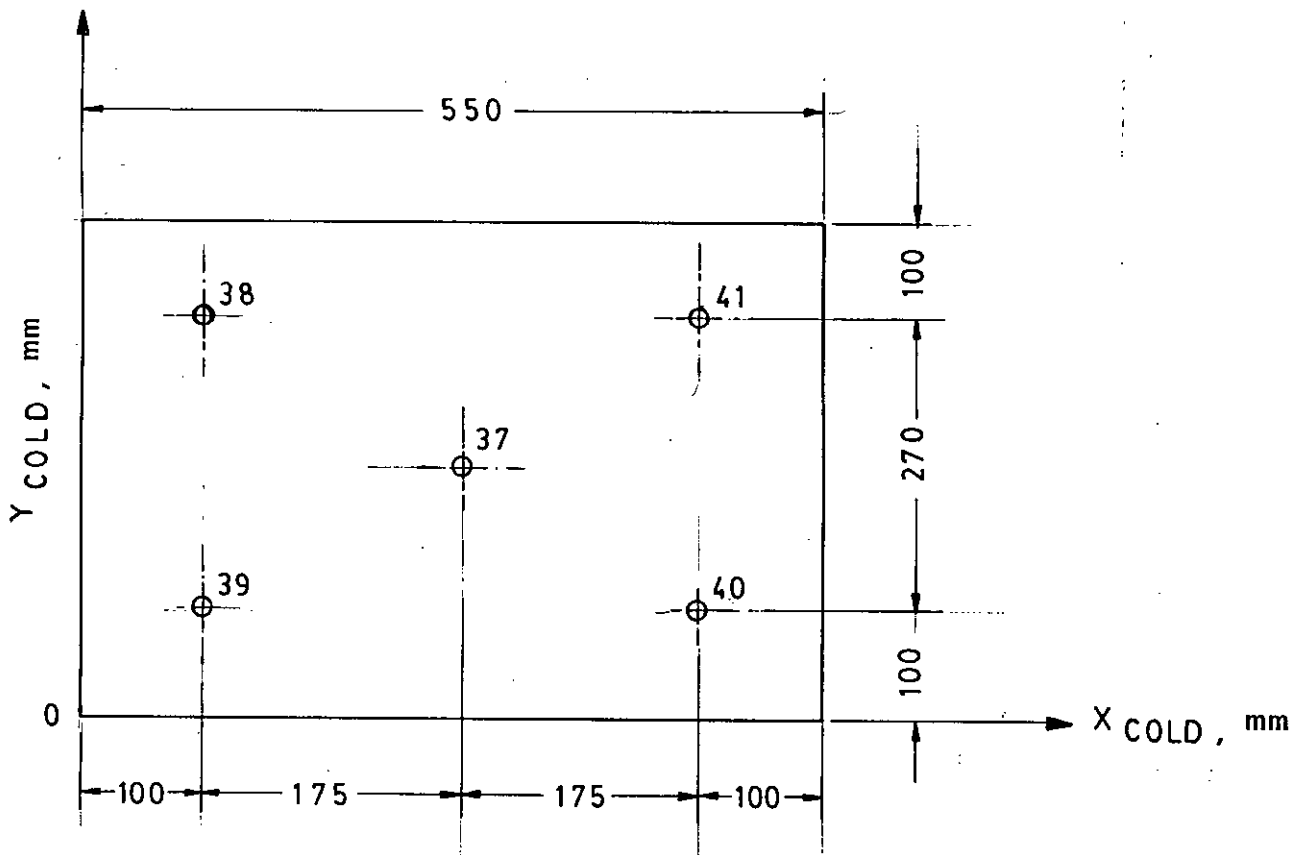


FIG. 6.3 TEMPERATURE DISTRIBUTION OVER THE COLD FLAT PLATE



POSITION OF THE THERMOCOUPLES IN THE COLD FLAT PLATE

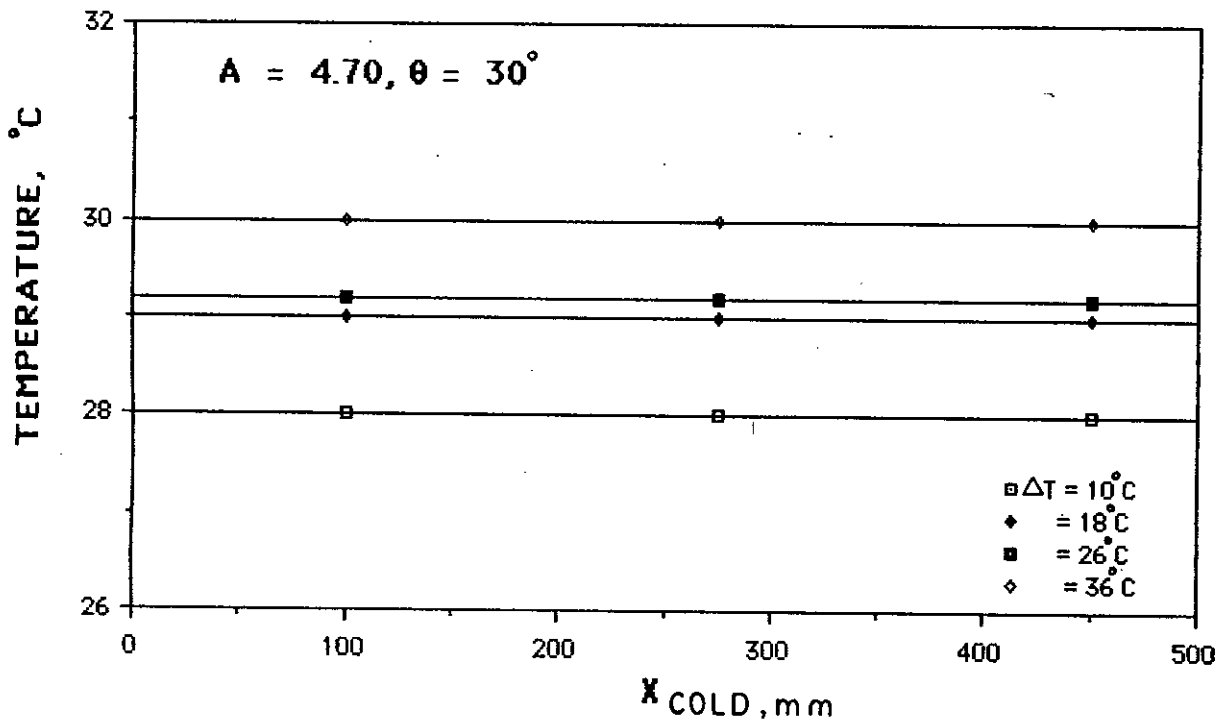


FIG. 6.4 TEMPERATURE DISTRIBUTION OVER THE COLD FLAT PLATE

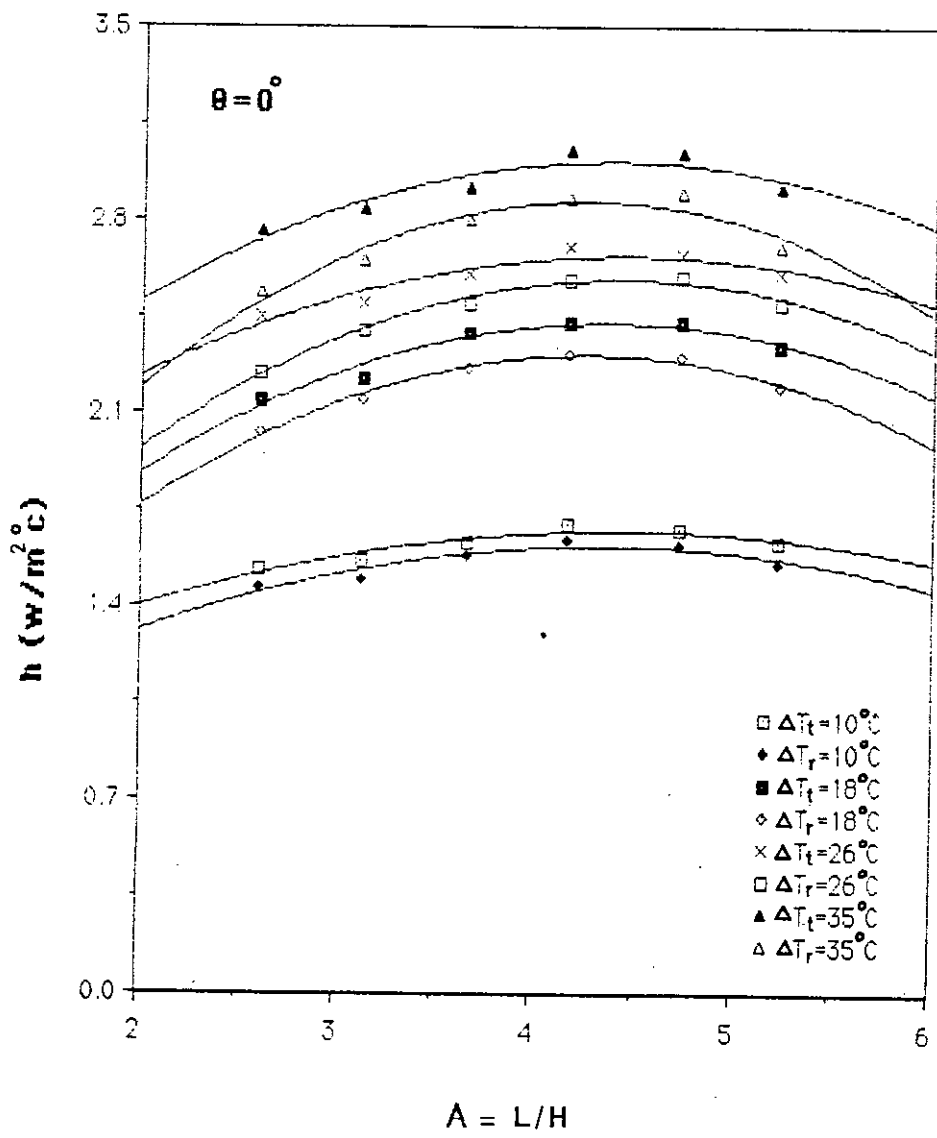


FIG.6.5 EFFECT OF ASPECT RATIO ON AVERAGE HEAT TRANSFER COEFFICIENT FOR $\theta = 0^\circ$

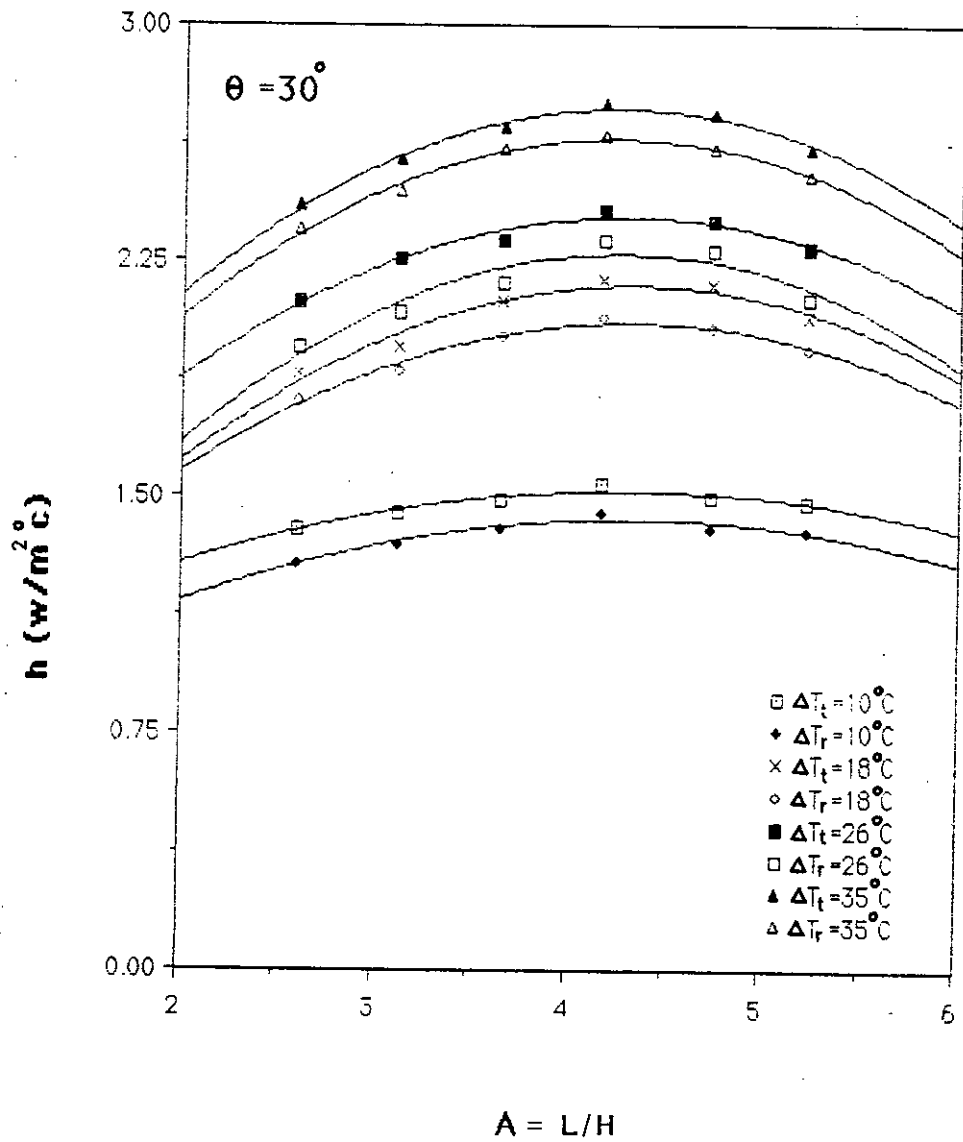


FIG. 6.6 EFFECT OF ASPECT RATIO ON AVERAGE HEAT TRANSFER COEFFICIENT FOR $\theta = 30^\circ$

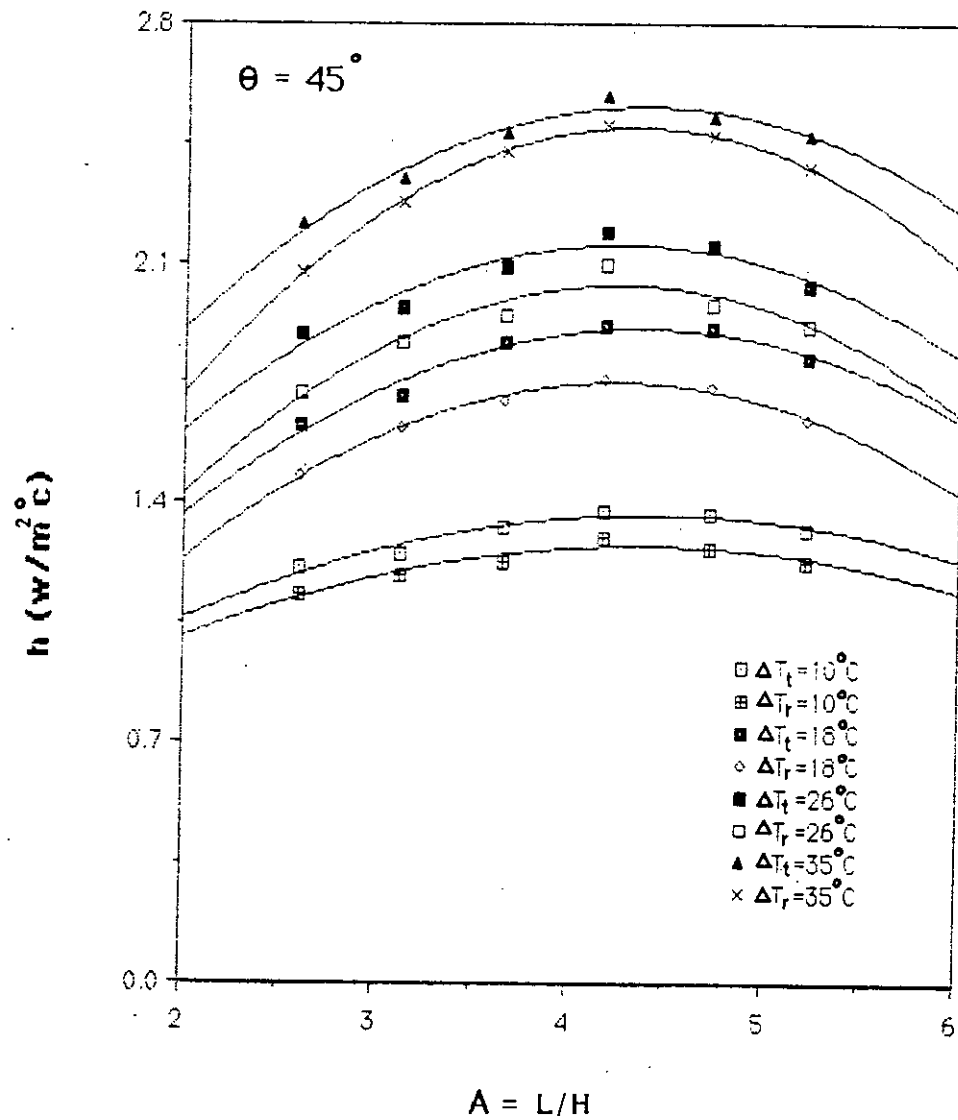


FIG.6.7 EFFECT OF ASPECT RATIO ON AVERAGE HEAT TRANSFER COEFFICIENT FOR $\theta = 45^\circ$

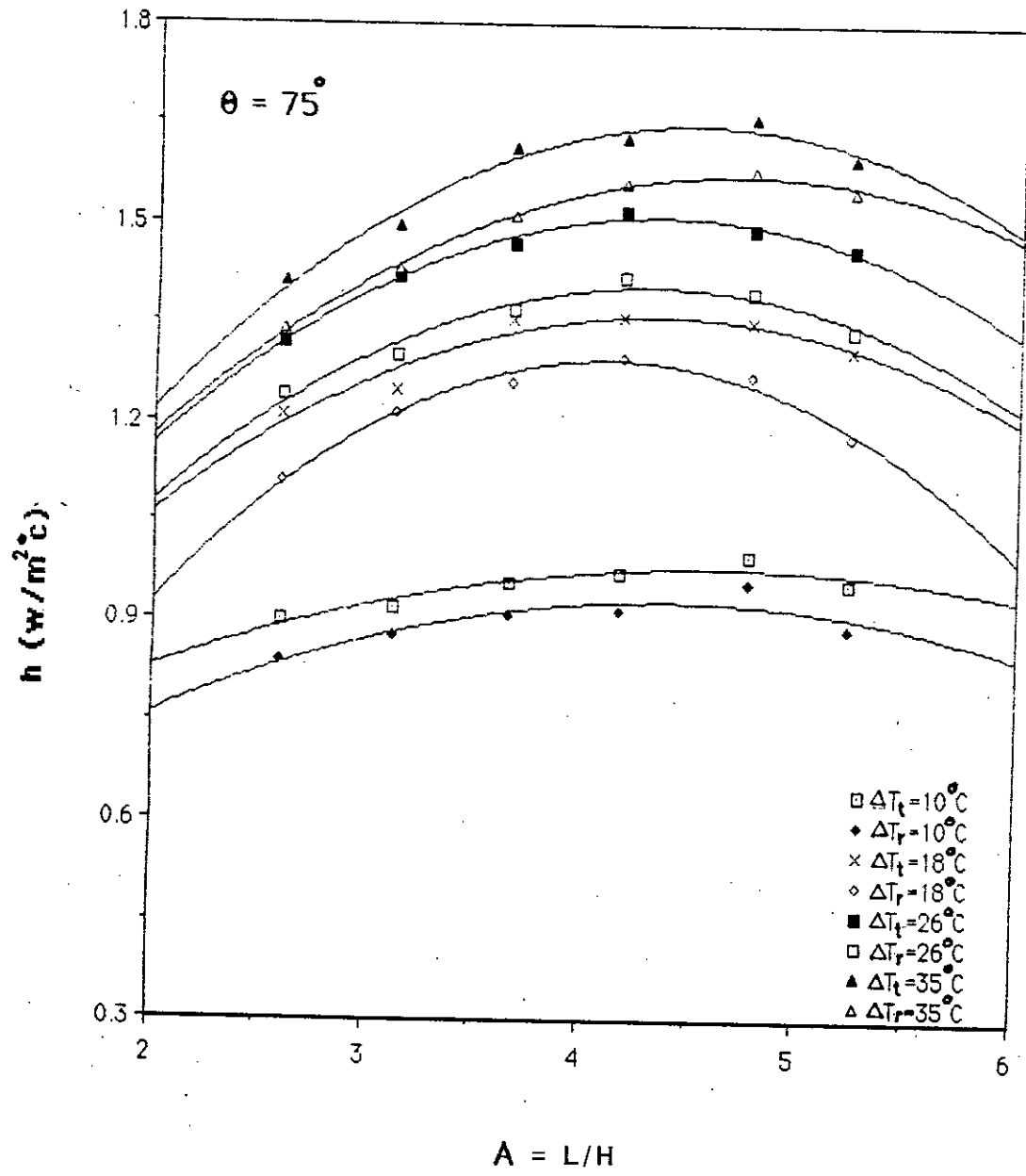


FIG.6.8 EFFECT OF ASPECT RATIO ON AVERAGE HEAT TRANSFER COEFFICIENT FOR $\theta = 75^\circ$

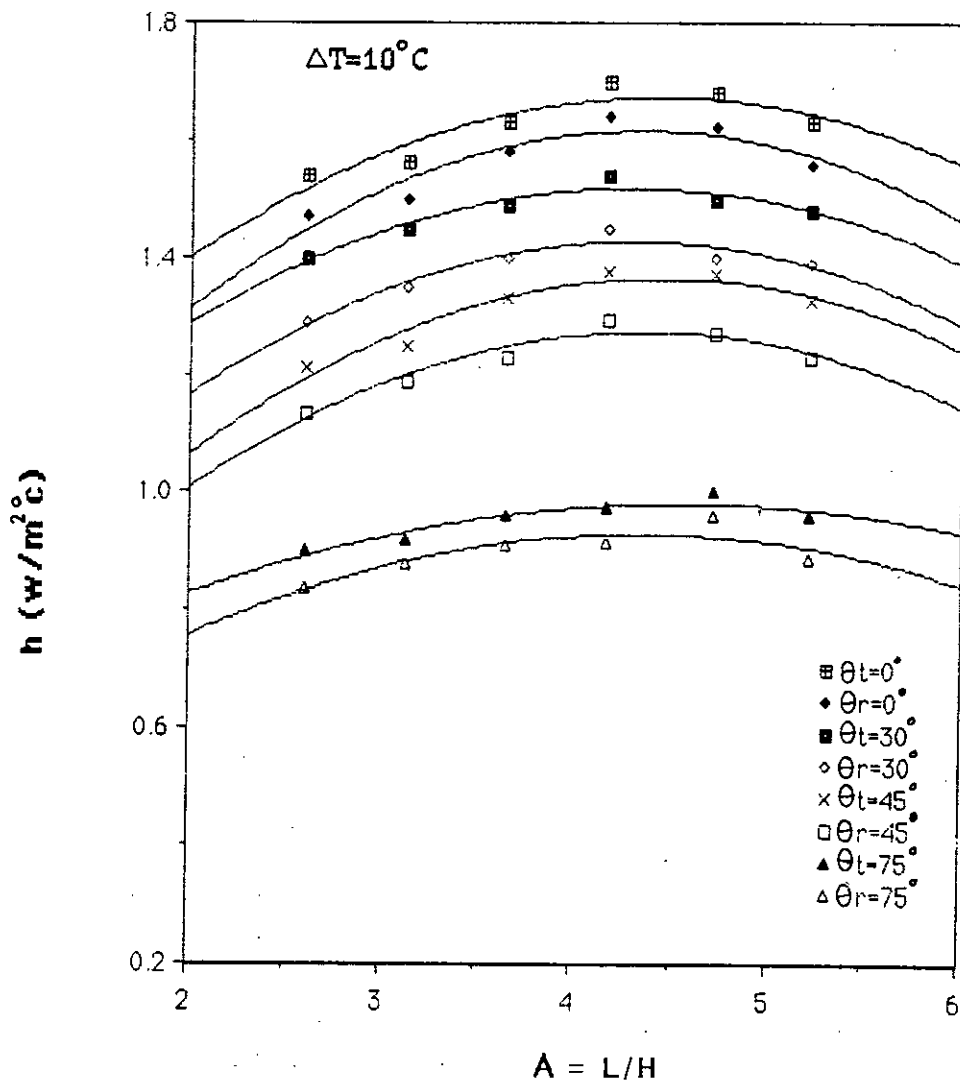


FIG.6.9 EFFECT OF ASPECT RATIO ON AVERAGE HEAT TRANSFER COEFFICIENT FOR $\Delta T = 10^\circ \text{C}$

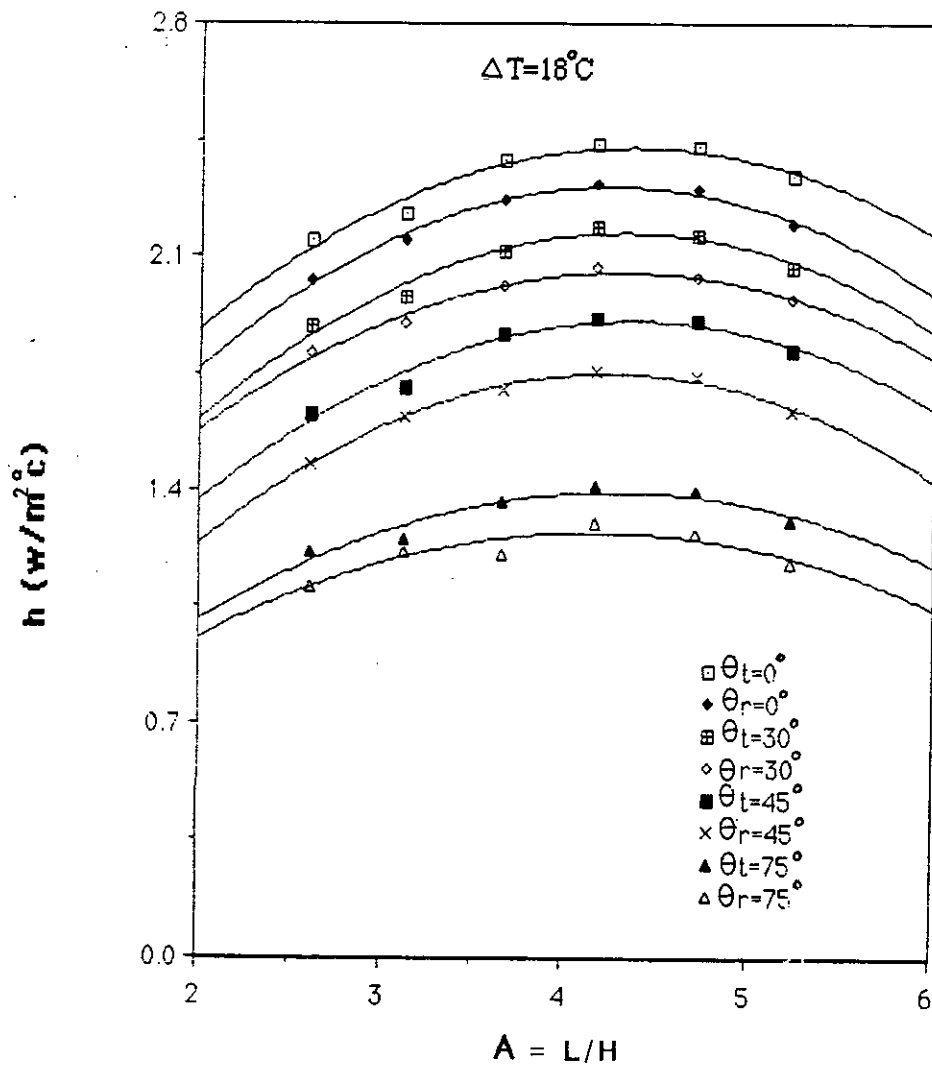


FIG.6.10 EFFECT OF ASPECT RATIO ON AVERAGE HEAT TRANSFER COEFFICIENT FOR $\Delta T = 18^\circ\text{C}$

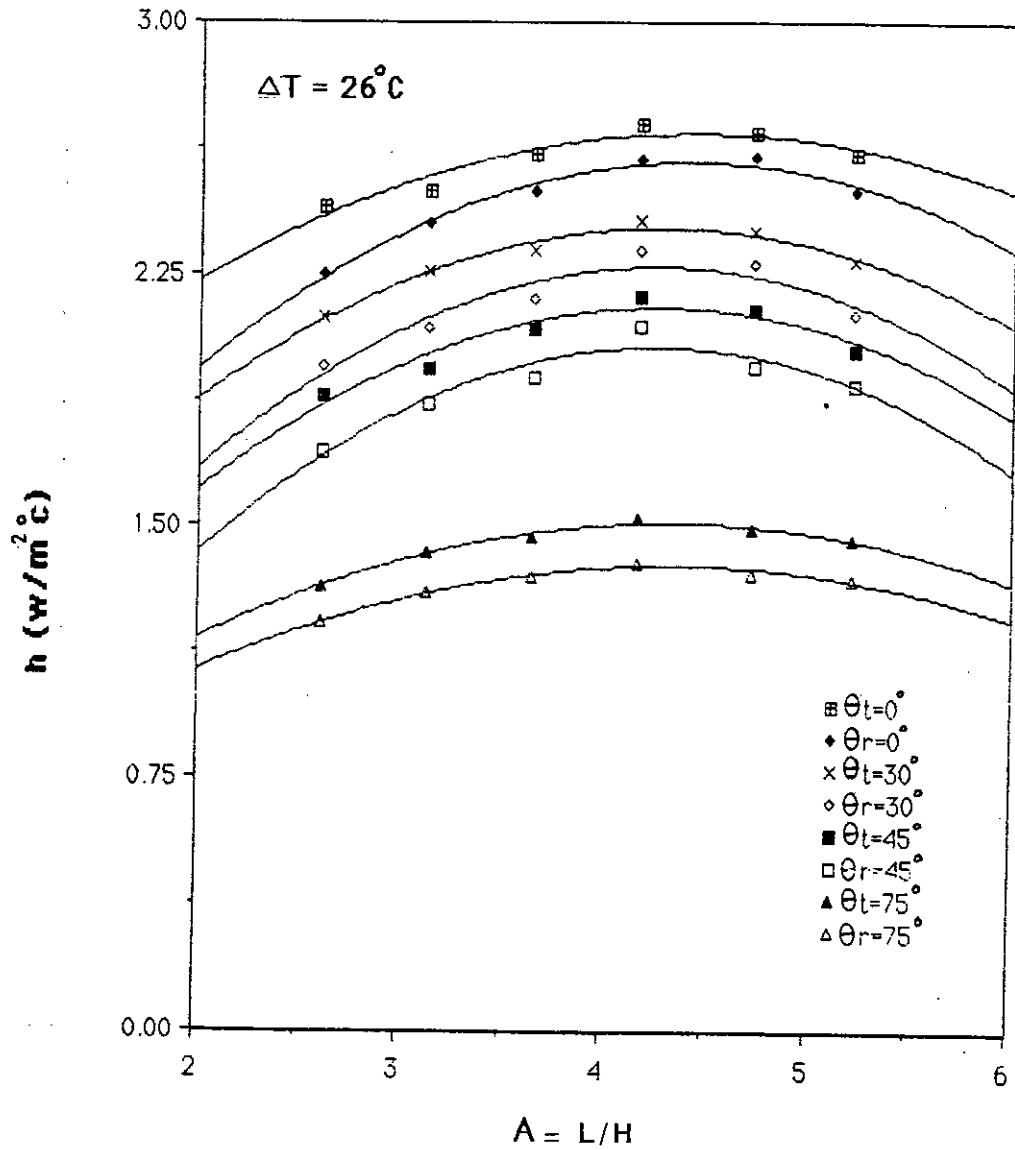


FIG.6.11 EFFECT OF ASPECT RATIO ON AVERAGE HEAT TRANSFER COEFFICIENT FOR $\Delta T = 26^\circ\text{C}$

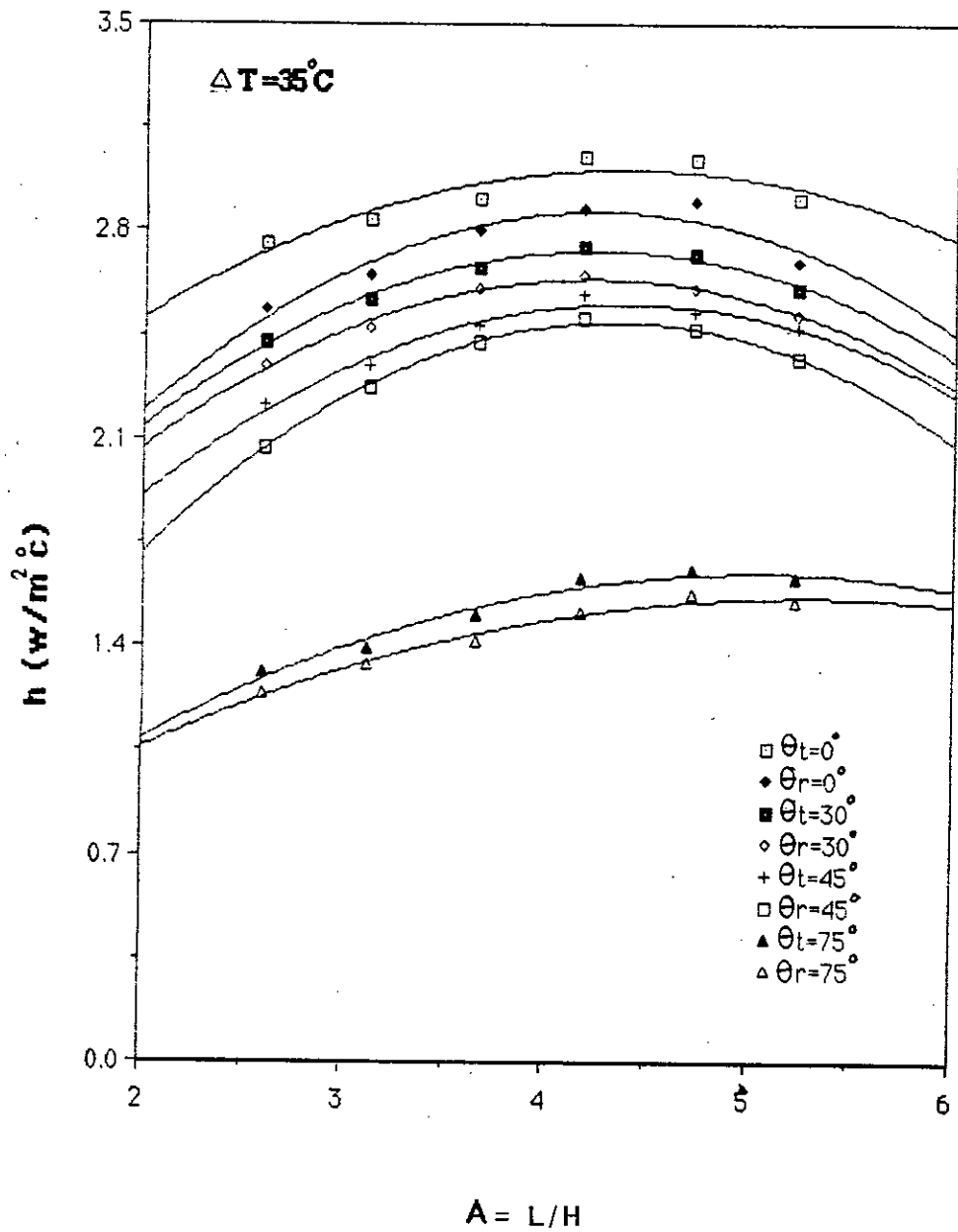


FIG.6.12 EFFECT OF ASPECT RATIO ON AVERAGE HEAT TRANSFER COEFFICIENT FOR $\Delta T = 35^\circ\text{C}$

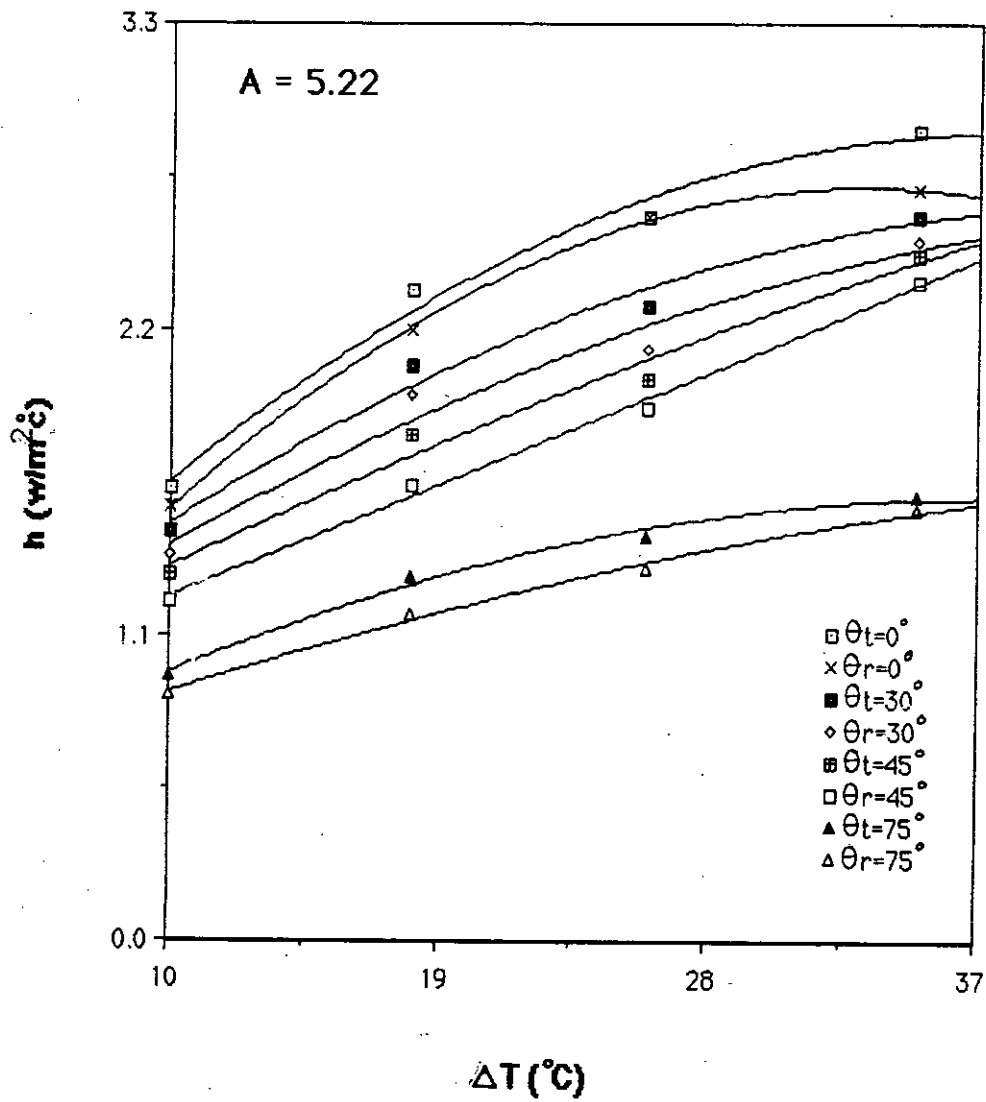


FIG. 6.13 EFFECT OF TEMPERATURE POTENTIAL ON AVERAGE HEAT TRANSFER COEFFICIENT FOR $A = 5.22$

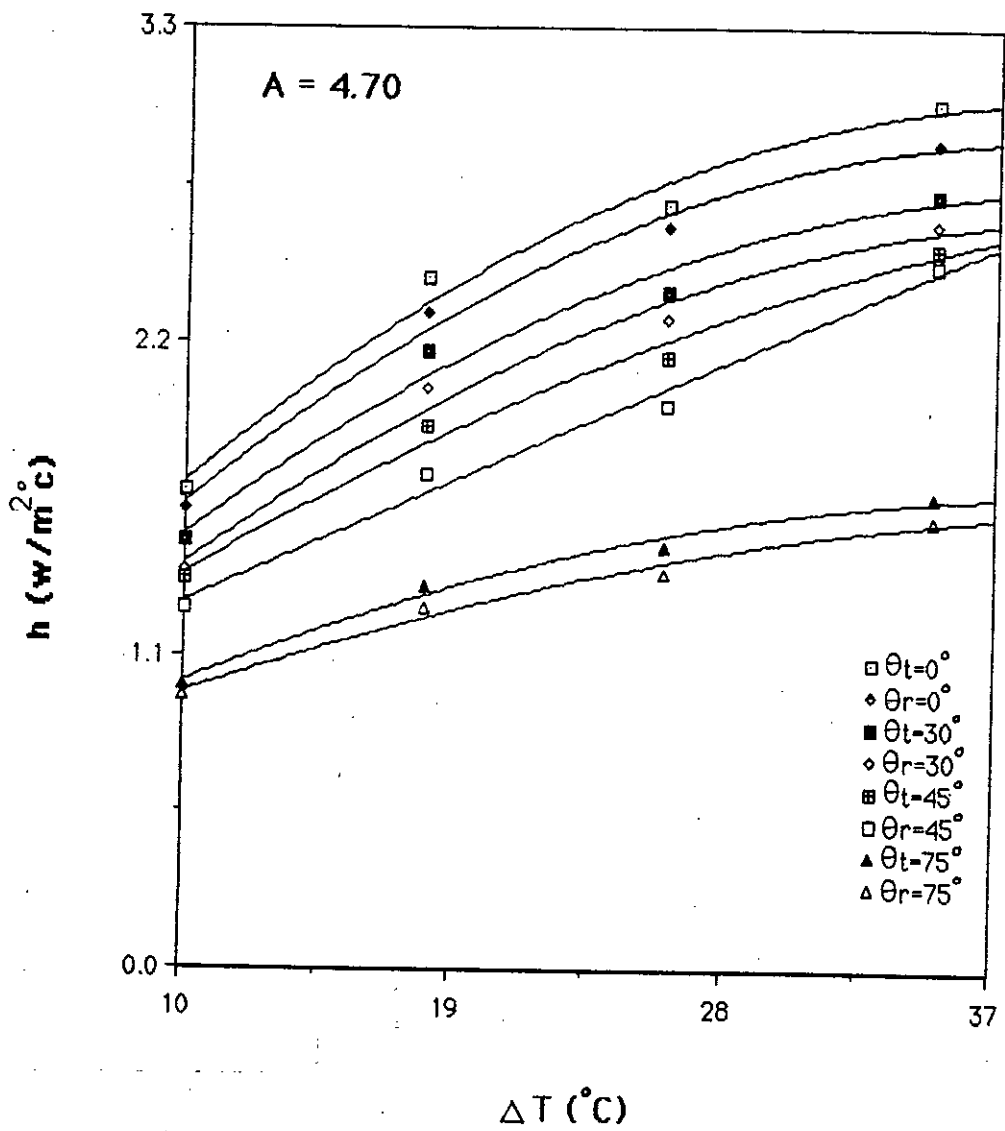


FIG. 6.14 EFFECT OF TEMPERATURE POTENTIAL ON AVERAGE HEAT TRANSFER COEFFICIENT FOR $A = 4.70$

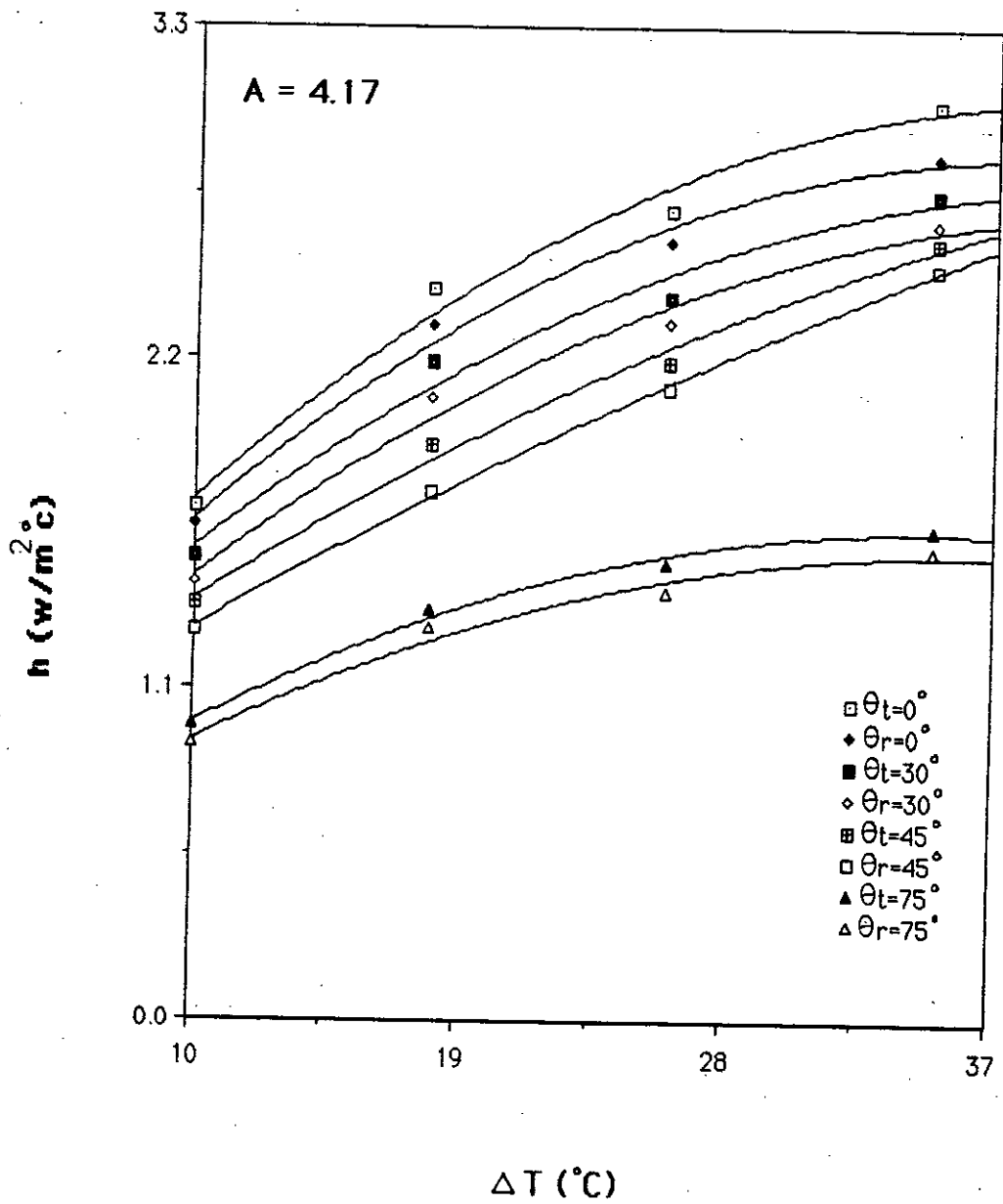


FIG. 6.15 EFFECT OF TEMPERATURE POTENTIAL ON AVERAGE HEAT TRANSFER COEFFICIENT FOR $A = 4.17$

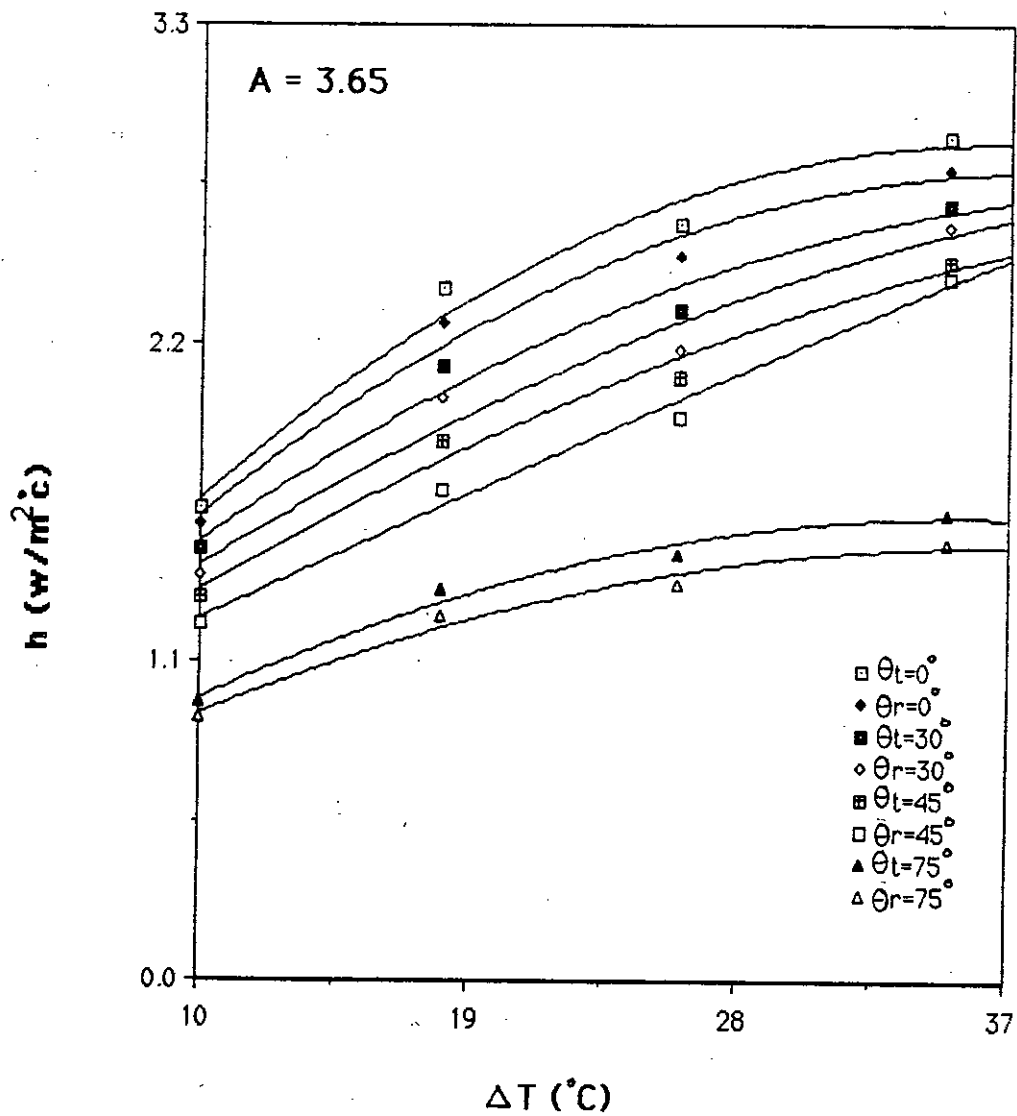


FIG. 6.16 EFFECT OF TEMPERATURE POTENTIAL ON AVERAGE HEAT TRANSFER COEFFICIENT FOR A = 3.65

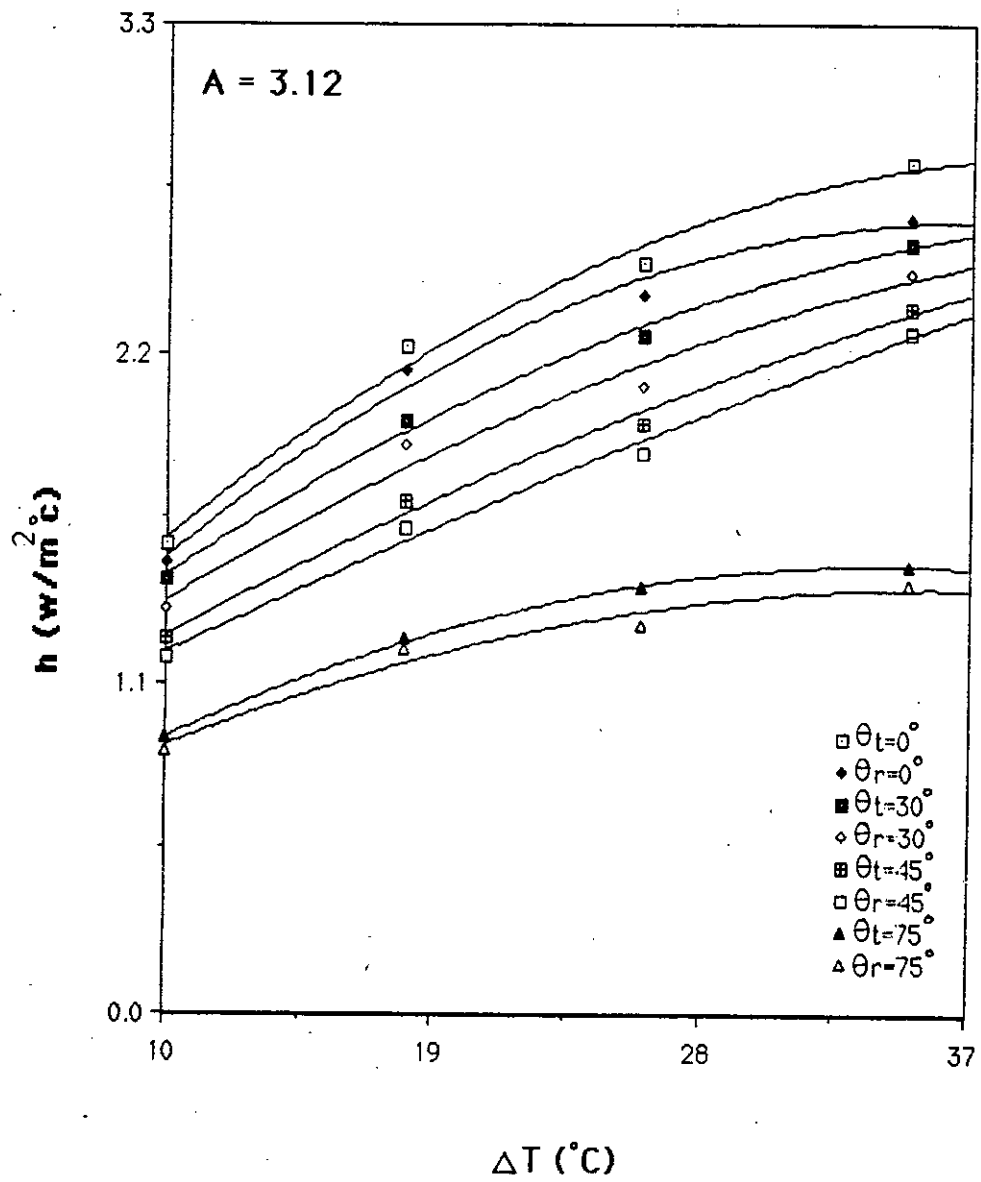


FIG. 6.17 EFFECT OF TEMPERATURE POTENTIAL ON AVERAGE HEAT TRANSFER COEFFICIENT FOR $A = 3.12$

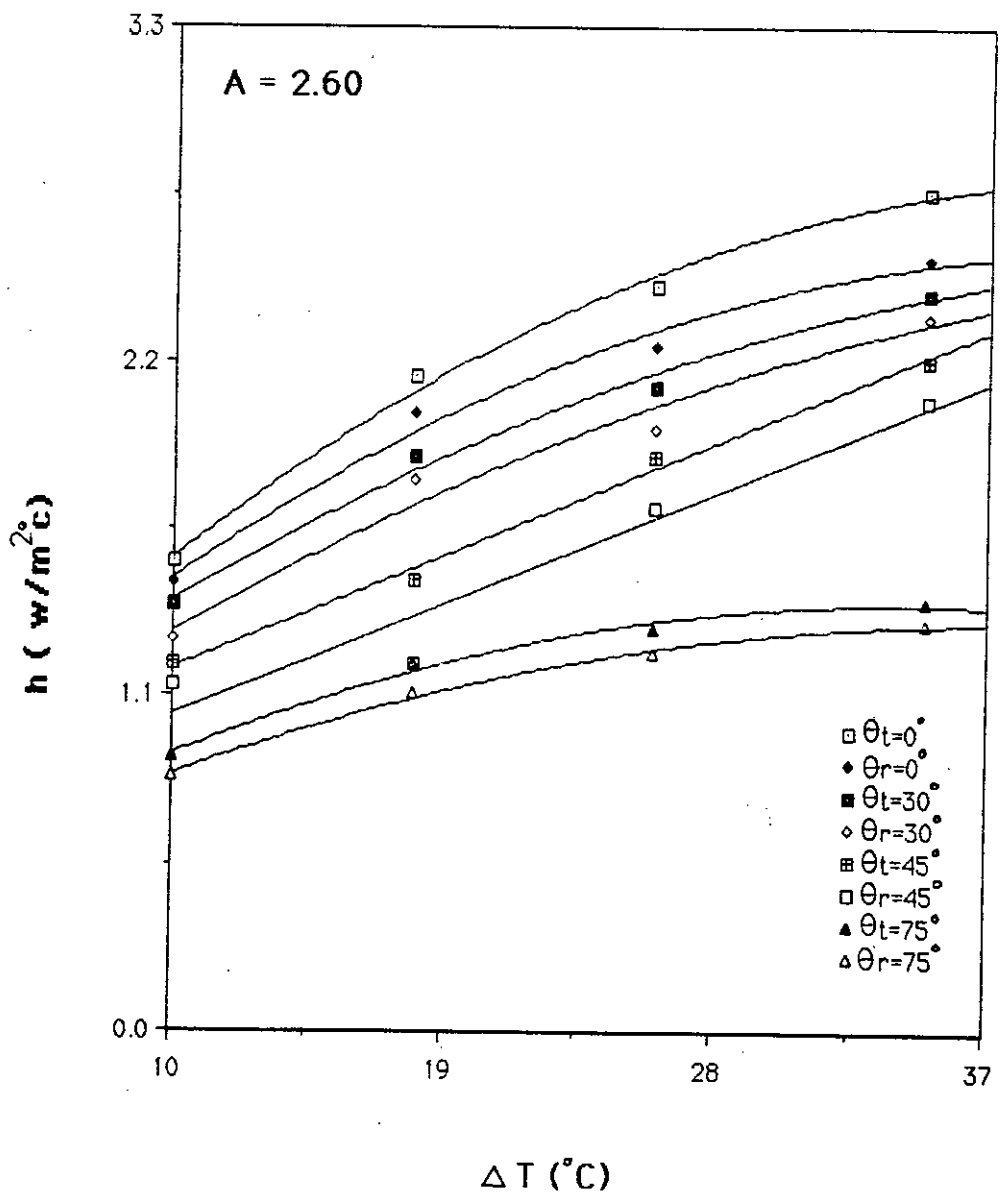


FIG. 6.18 EFFECT OF TEMPERATURE POTENTIAL ON AVERAGE HEAT TRANSFER COEFFICIENT FOR A = 2.60

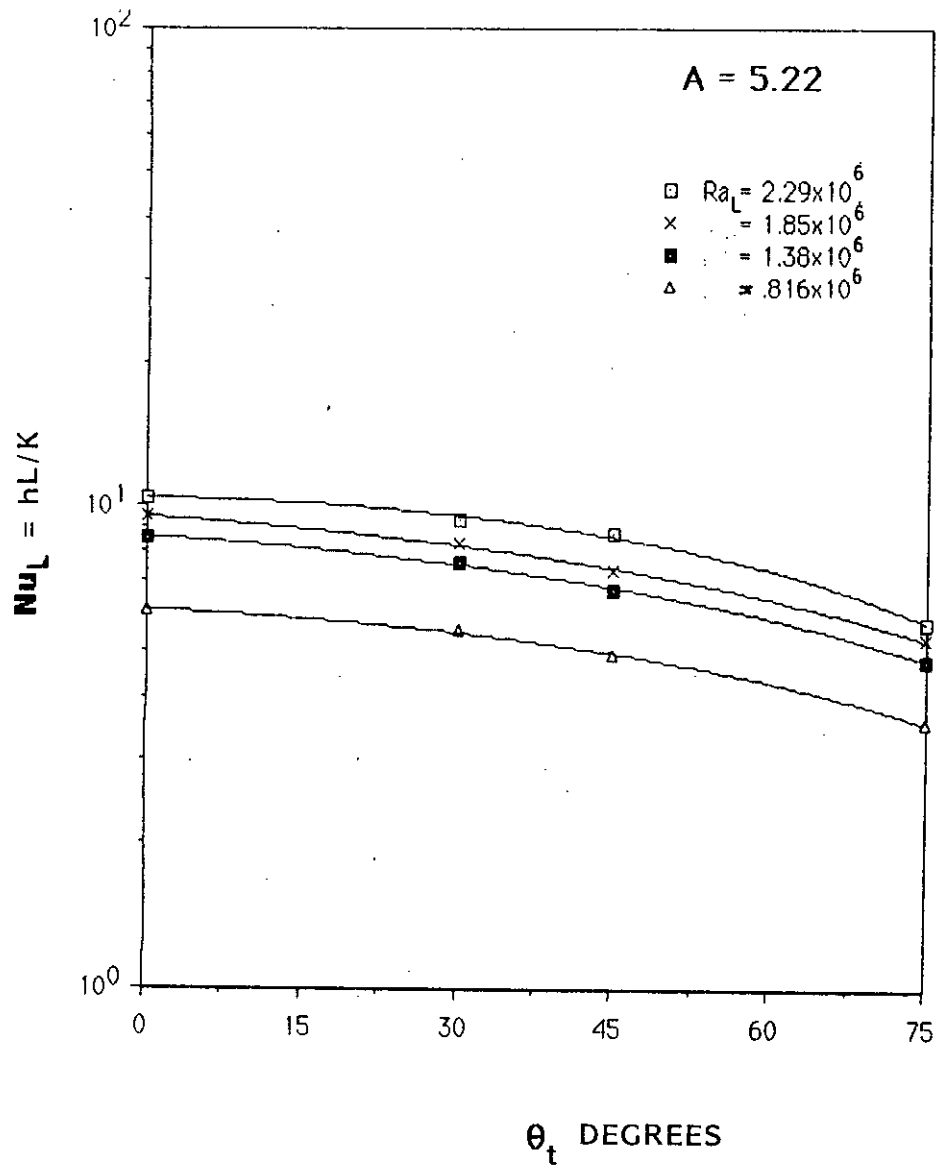


FIG. 6.19 EFFECT OF ANGLE OF INCLINATION OF TRAPEZOIDAL CORRUGATION ON NUSSELT NUMBER FOR $A = 5.22$

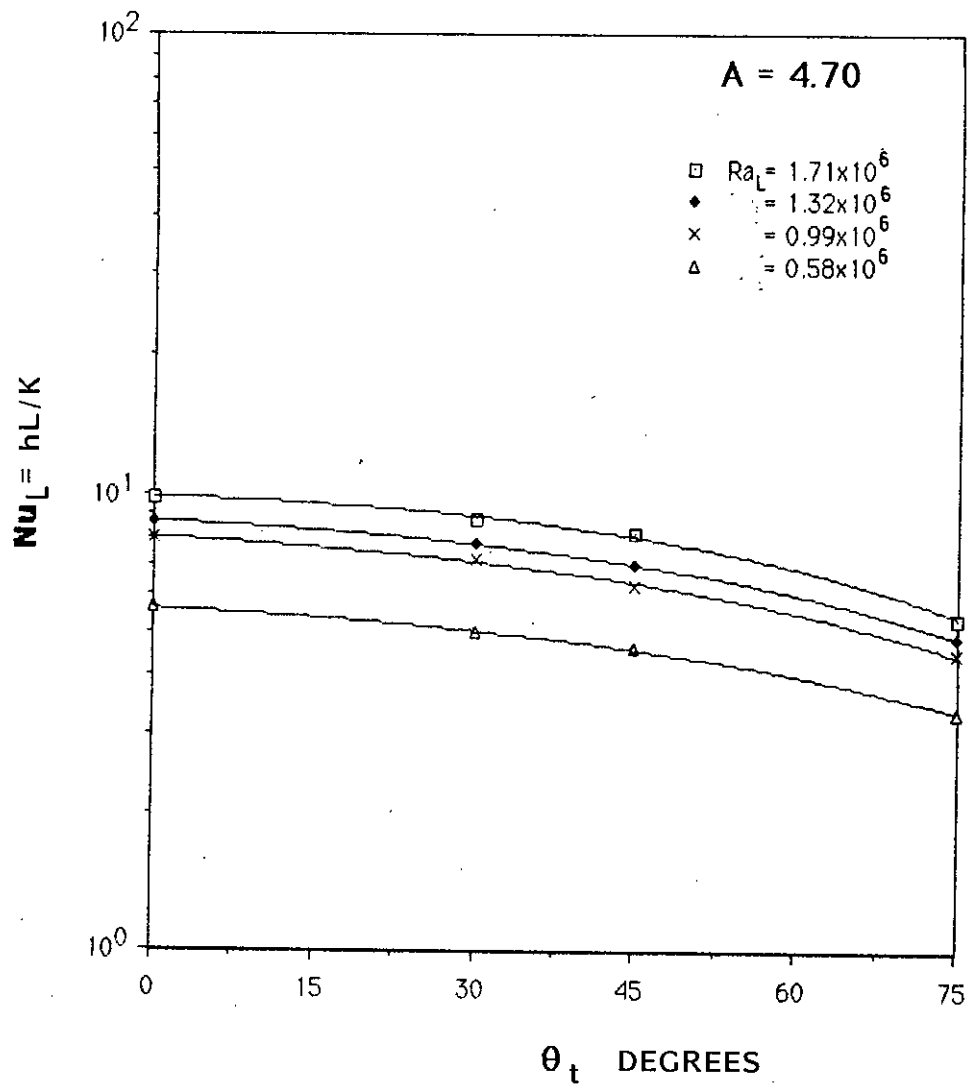


FIG. 6.20 EFFECT OF ANGLE OF INCLINATION OF TRAPEZOIDAL CORRUGATION ON NUSSELT NUMBER FOR $A = 4.70$

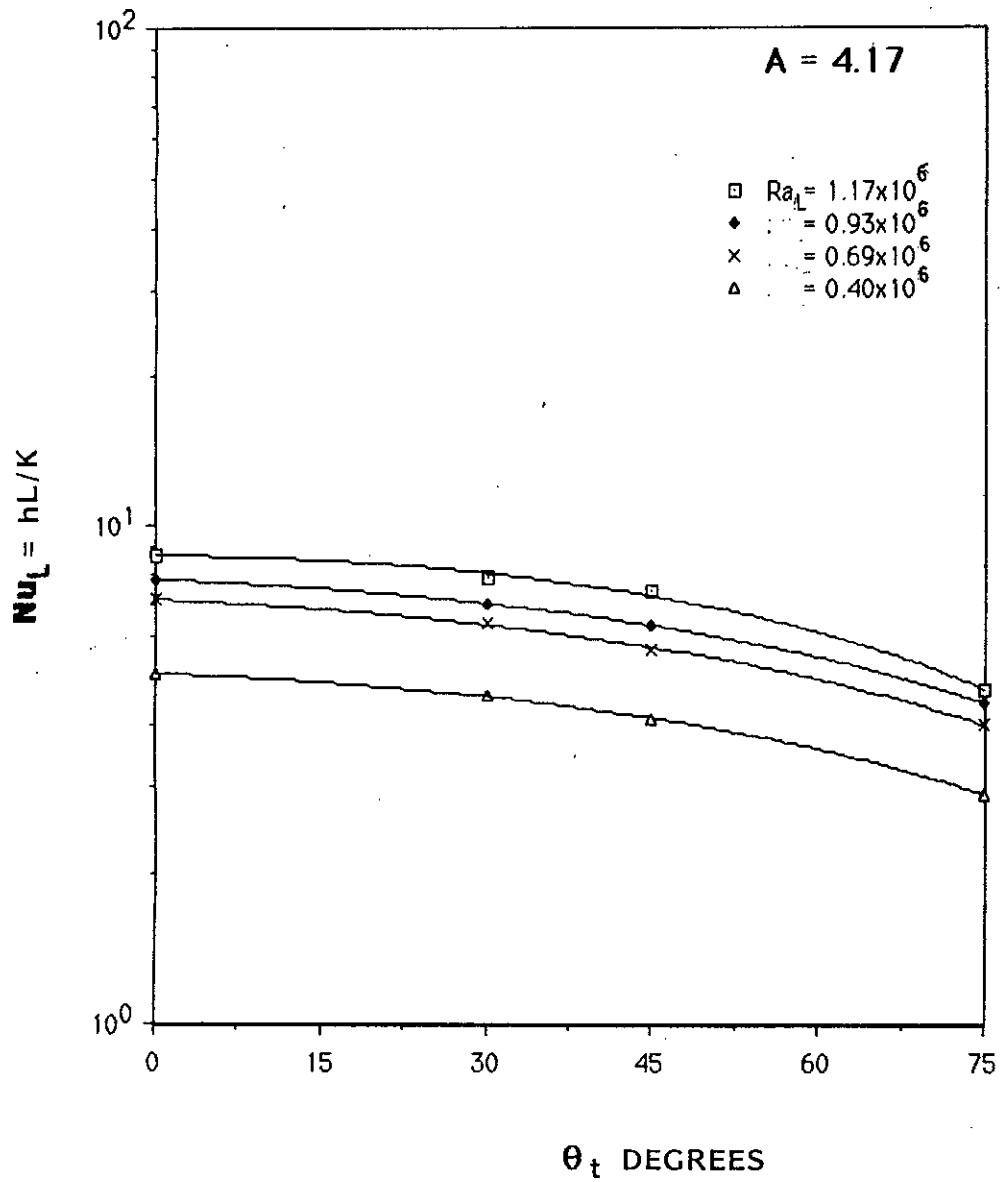


FIG.6.21 EFFECT OF ANGLE OF INCLINATION OF TRAPEZOIDAL CORRUGATION ON NUSSELT NUMBER FOR $A = 4.17$

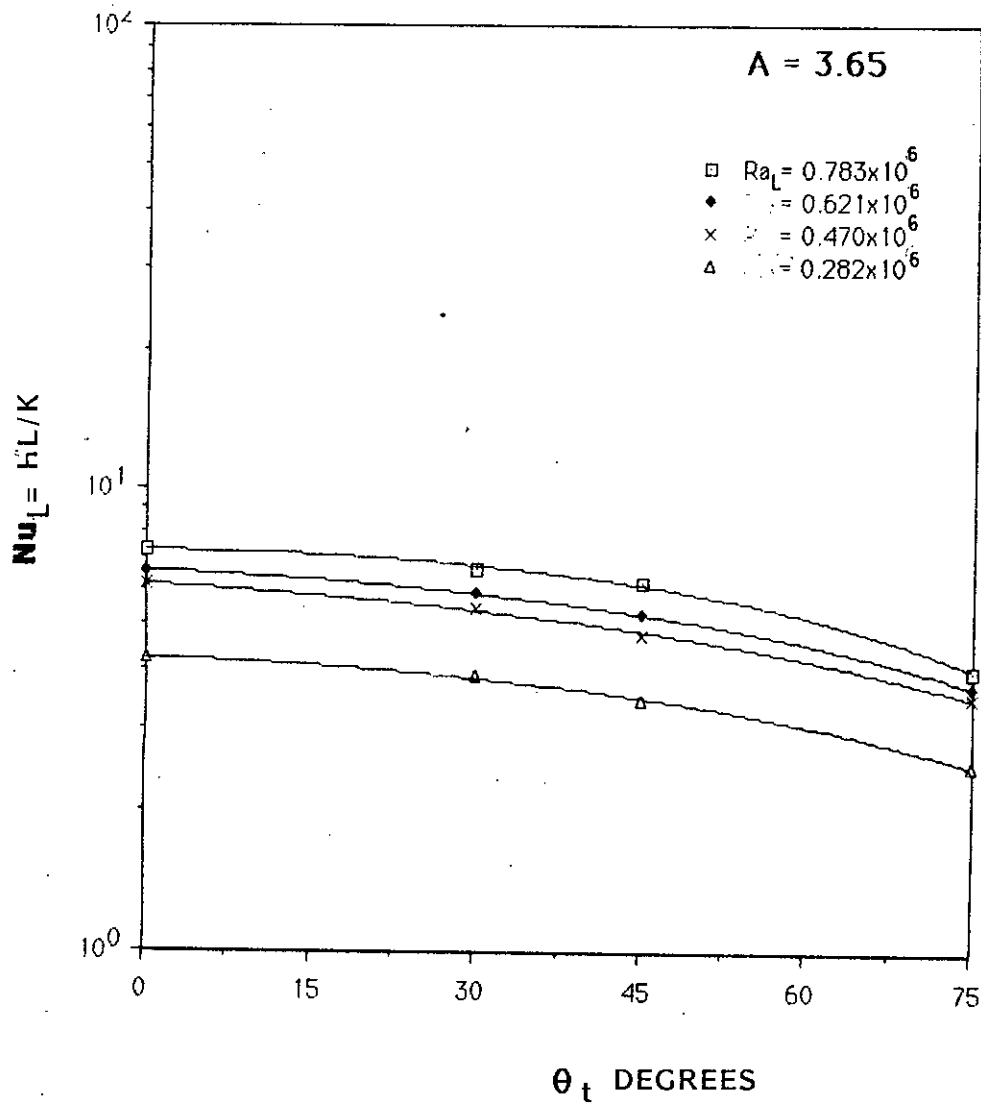


FIG.6.22 EFFECT OF ANGLE OF INCLINATION OF TRAPEZOIDAL CORRUGATION ON NUSSELT NUMBER FOR A = 3.65

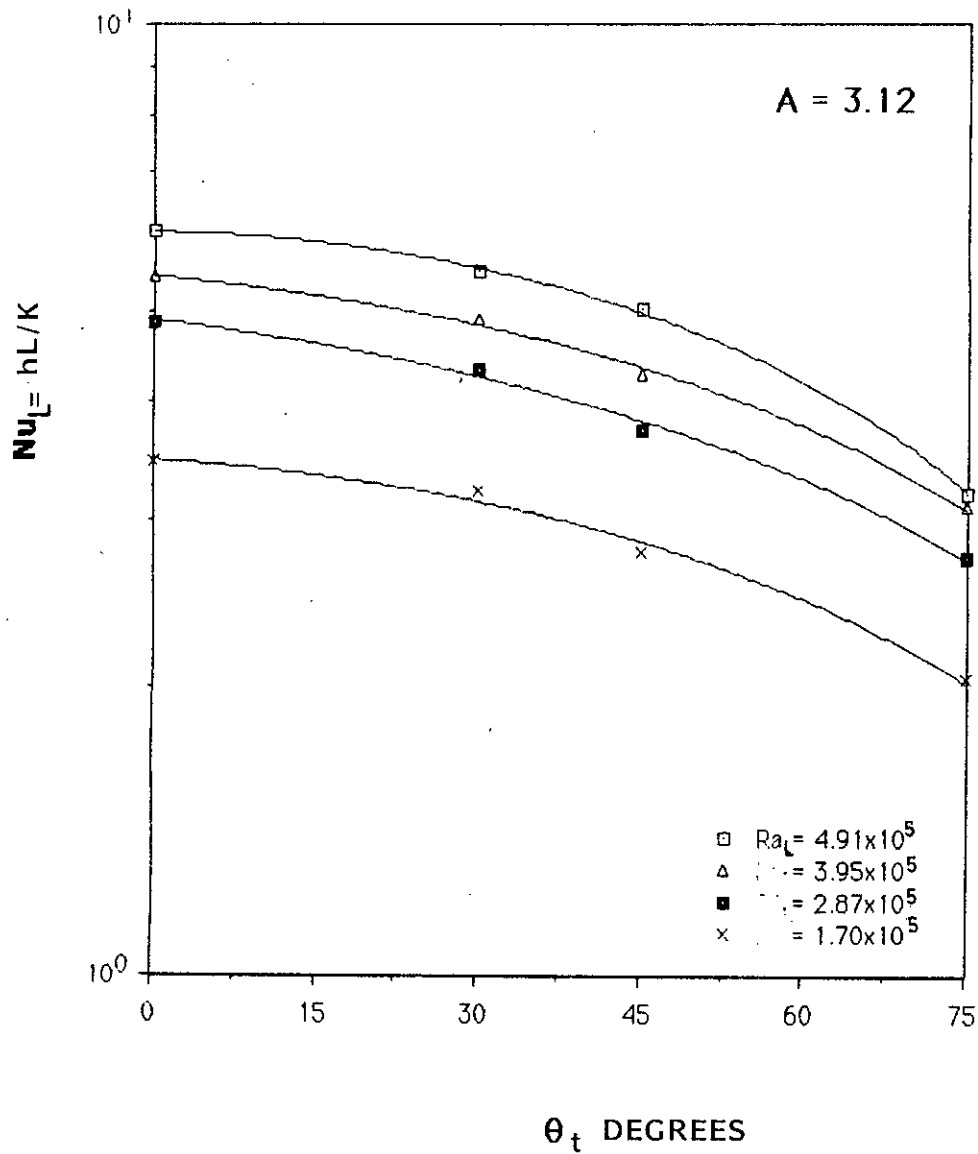


FIG. 6.23 EFFECT OF ANGLE OF INCLINATION OF TRAPEZOIDAL CORRUGATION ON NUSSELT NUMBER FOR $A = 3.12$

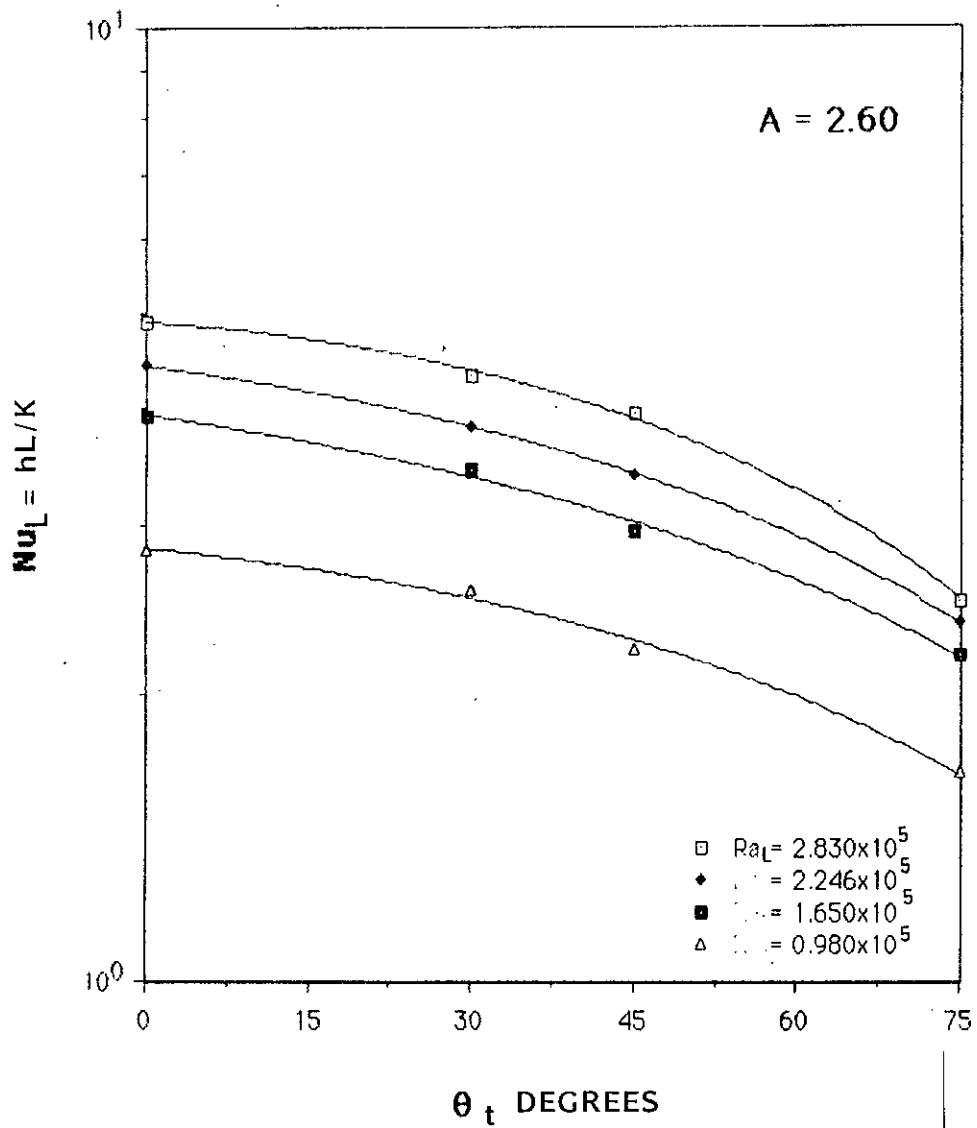


FIG. 6.24 EFFECT OF ANGLE OF INCLINATION OF TRAPEZOIDAL CORRUGATION ON NUSSELT NUMBER FOR $A = 2.60$

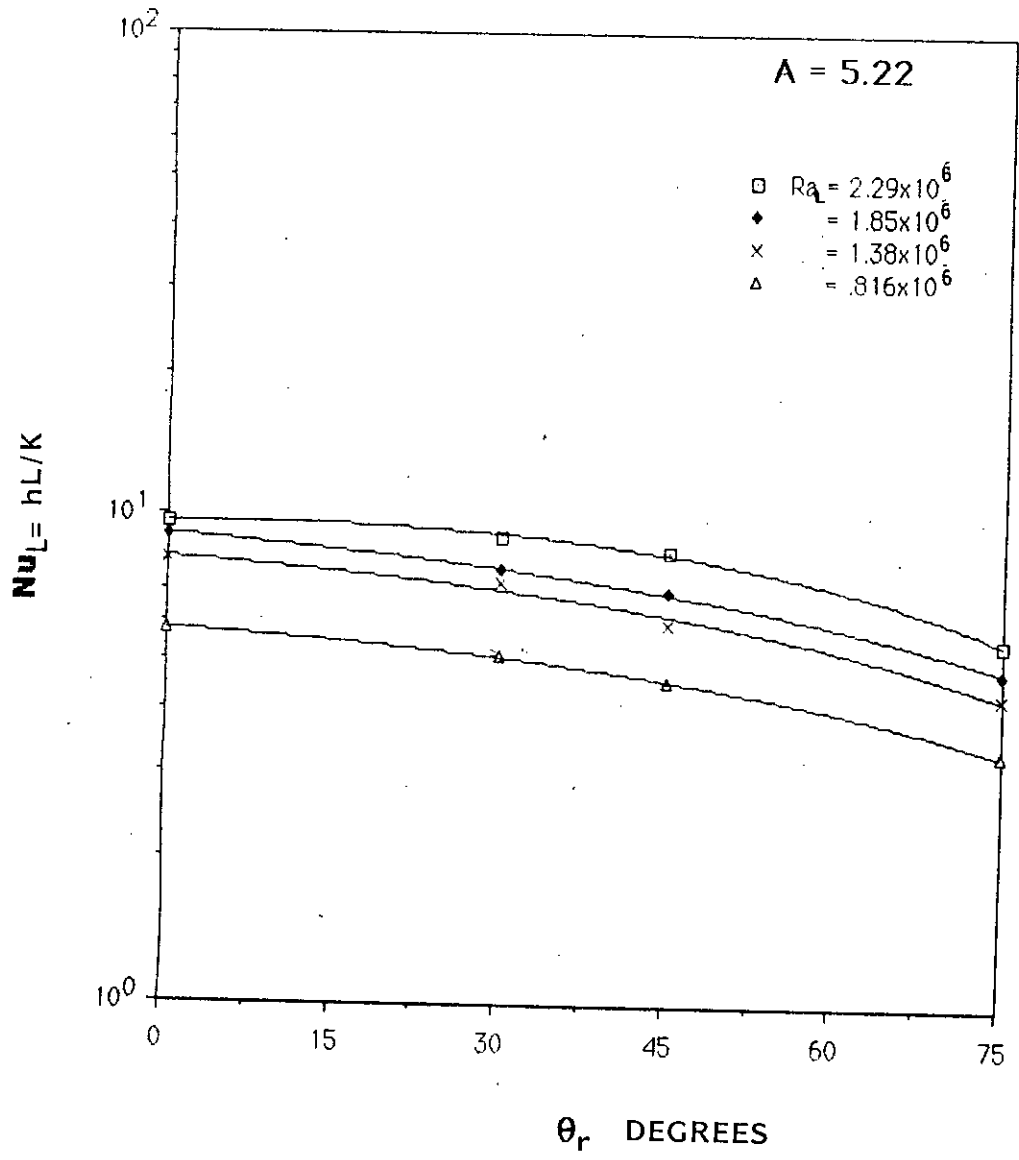


FIG.6.25 EFFECT OF ANGLE OF INCLINATION OF RECTANGULAR CORRUGATION ON NUSSELT NUMBER FOR $A = 5.22$

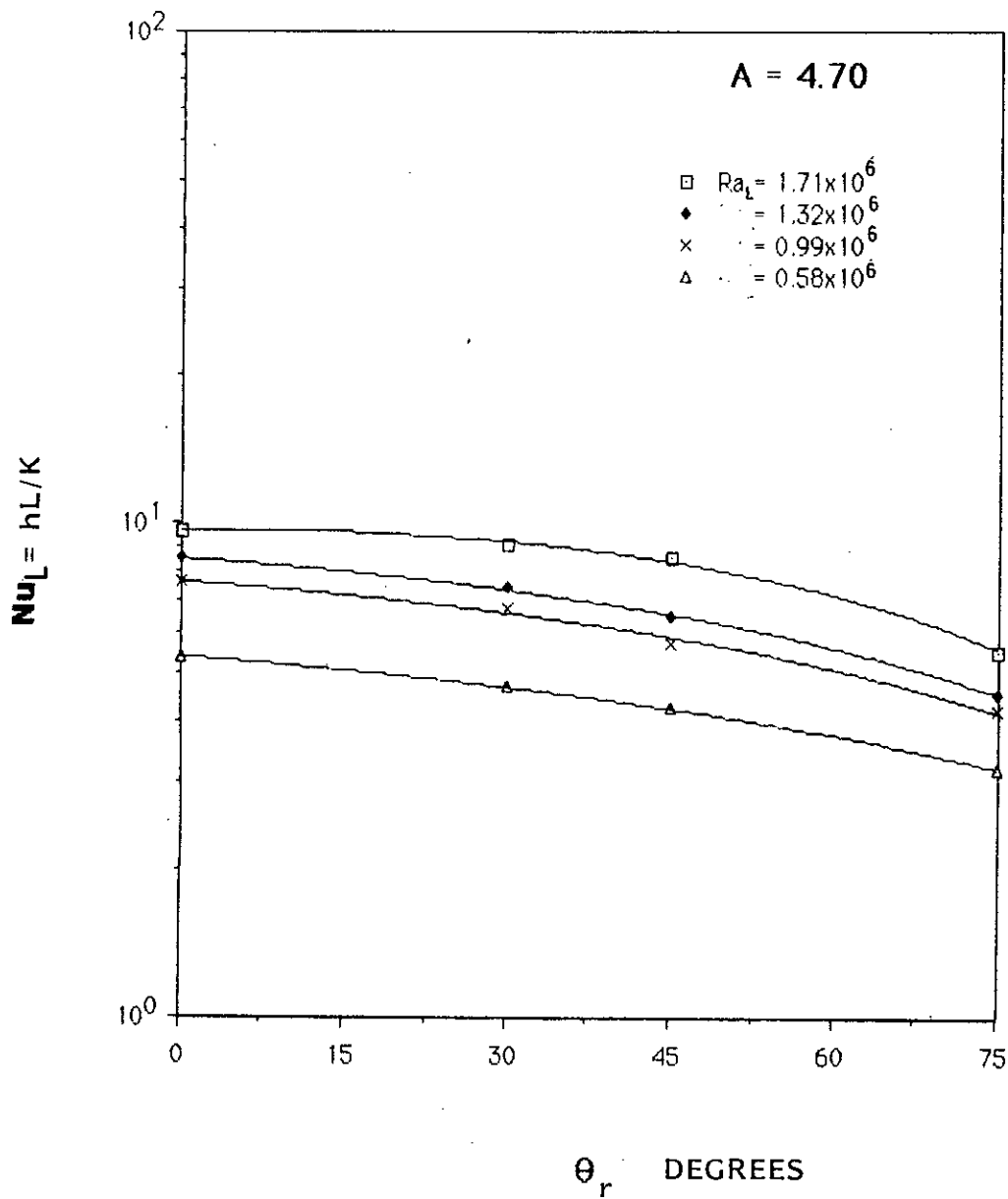


FIG. 6.26 EFFECT OF ANGLE OF INCLINATION OF RECTANGULAR CORRUGATION ON NUSSELT NUMBER FOR $A = 4.70$

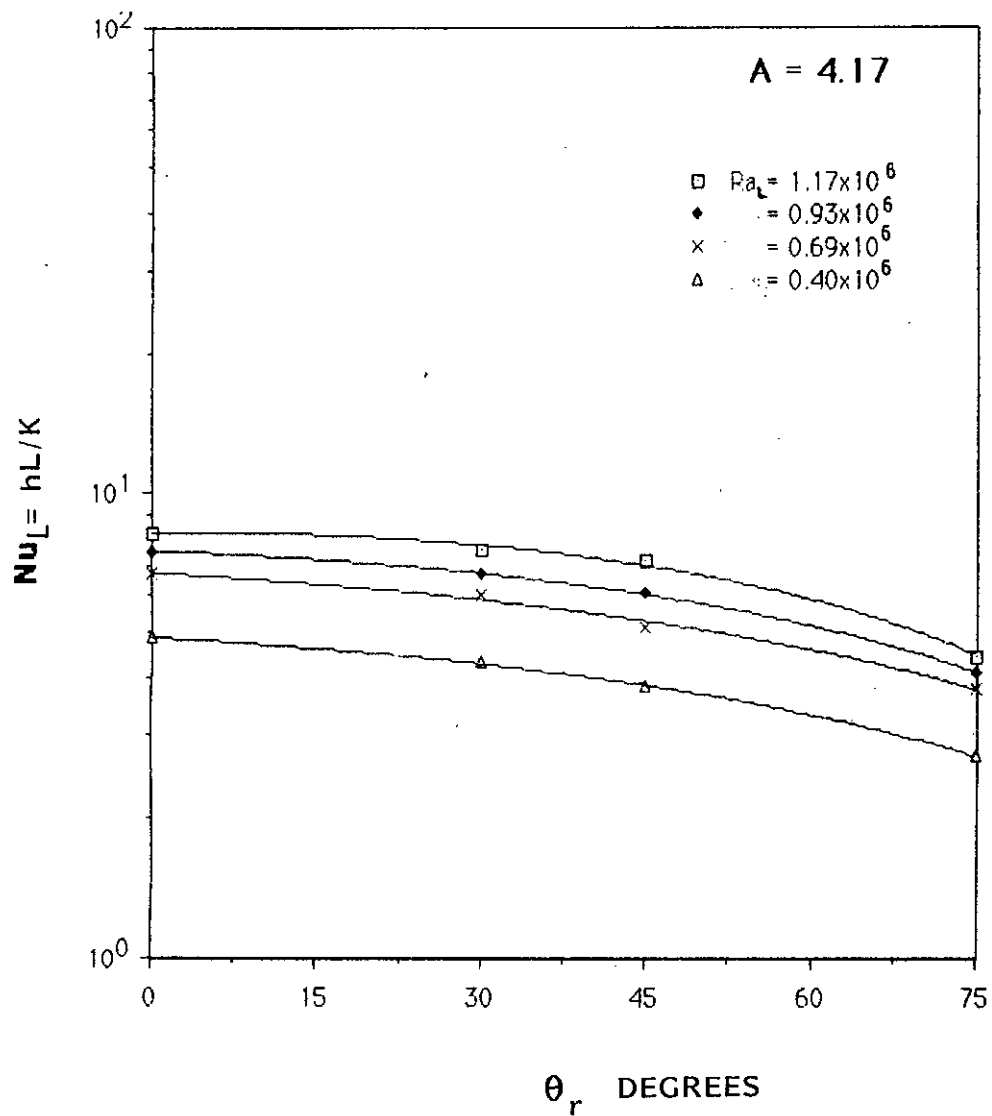


FIG. 6.27 EFFECT OF ANGLE OF INCLINATION OF RECTANGULAR CORRUGATION ON NUSSELT NUMBER FOR $A = 4.17$

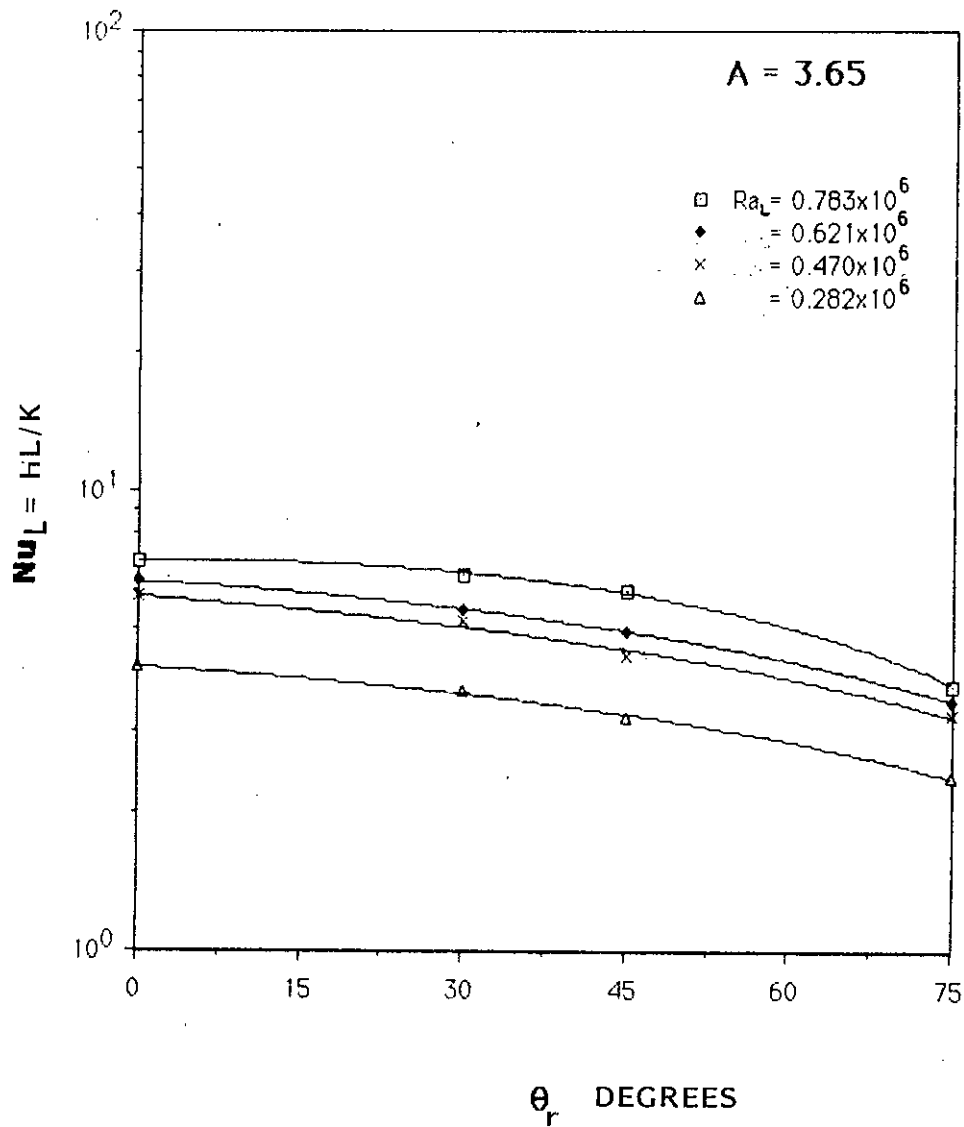


FIG. 6.28 EFFECT OF ANGLE OF INCLINATION OF RECTANGULAR CORRUGATION ON NUSSELT NUMBER FOR $A = 3.65$

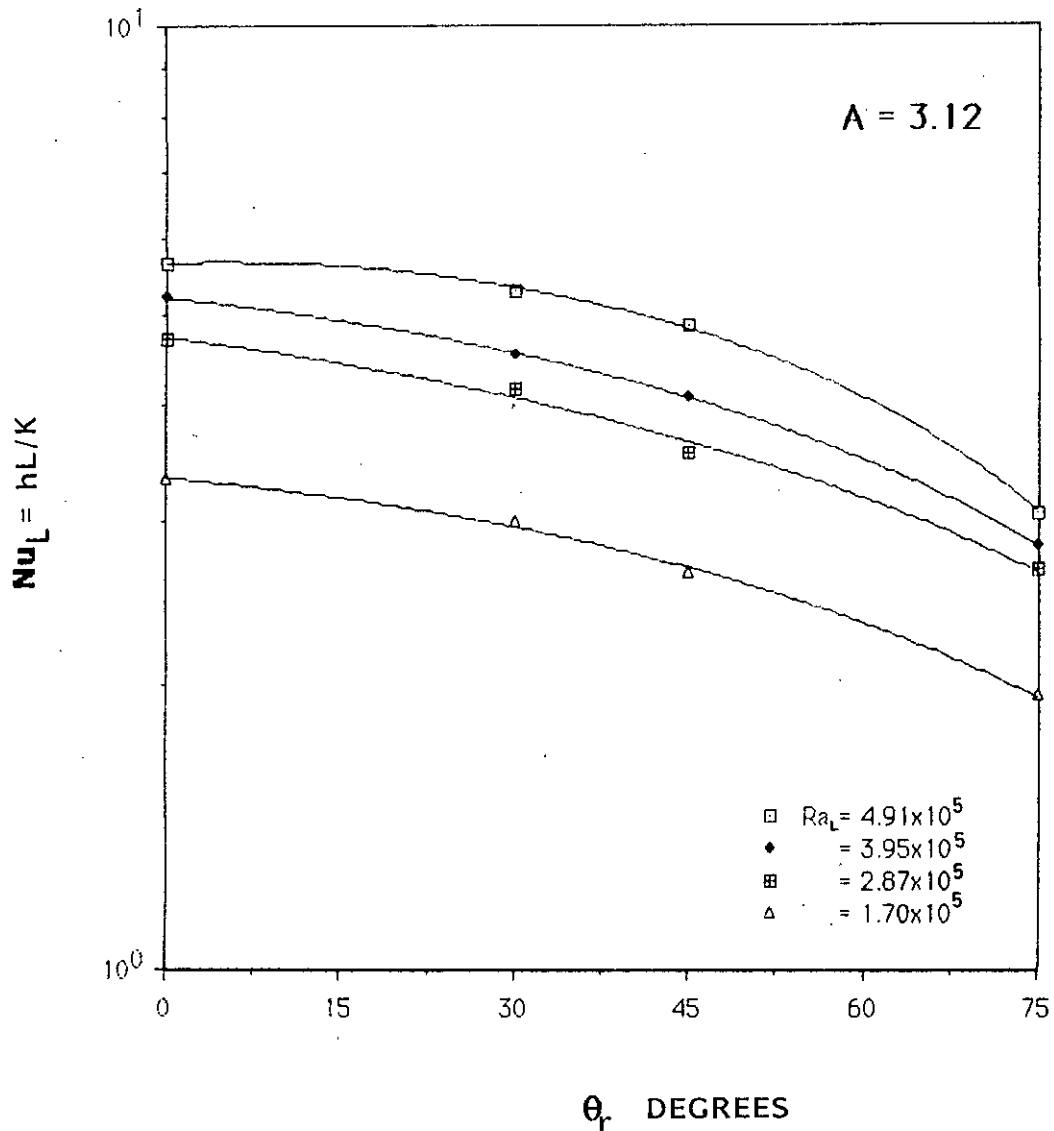


FIG. 6.29 EFFECT OF ANGLE OF INCLINATION OF RECTANGULAR CORRUGATION ON NUSSELT NUMBER FOR $A = 3.12$

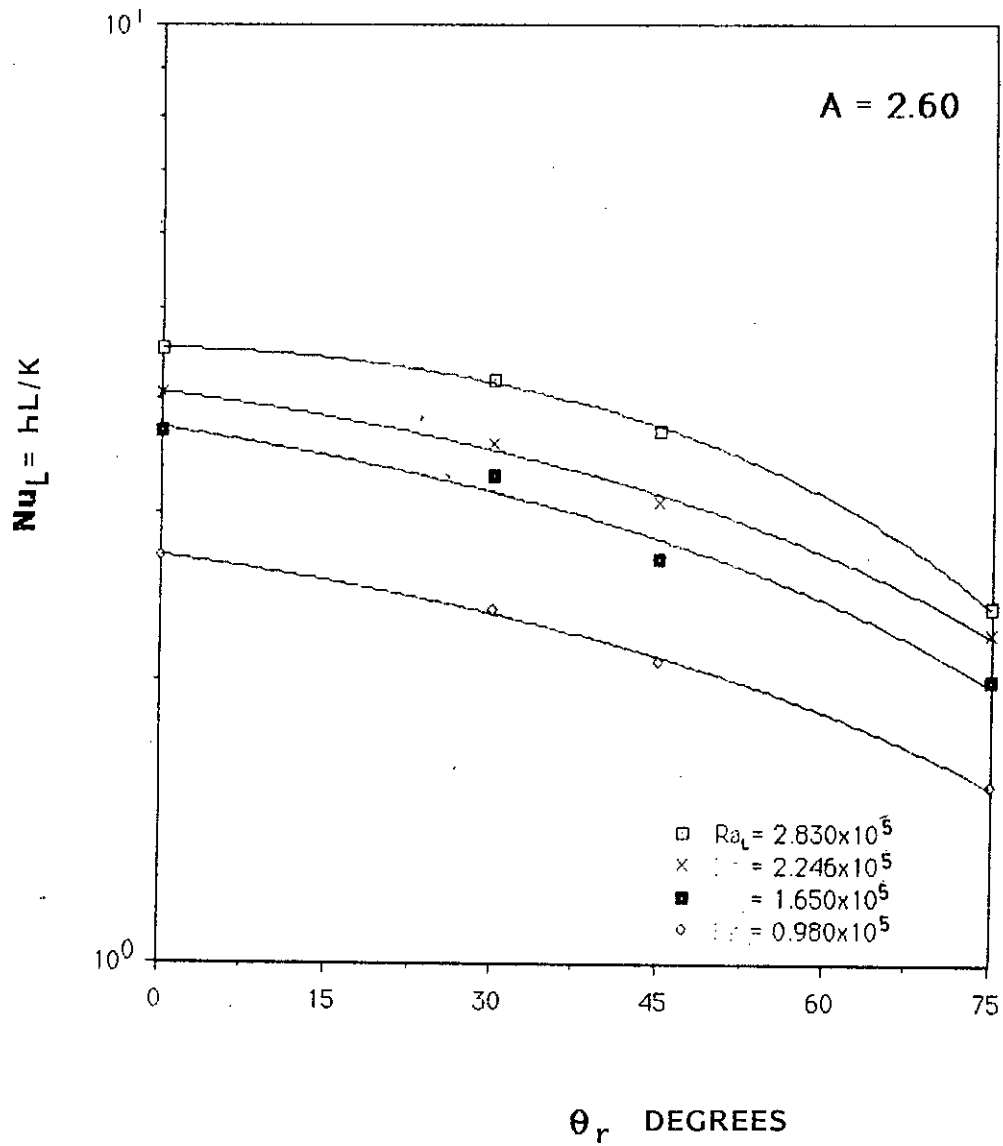


FIG. 6.30 EFFECT OF ANGLE OF INCLINATION OF RECTANGULAR CORRUGATION ON NUSSELT NUMBER FOR $A = 2.60$

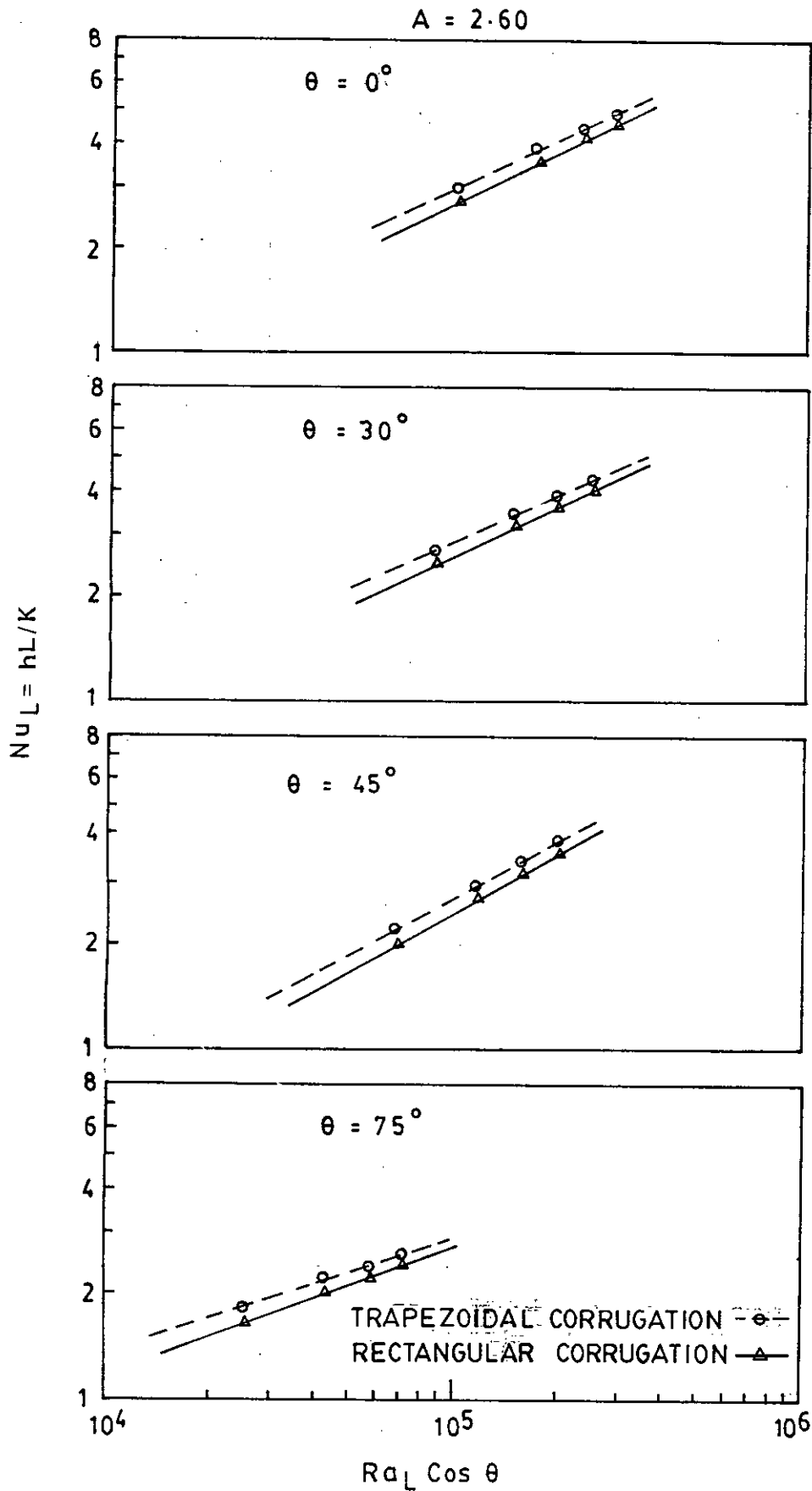


FIG. 6-31 PLOT OF AVERAGE NUSSELT NUMBER VS $Ra_L \cos \theta$ FOR $A = 2.60$

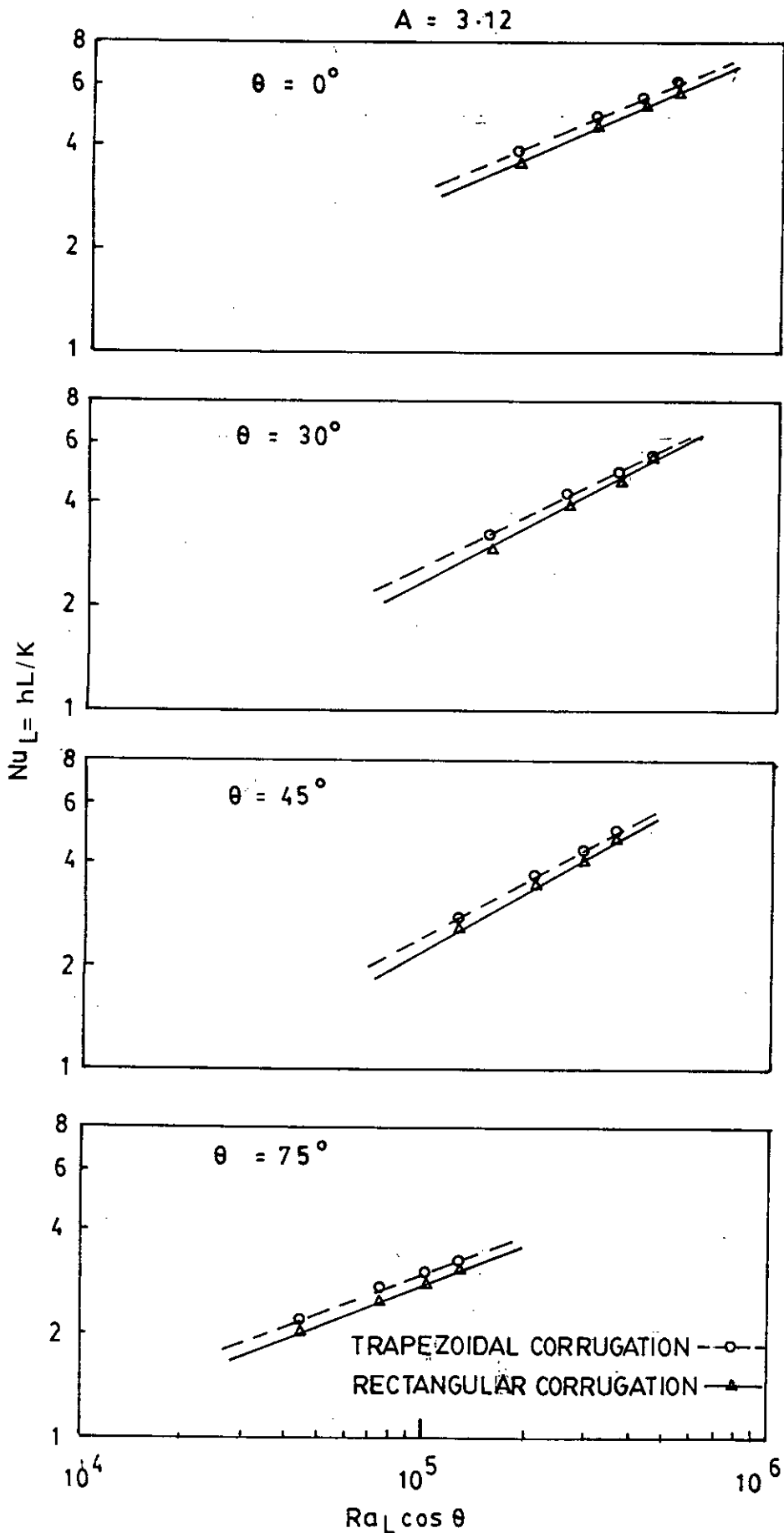


FIG 6.32 PLOT OF AVERAGE NUSSELT NUMBER
Vs $Ra_L \cos \theta$ FOR $A = 3.12$

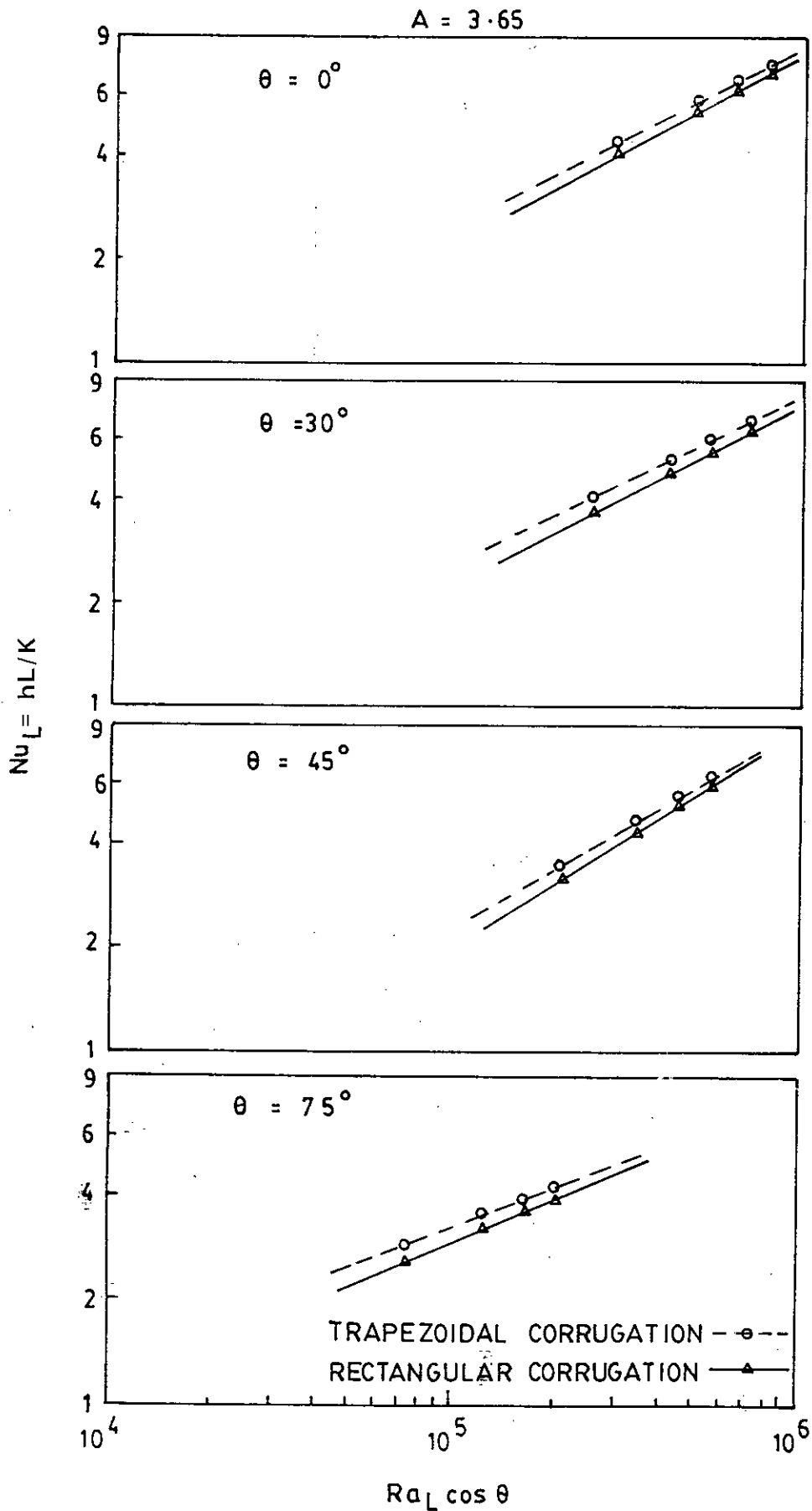


FIG. 6.33 PLOT OF AVERAGE NUSSELT NUMBER
Vs $Ra_L \cos \theta$ FOR $A = 3.65$

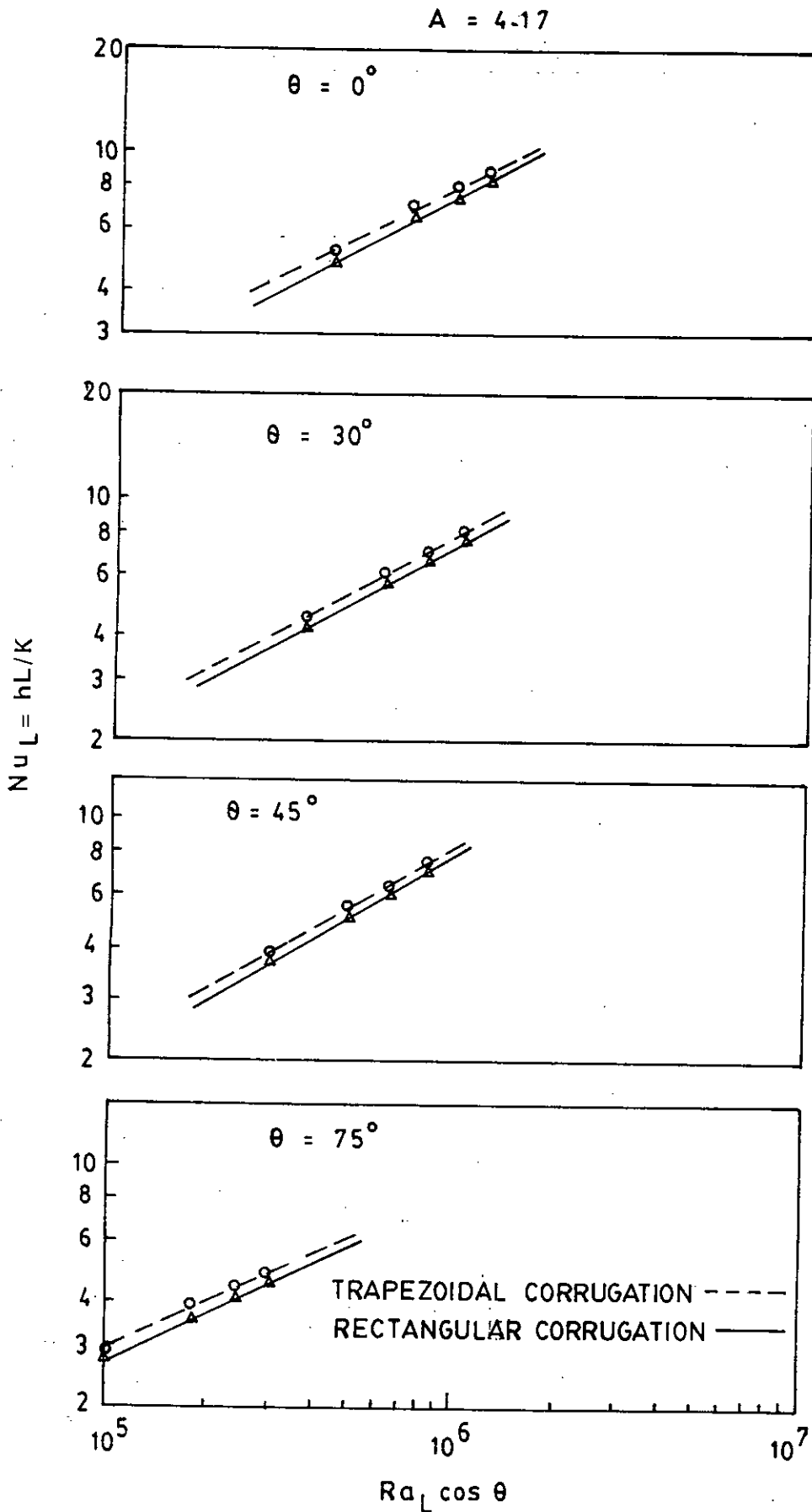


FIG 6.34 PLOT OF AVERAGE NUSSLETT NUMBER
Vs $Ra_L \cos \theta$ FOR $A = 4.17$

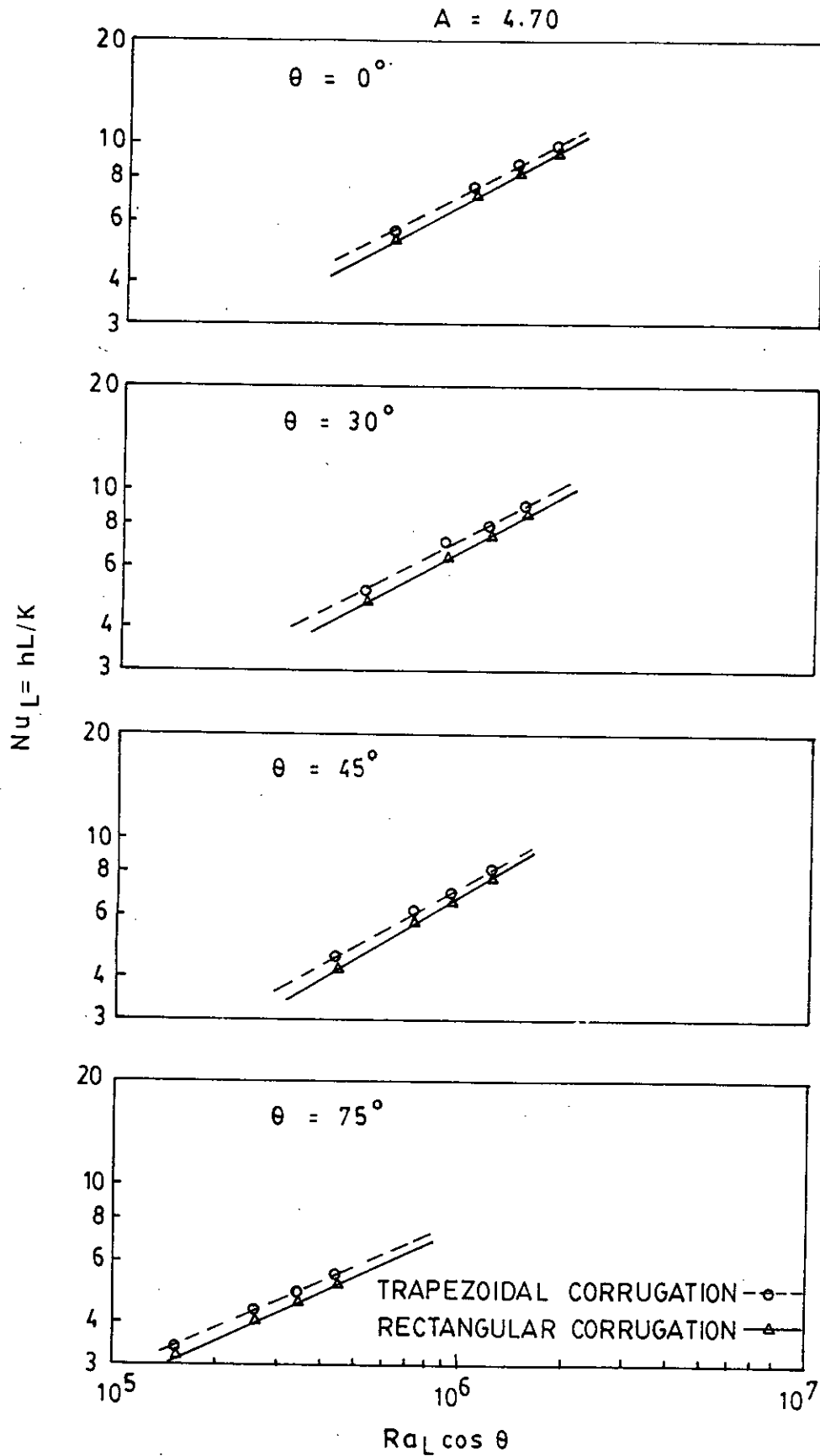


FIG. 6.35 PLOT OF AVERAGE NUSSELT NUMBER
Vs $Ra_L \cos \theta$ FOR $A = 4.70$

A = 5.22

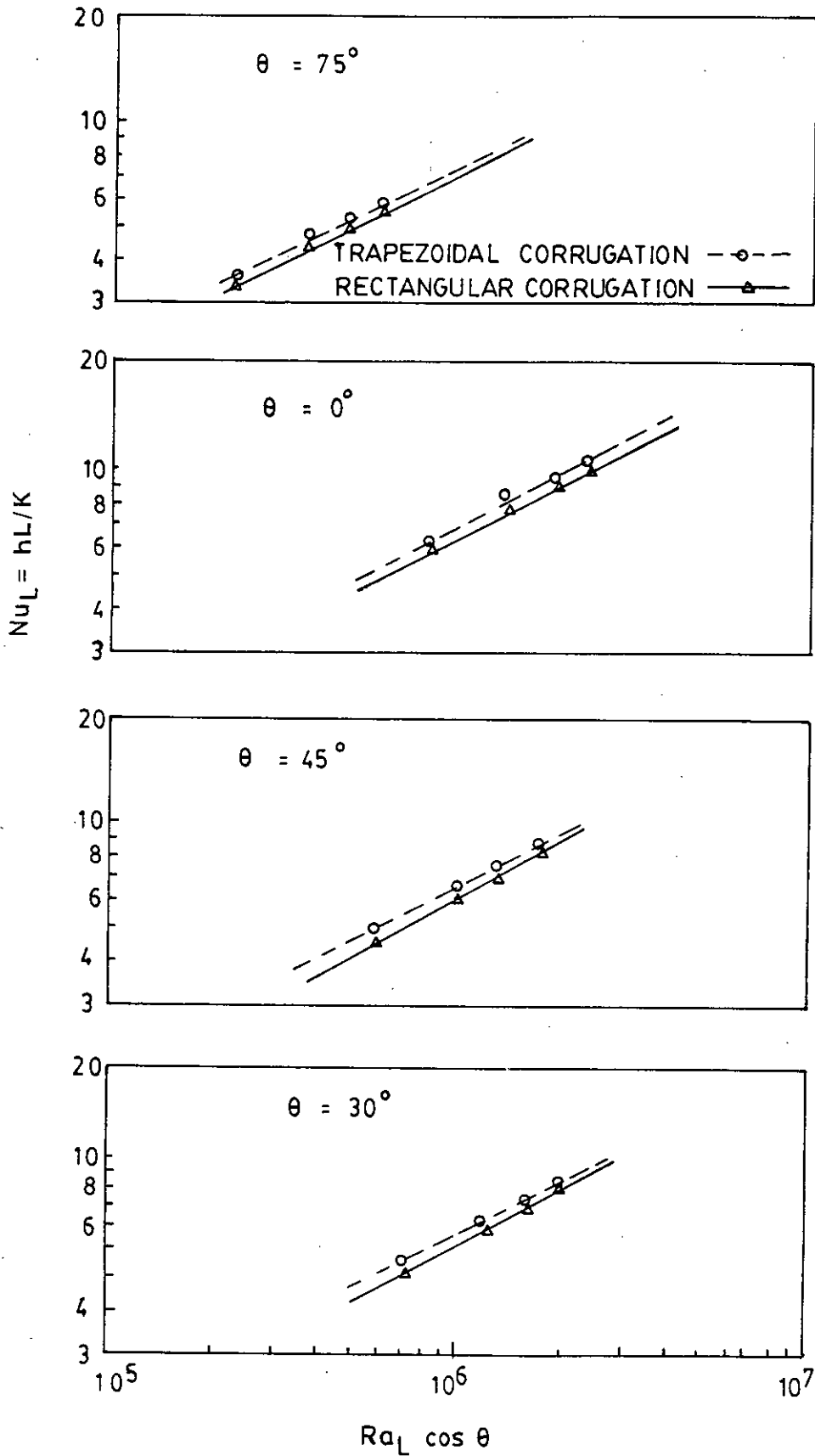


FIG. 6-36 PLOT OF AVERAGE NUSSELT NUMBER Vs. $Ra_L \cos \theta$ FOR A = 5.22

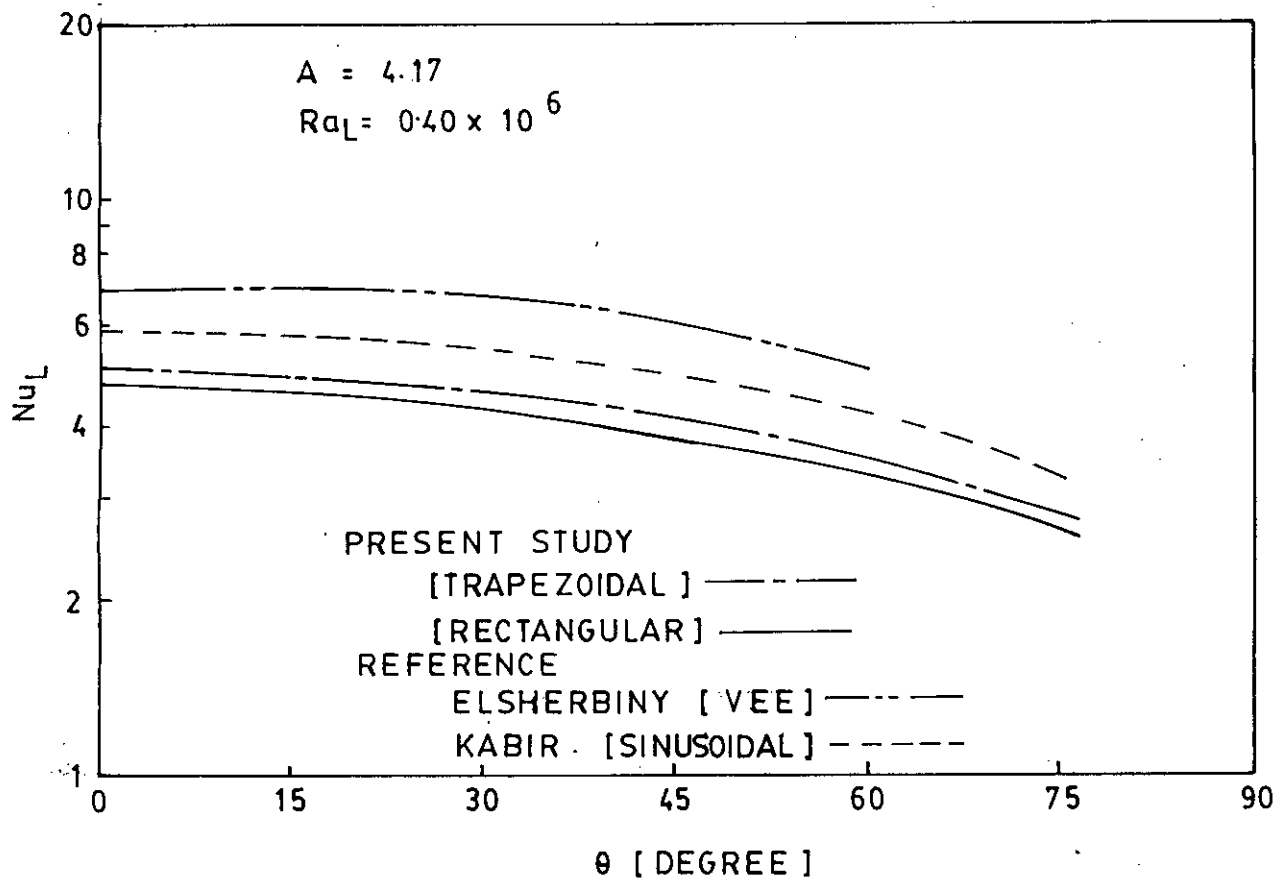


FIG. 6.37 COMPERISON THE EFFECT OF ANGLE OF INCLINATION ON NUSSELT NUMBER OF THE PRESENT STUDY WITH NUSSELT NUMBER OF OTHER RELATED WORKS

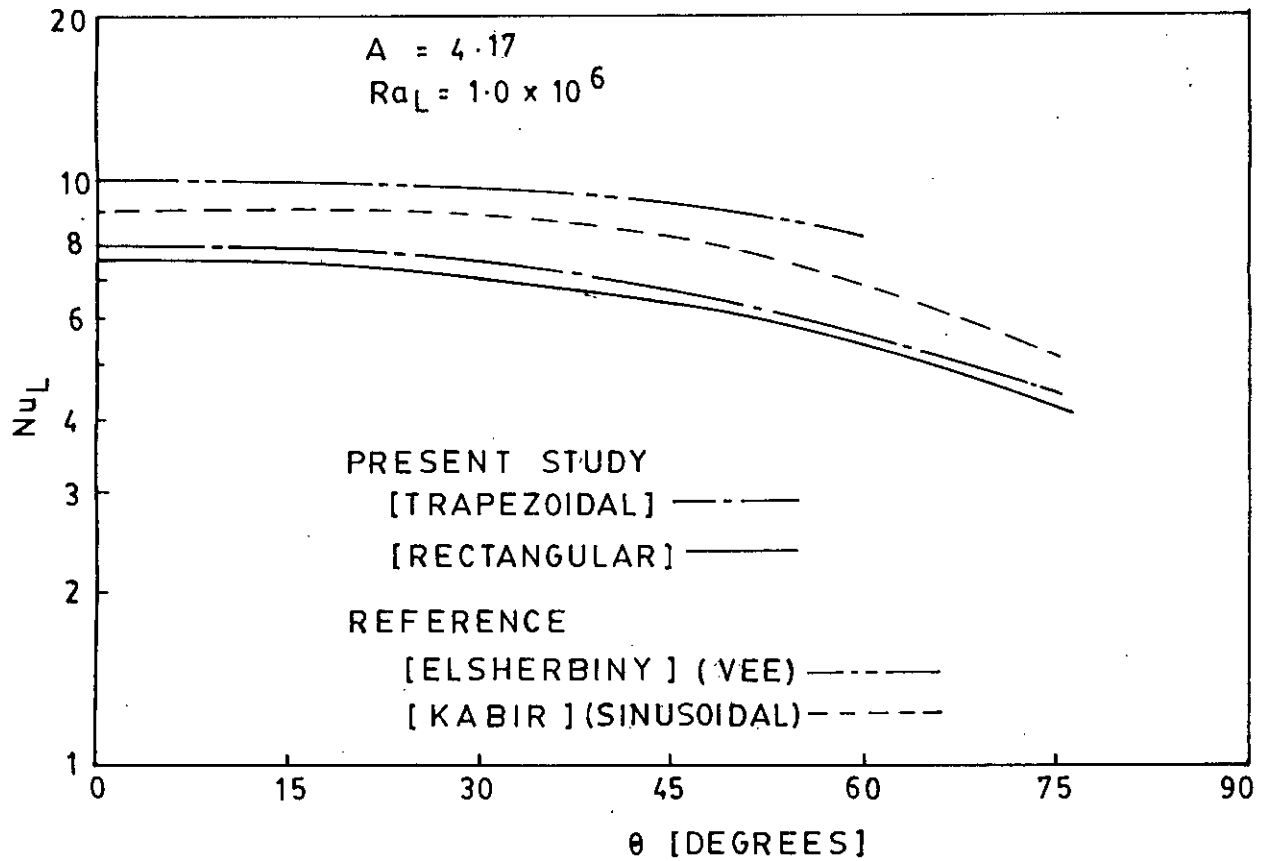


FIG. 6.38 COMPERISON THE EFFECT OF ANGLE OF INCLINATION ON NUSSLELT NUMBER OF THE PRESENT STUDY WITH NUSSLELT NUMBER OF OTHER RELATED WORKS

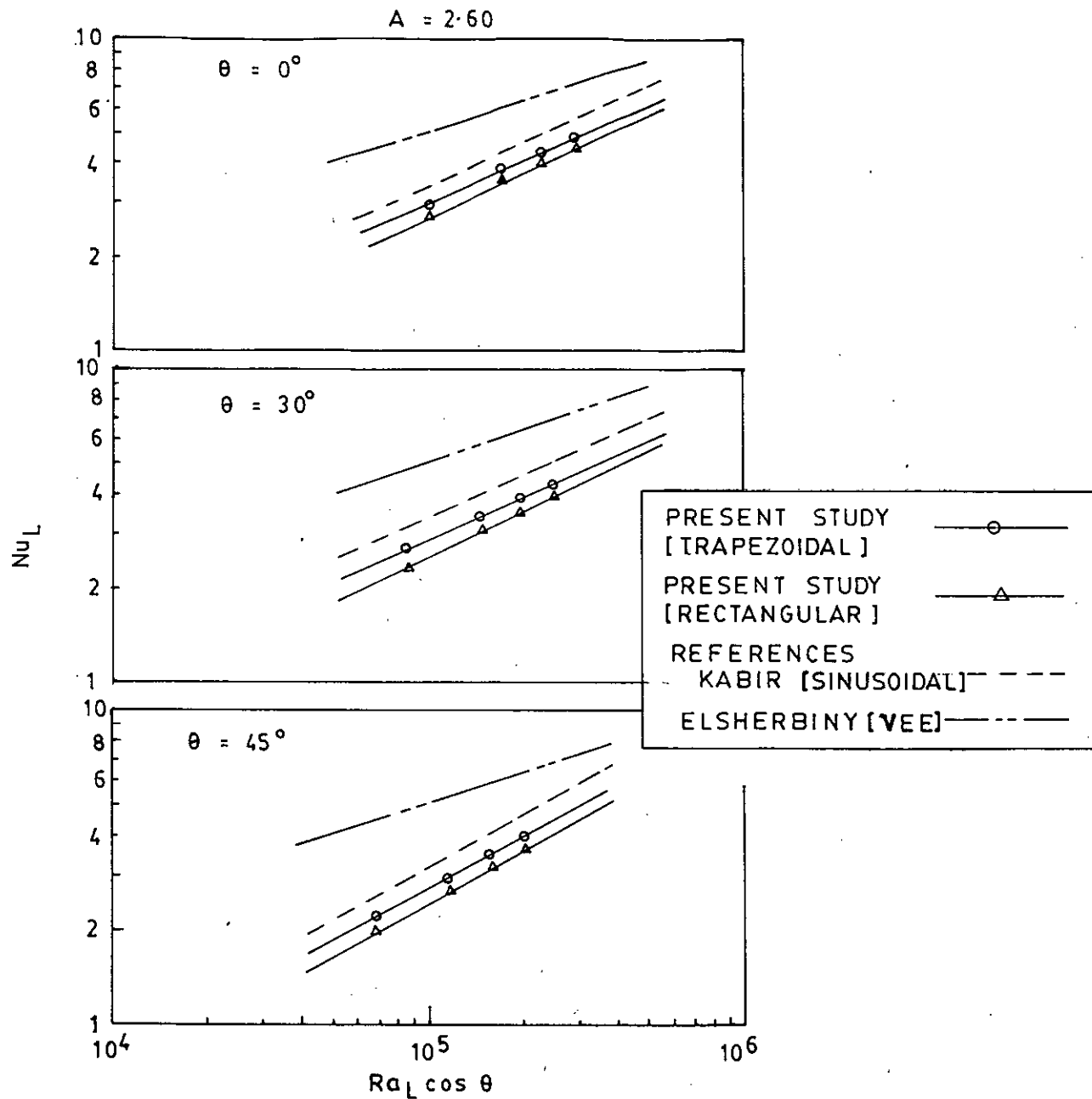


FIG. 6.39 COMPARISON OF NUSSELT NUMBER OF THE PRESENT STUDY WITH NUSSELT NUMBER OF OTHER RELATED WORKS.

$$A' = 4.17$$

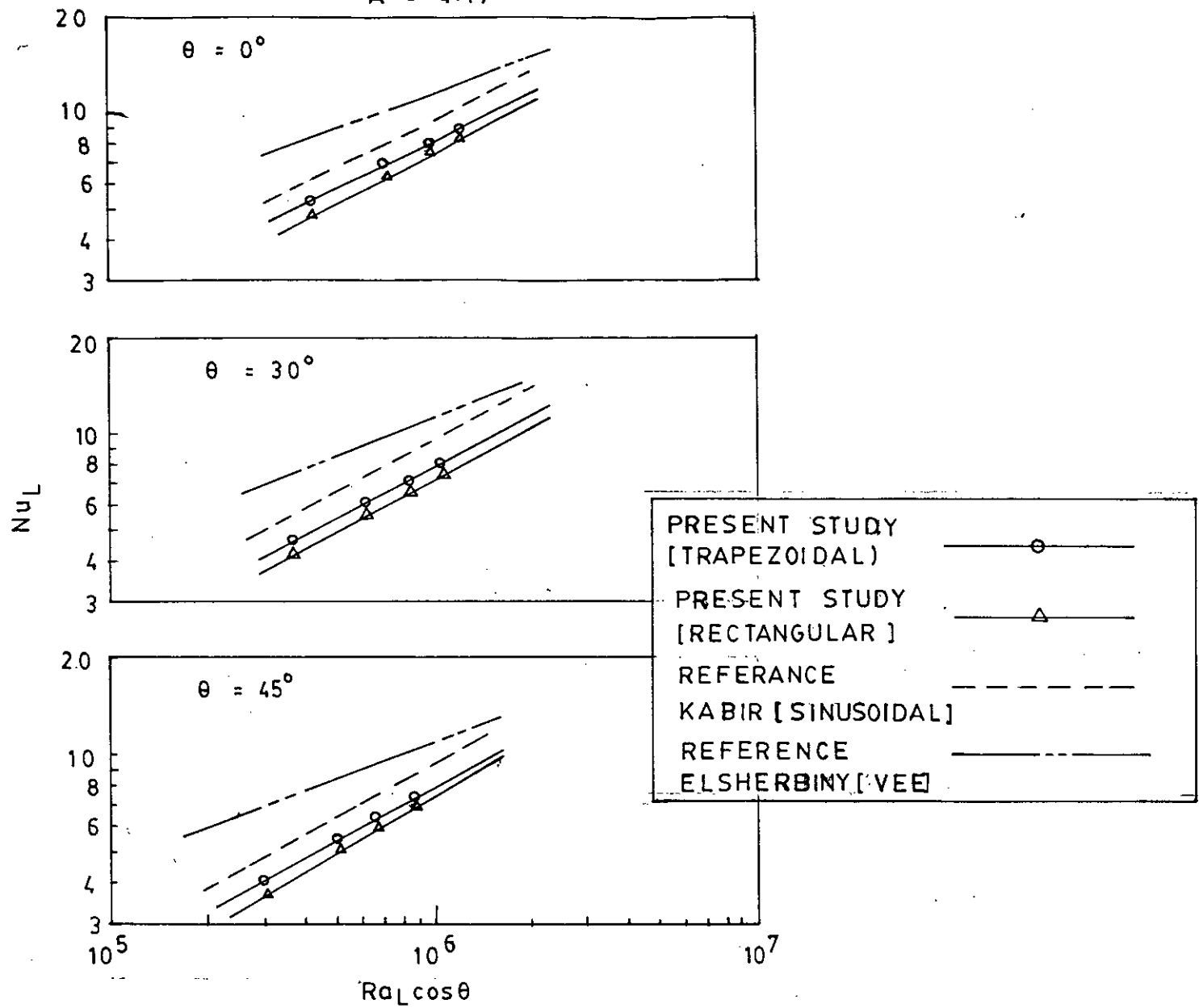


FIG 6.40 COMPERISON OF NUSSELT NUMBER OF THE PRESENT STUDY WITH NUSSELT NUMBER OF OTHER RELATED WORKS

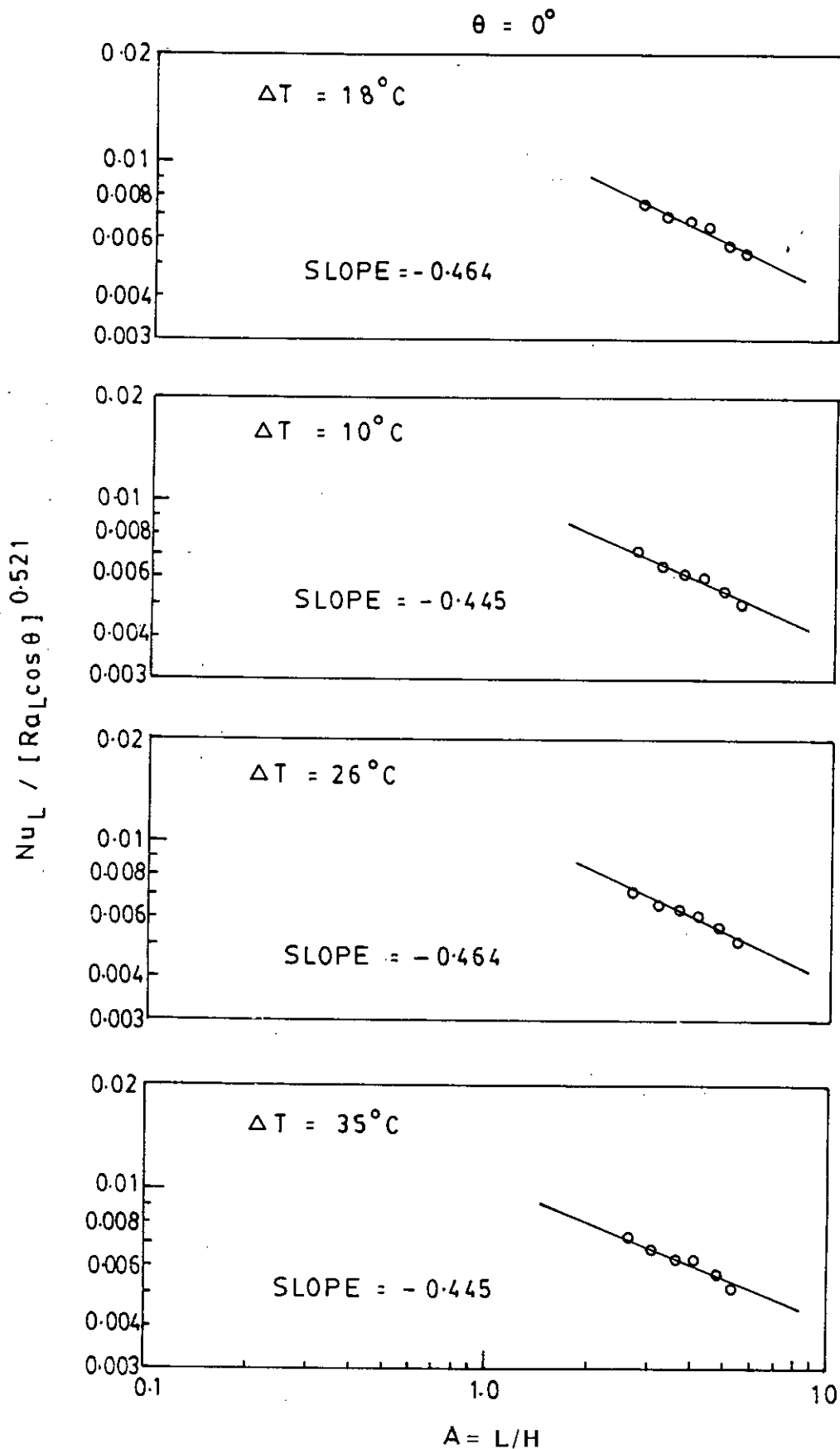


FIG. 7.1 DETERMINATION OF EXPONENT m_t FOR TRAPEZOIDAL CORRUGATED SURFACE

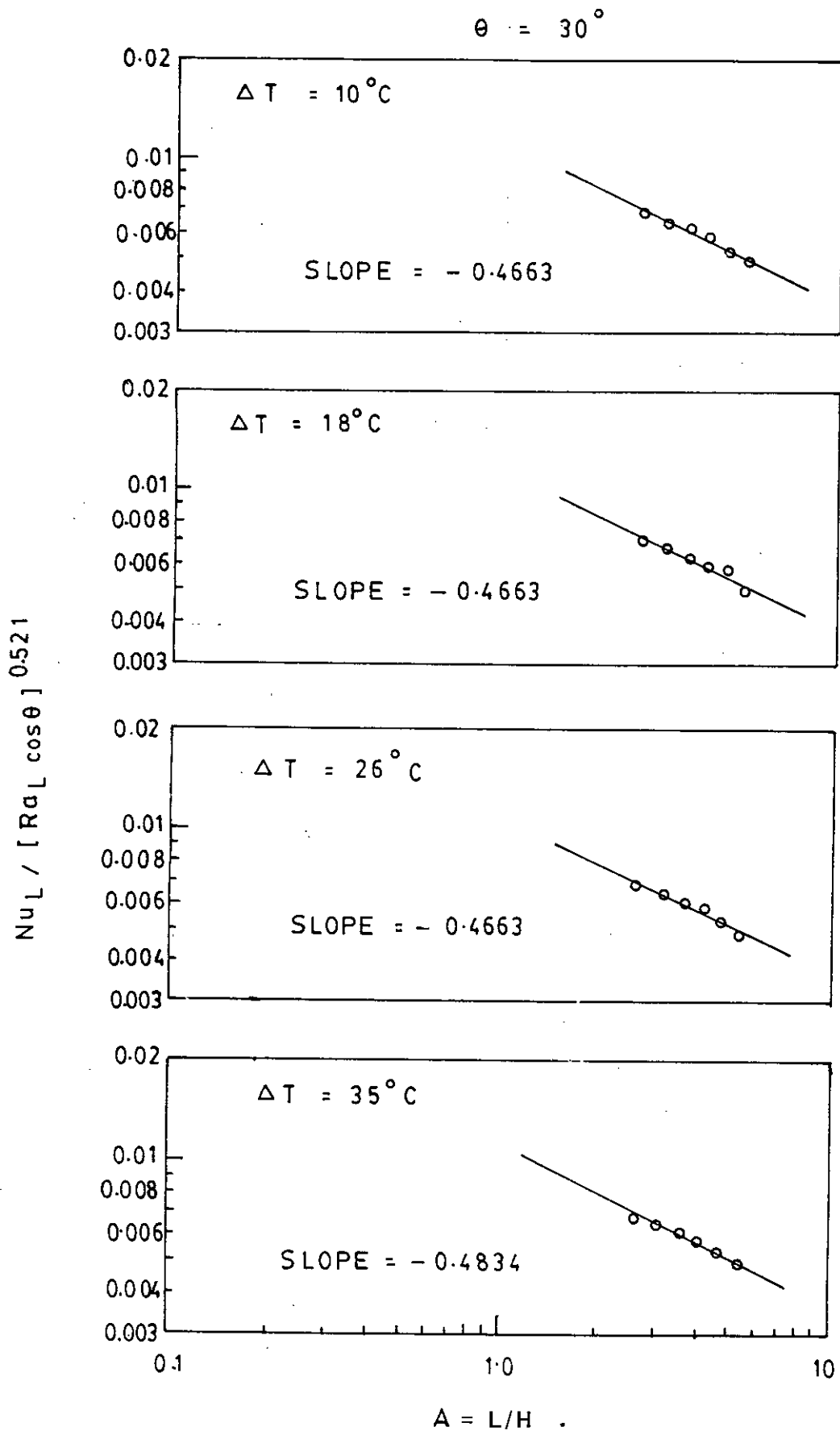


FIG. 7.2 DETERMINATION OF EXPONENT m_t FOR TRAPEZOIDAL CORRUGATED SURFACE

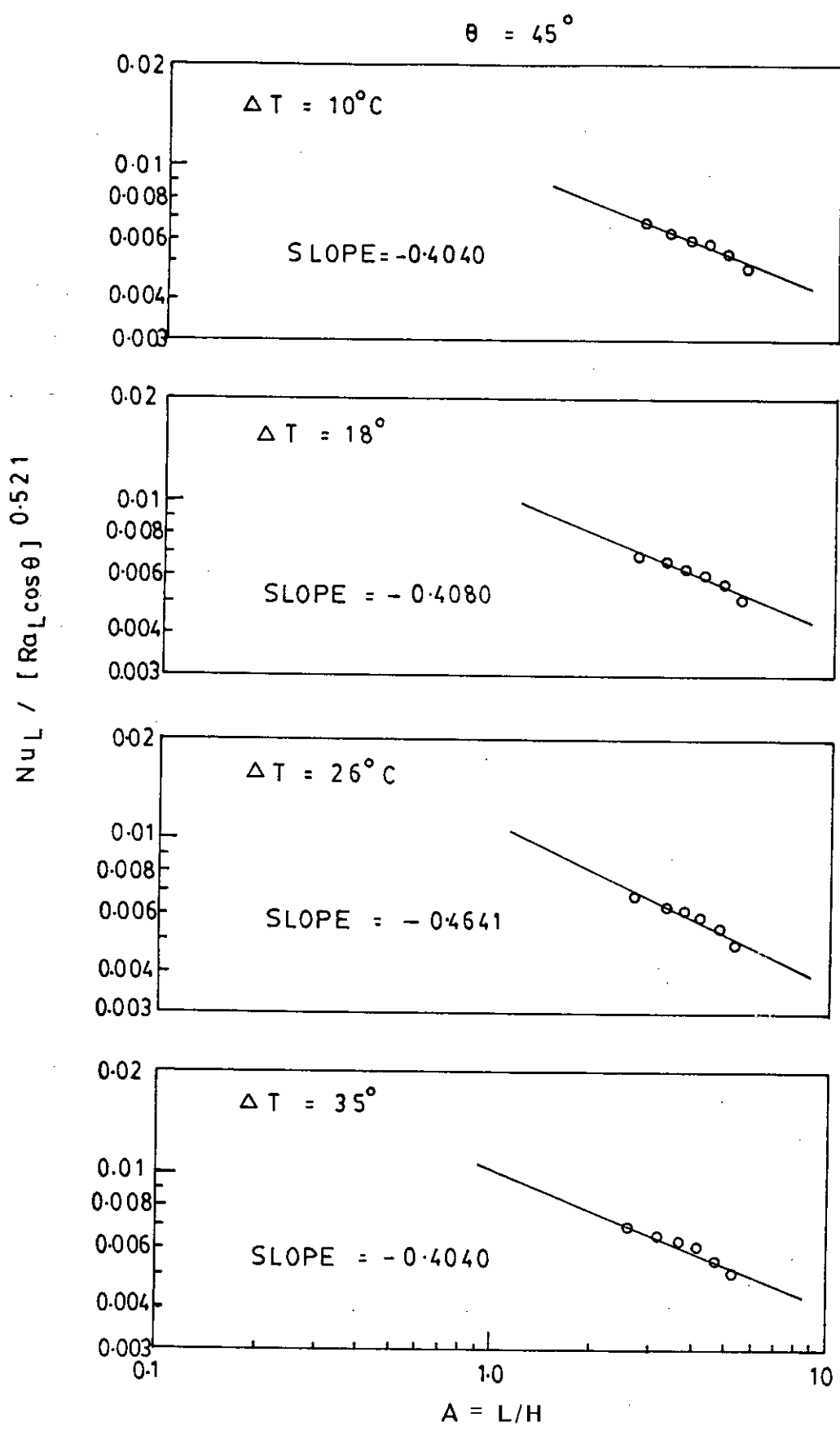


FIG. 7.3 DETERMINATION OF EXPONENT m_t FOR TRAPEZOIDAL CORRUGATED SURFACE

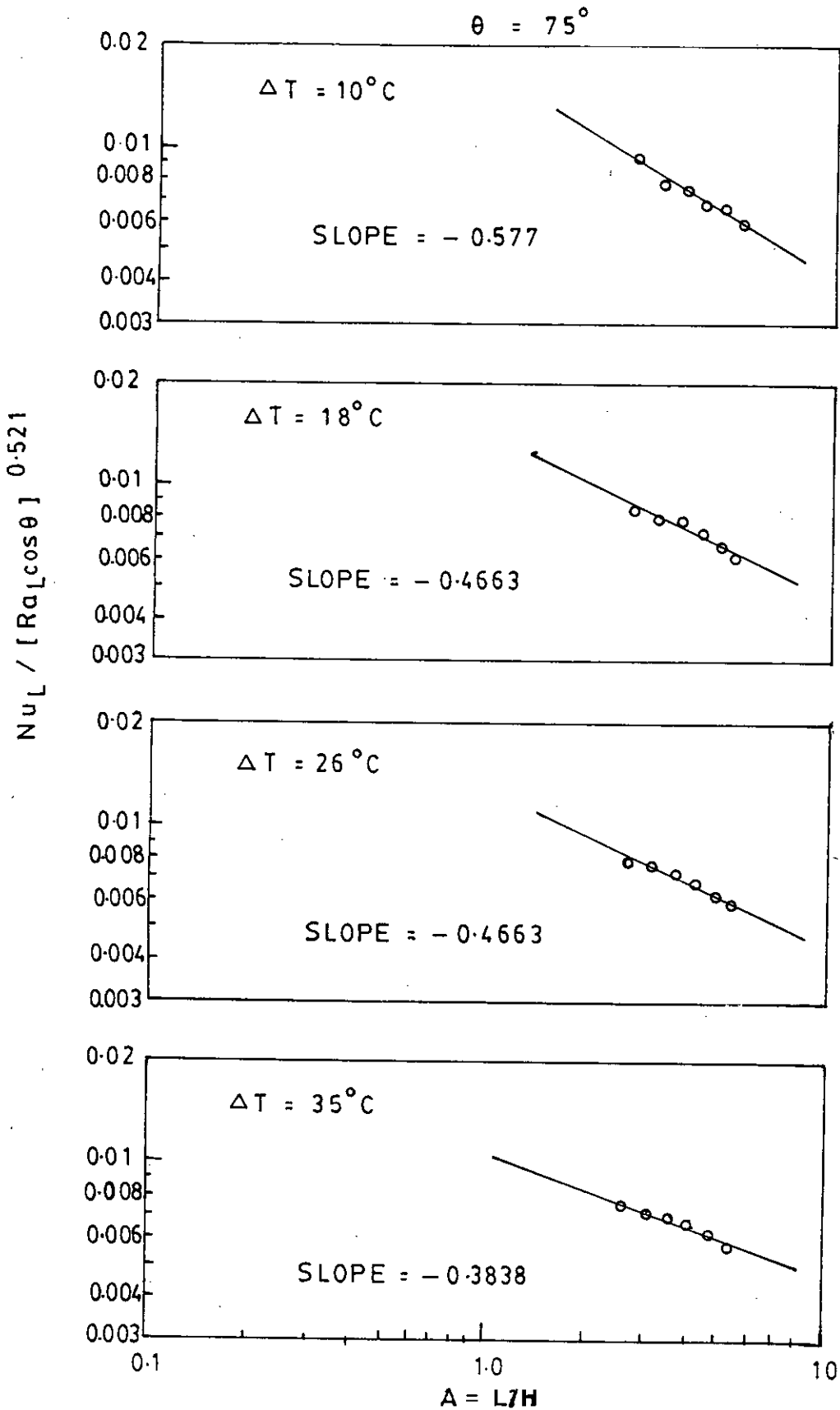


FIG. 7.4 DETERMINATION OF EXPONENT m_t FOR TRAPEZOIDAL CORRUGATED SURFACE.

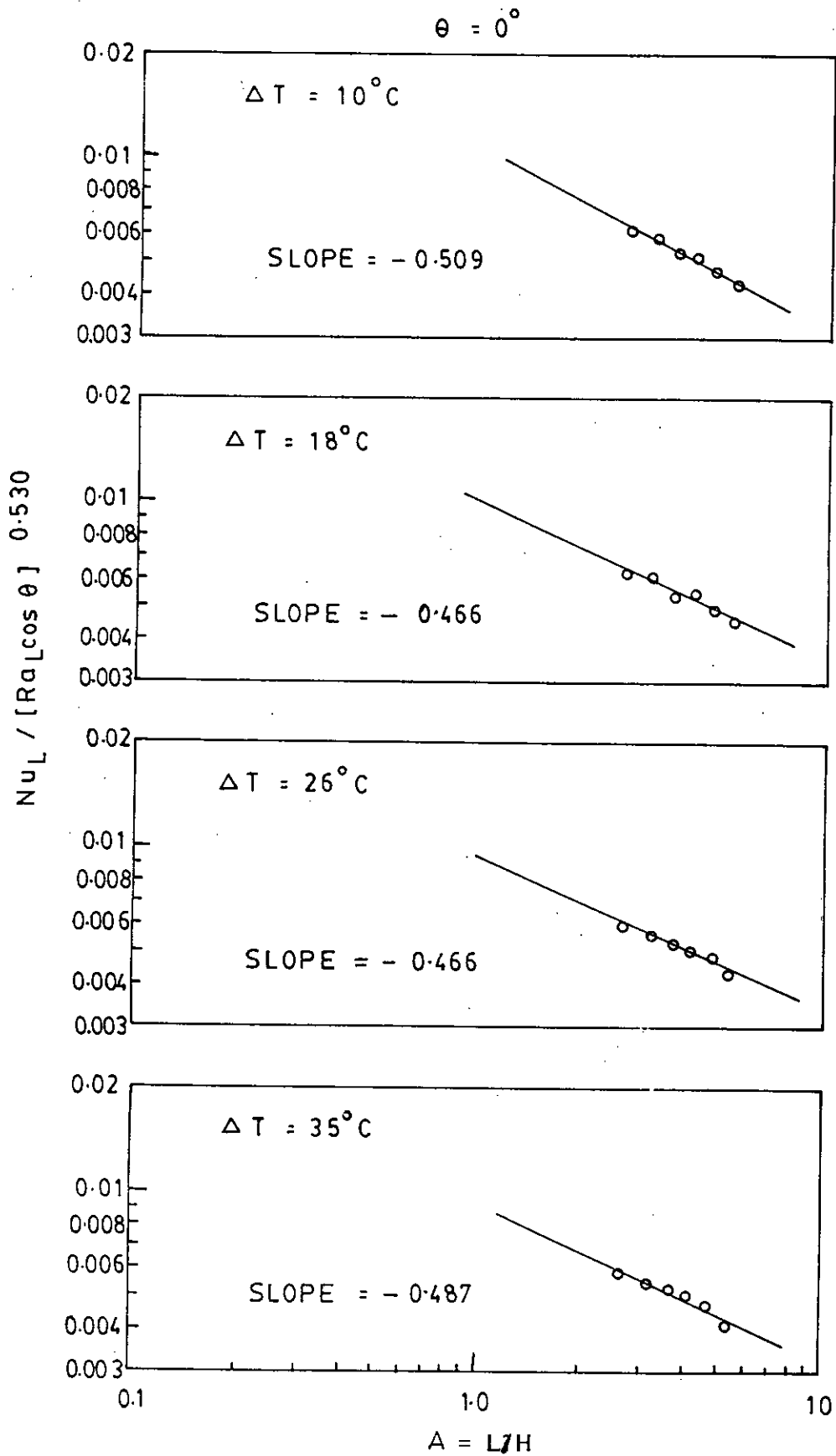


FIG. 7.5 DETERMINATION OF EXPONENT m_r FOR RECTANGULAR CORRUGATED SURFACE

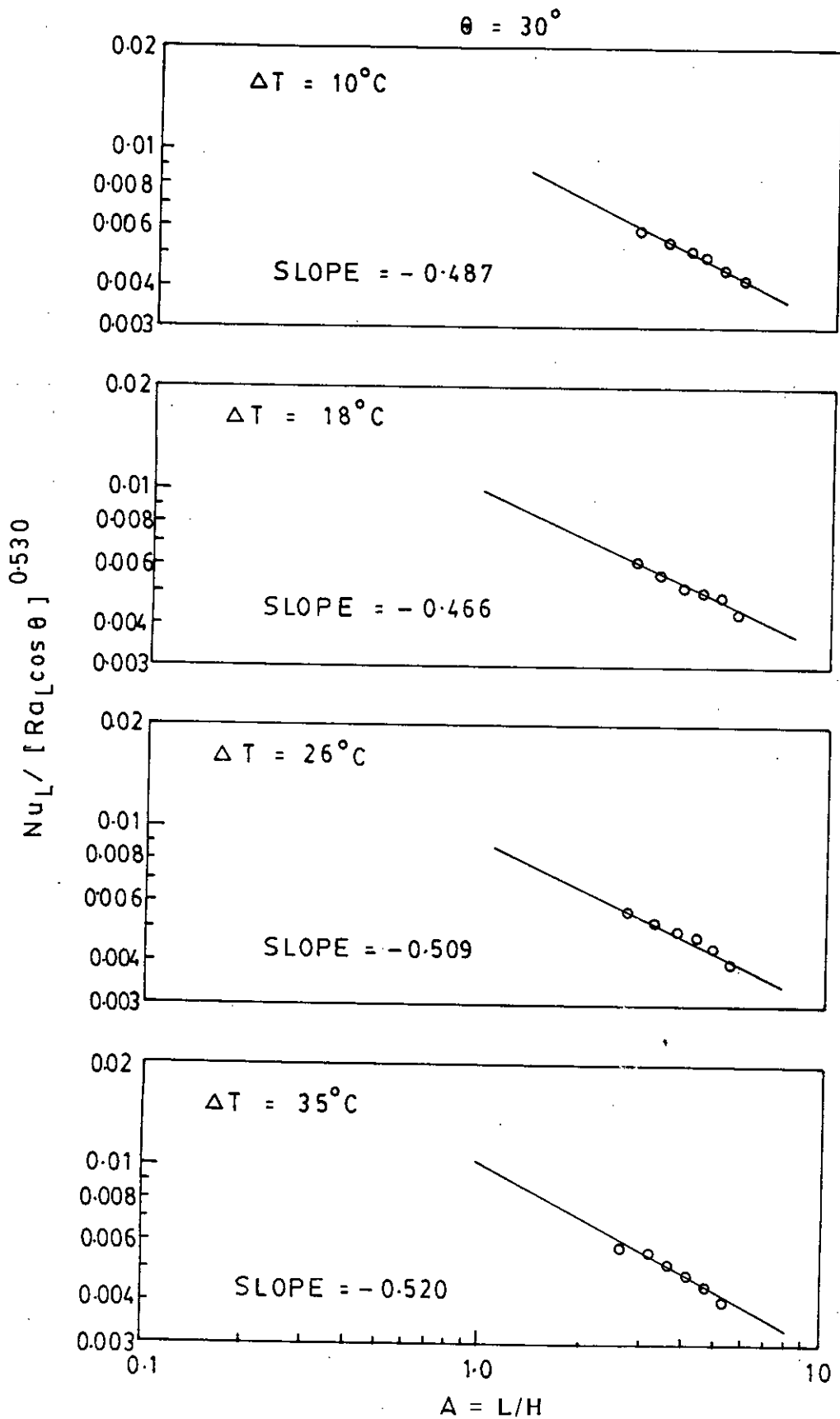


FIG. 7.6 DETERMINATION OF EXPONENT m_r FOR RECTANGULAR CORRUGATED SURFACE.

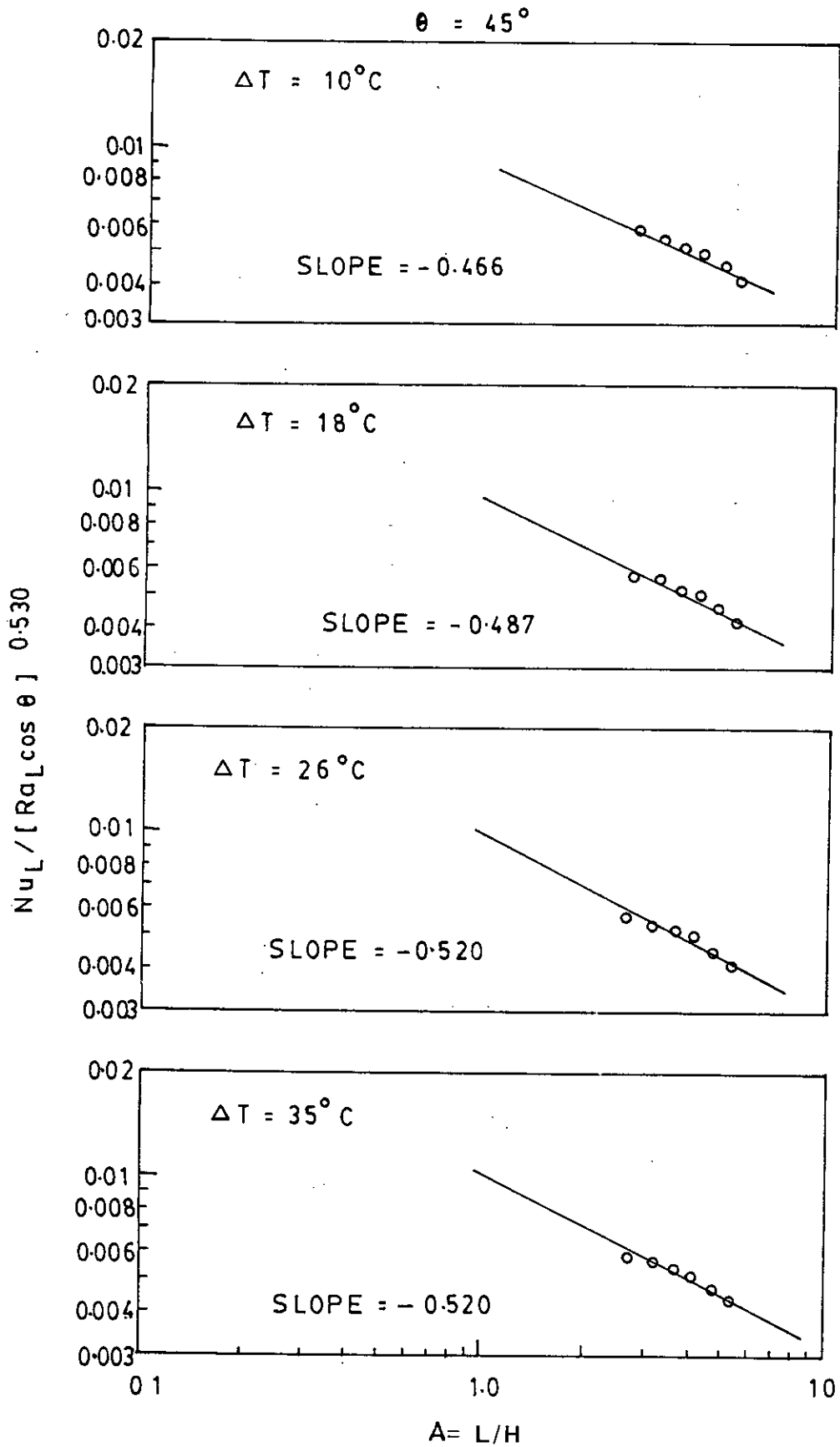


FIG. 7.7 DETERMINATION OF EXPONENT m_r FOR RECTANGULAR CORRUGATED SURFACE

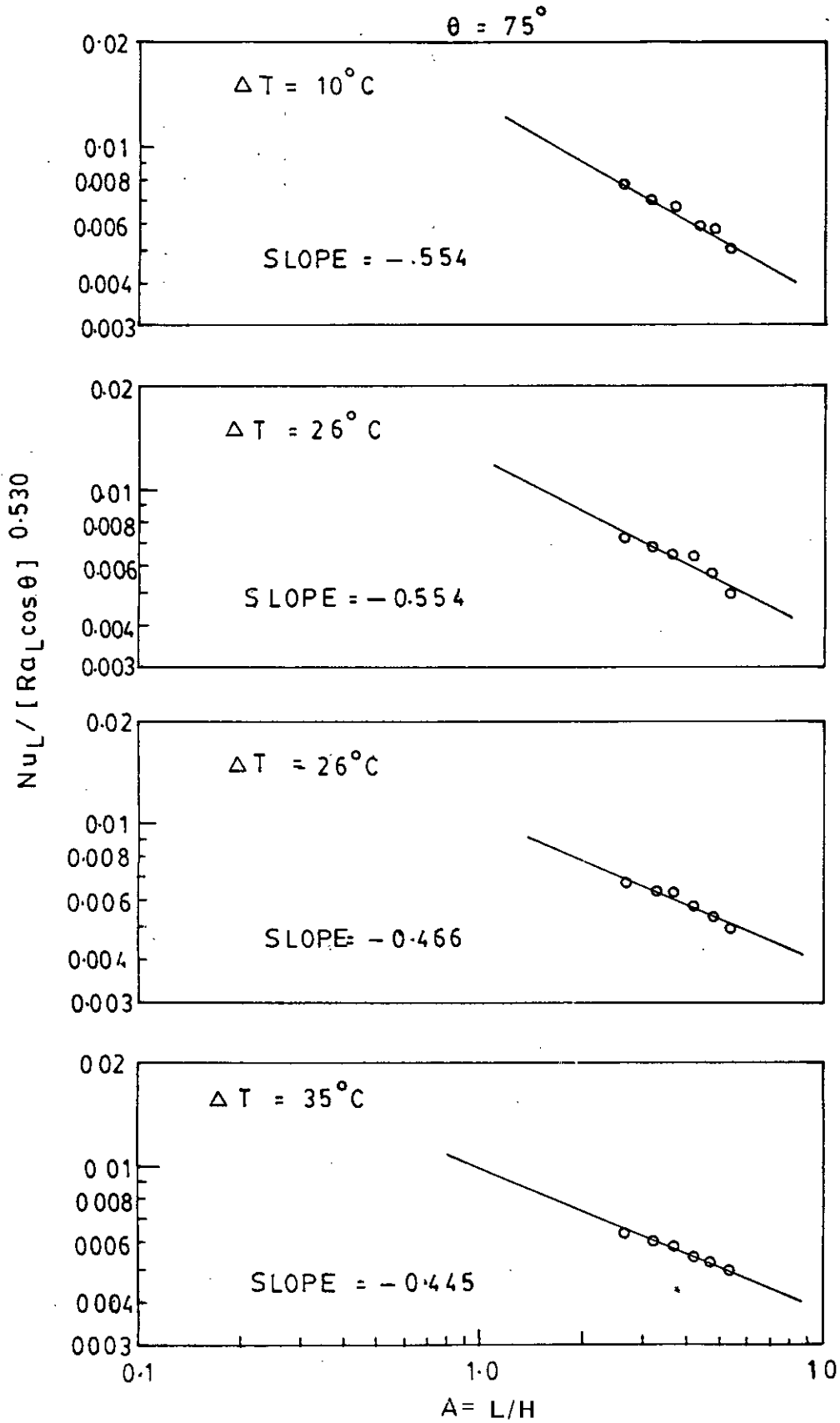


FIG. 7.8 DETERMINATION OF EXPONENT m_r FOR RECTANGULAR CORRUGATED SURFACE

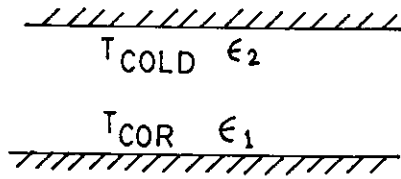


FIG. A.1

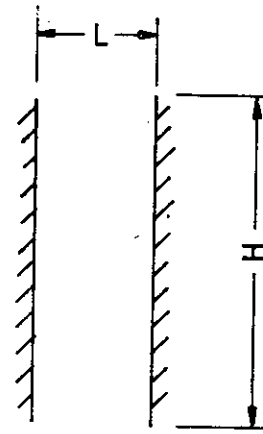


FIG. A.2

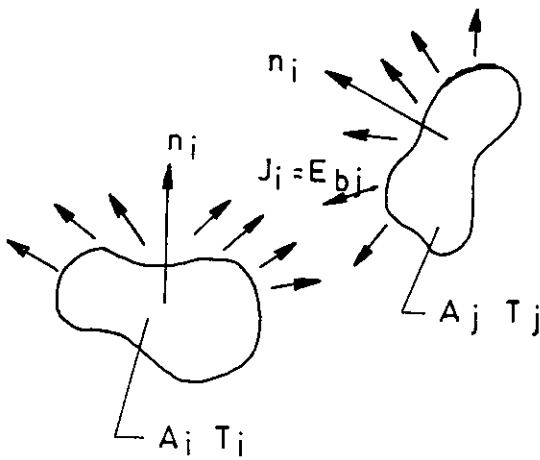


FIG. A.3

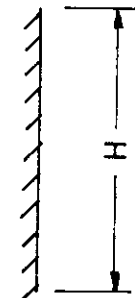


FIG. A.4

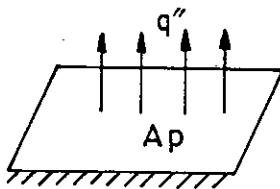


FIG. A.5

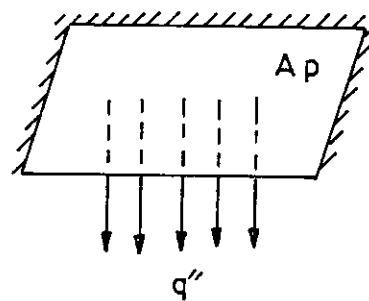


FIG. A.6

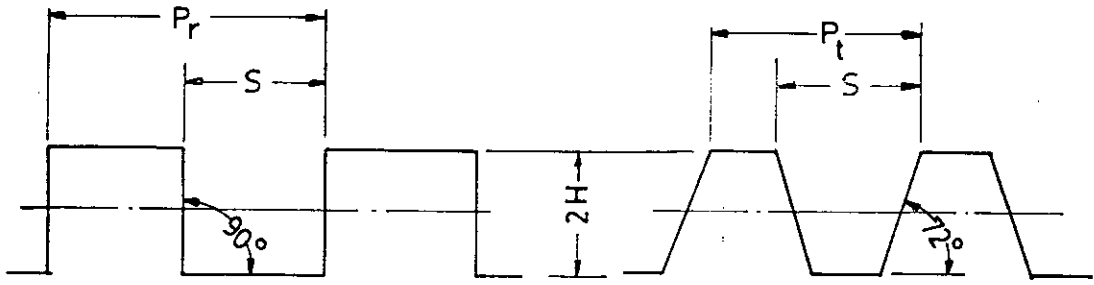


FIG. C.1 CORRUGATION GEOMETRY

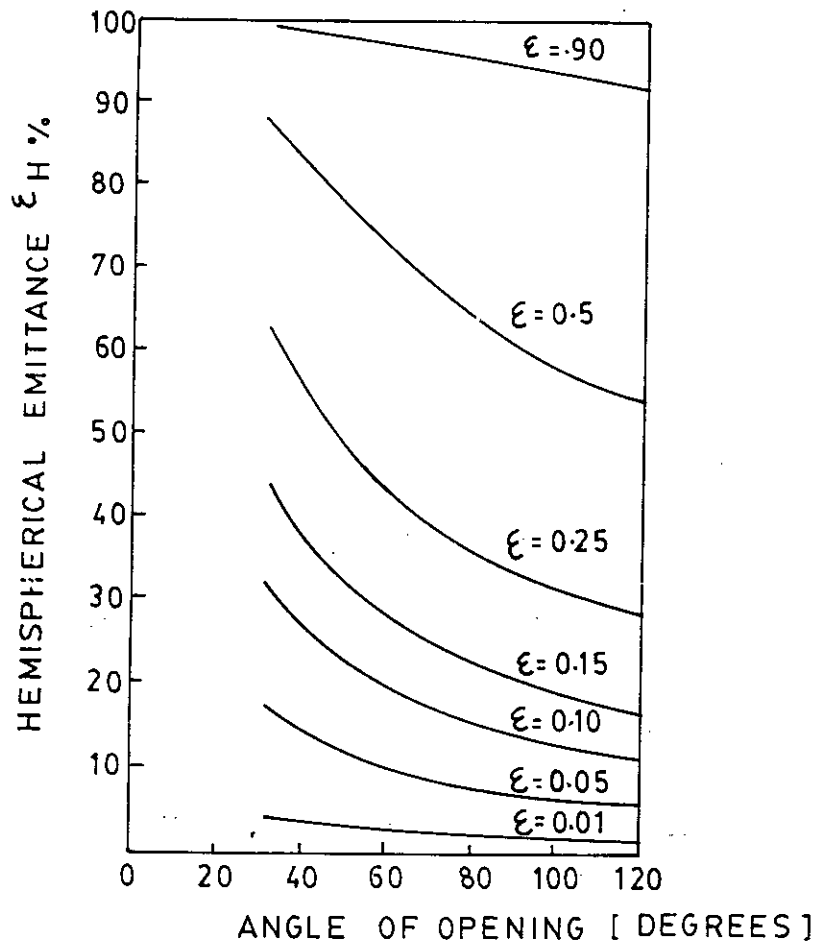


FIG. C.2 HEMISPHERICAL EMITTANCE Vs ANGLE OF OPENING FOR SEVERAL PLANE LONG WAVE EMISSIVITIES

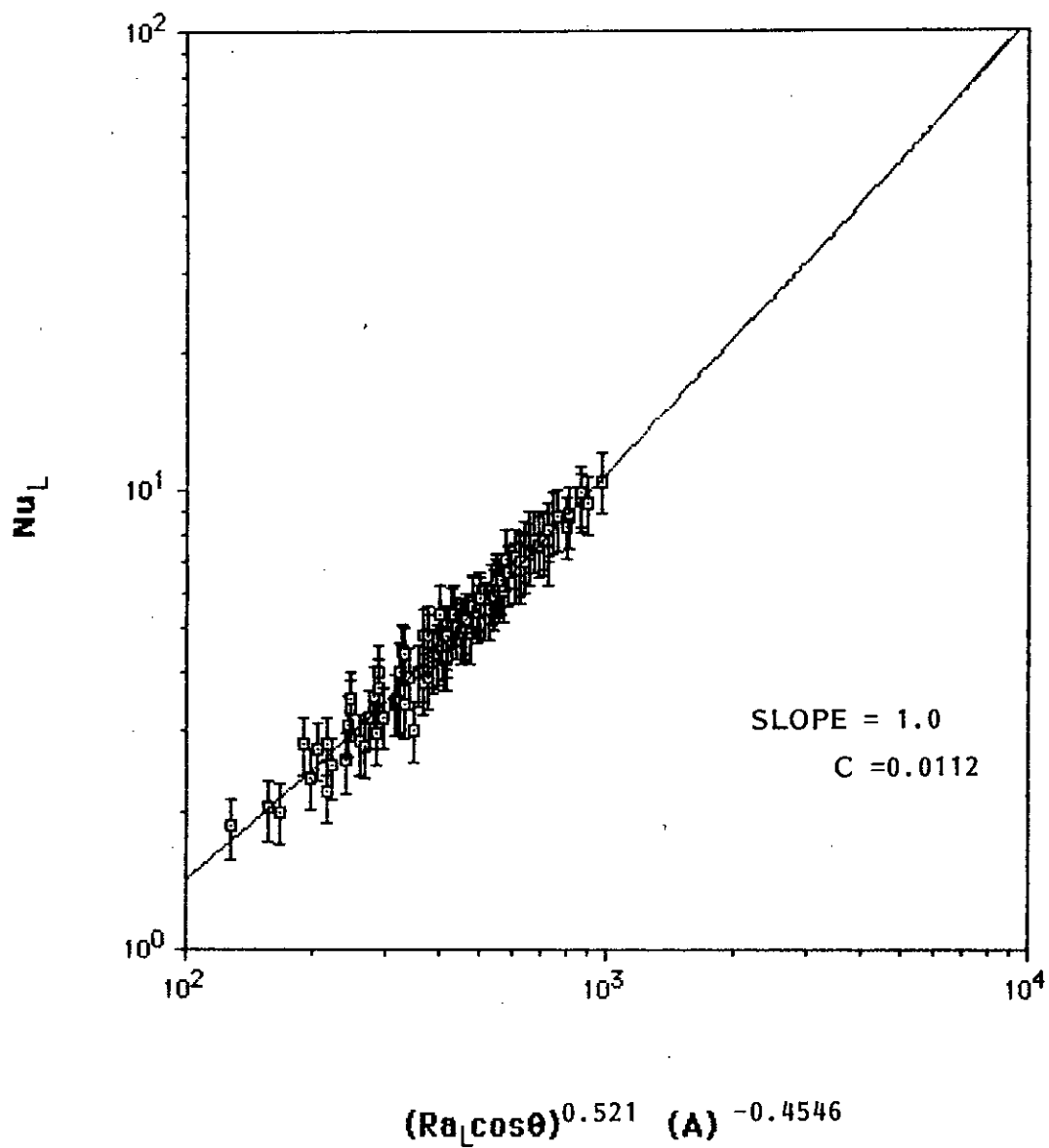
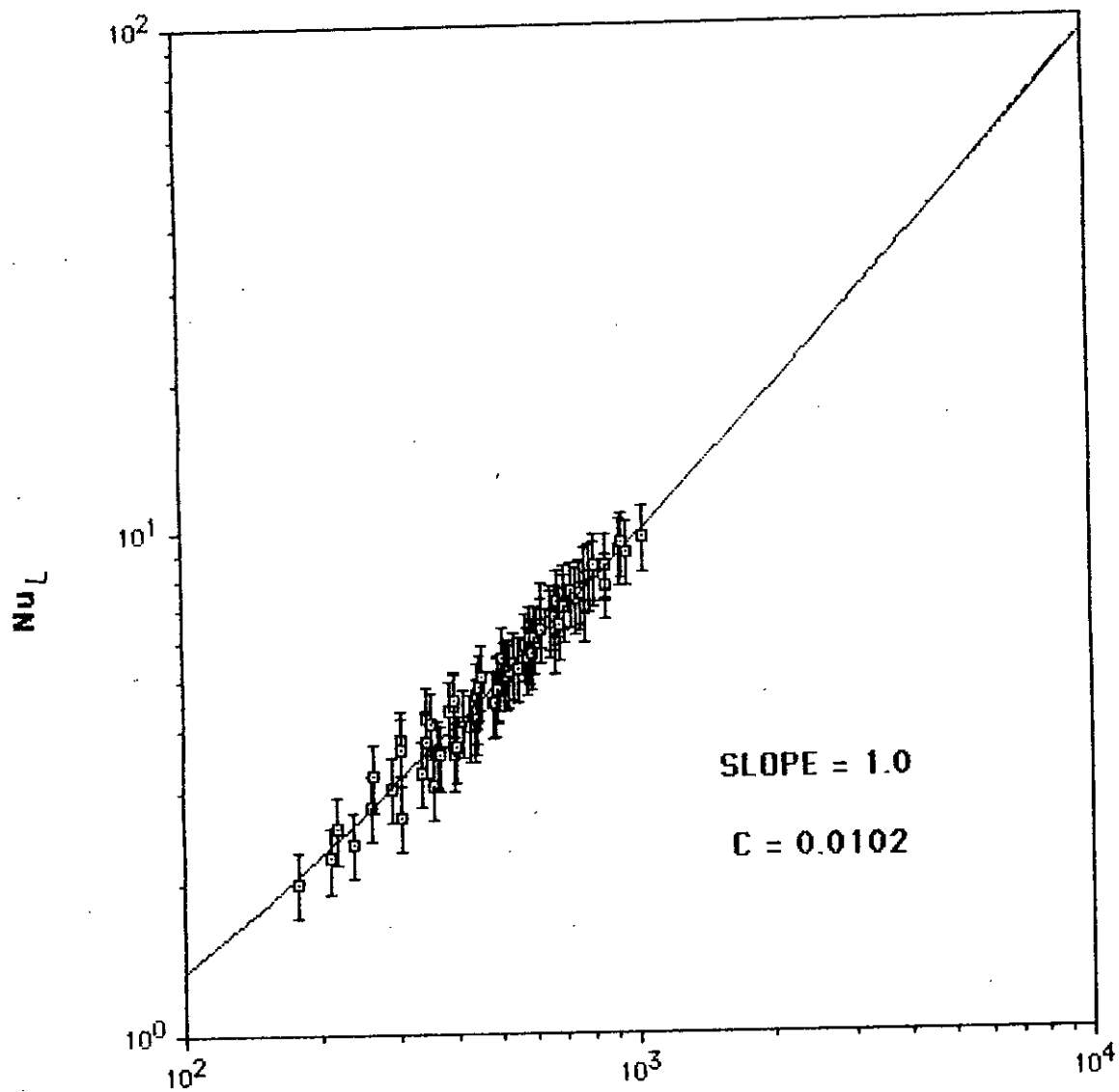


FIG. D.1 GRAPHICAL REPRESENTATION OF THE CORRELATION FOR TRAPEZOIDAL CORRUGATION



$$(Ra \cos \theta)^{0.530} (A)^{-0.4923}$$

FIG. D.2 GRAPHICAL REPRESENTATION OF THE CORRELATION FOR RECTANGULAR CORRUGATION

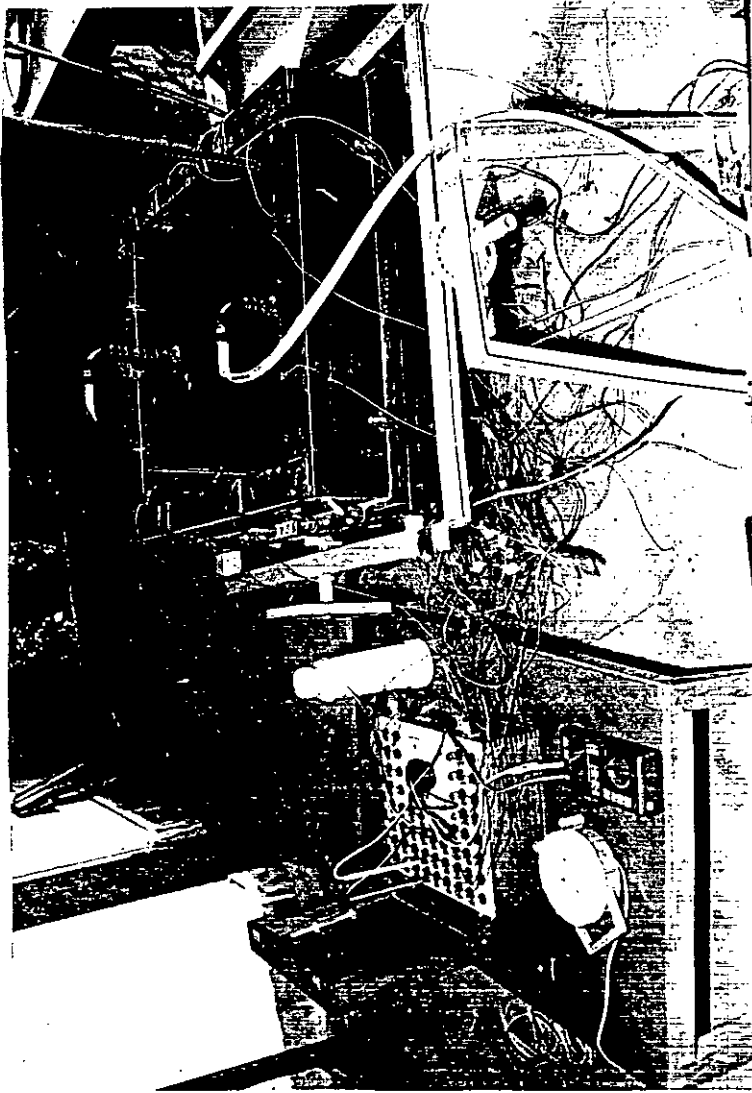


FIG. PHOTOGRAPH OF THE TEST SECTION

